

Spring 2018

REGULATION OF GABA RELEASE BY PRESYNAPTIC CAV2.2 IN THE BASOLATERAL AMYGDALA AND INFRALIMBIC CORTEX

Maxwell Robert Blazon
University of New Hampshire, Durham

Follow this and additional works at: <https://scholars.unh.edu/thesis>

Recommended Citation

Blazon, Maxwell Robert, "REGULATION OF GABA RELEASE BY PRESYNAPTIC CAV2.2 IN THE BASOLATERAL AMYGDALA AND INFRALIMBIC CORTEX" (2018). *Master's Theses and Capstones*. 1178.
<https://scholars.unh.edu/thesis/1178>

This Thesis is brought to you for free and open access by the Student Scholarship at University of New Hampshire Scholars' Repository. It has been accepted for inclusion in Master's Theses and Capstones by an authorized administrator of University of New Hampshire Scholars' Repository. For more information, please contact nicole.hentz@unh.edu.

REGULATION OF GABA RELEASE BY PRESYNAPTIC $CA_{v2.2}$ IN THE BASOLATERAL
AMYGDALA AND INFRALIMBIC CORTEX

BY

MAXWELL ROBERT BLAZON

Bachelor of Science in Physiology and Neurobiology, The University of Connecticut, 2016

THESIS

Submitted to the University of New Hampshire

in Partial Fulfillment of

the Requirements for the Degree of

Master of Science

in

Integrative and Organismal Biology

May, 2018

This thesis has been examined and approved in partial fulfillment of the requirements for the degree of Master of Science in Integrative and Organismal Biology by:

Thesis Director, Dr. Arturo S. Andrade, Assistant Professor of Neurobiology

Dr. Jill A. McGaughy, Associate Professor of Psychology

Dr. Winsor H. Watson, Professor of Zoology

On April 19, 2018

Original approval signatures are on file with the University of New Hampshire Graduate School.

TABLE OF CONTENTS

AKNOWLEDGEMENTS..... v

LIST OF FIGURES AND TABLES..... vi

ABSTRACT..... viii

INTRODUCTION..... 1

 Master's Thesis Research..... 23

CHAPTER 1: CA_v2.2-MEDIATED GABA RELEASE FROM CCK+ INTERNEURONS ONTO PYRAMIDAL CELLS IN THE BASOLATERAL AMYGDALA..... 27

 Abstract 27

 Introduction..... 27

 Methods 30

 Results..... 43

 Discussion 51

 Additional Considerations for Future Research..... 56

CHAPTER 2: CB₁-MEDIATED MODULATION OF GABA RELEASE FROM CCK+ INTERNEURONS ONTO PYRAMIDAL CELLS IN THE BASOLATERAL AMYGDALA... 58

 Abstract 58

 Introduction..... 58

 Methods 61

 Results..... 65

 Discussion 70

Additional Considerations for Future Research.....	74
<i>CHAPTER 3: ASSESSING REGULATION OF GABA RELEASE AND INTRINSIC FIRING BY CA_v2.2 IN THE INFRALIMBIC CORTEX.....</i>	76
Abstract	76
Introduction.....	76
Methods	80
Results.....	86
Discussion	93
Additional Considerations for Future Research.....	100
 <i>OVERALL CONCLUSIONS.....</i>	 102
 <i>LIST OF REFERENCES</i>	 105

ACKNOWLEDGEMENTS

I would like to acknowledge Dr. Arturo Andrade. Thank you for trusting and challenging me with research projects, grant proposals, and teaching positions. I will apply the level of quality and thoroughness you have showed me to all that I seek to achieve in my professional career. I would like to acknowledge Dr. Win Watson, Dr. Katherine Lockwood, and Dr. Robert Ross. I value the many lessons I learned from you as a teaching assistant, interacting with students and making important, difficult decisions. I am a better leader as a result, and I will apply this knowledge as a healthcare provider in the future. I would like to acknowledge Dr. Aaron Bradford. We would not have accomplished the electrophysiology research we did if not for your help. Your unique insight and knowledgeability was very much appreciated.

I would like to acknowledge Bri LaCarubba. From creating the mouse model for my research, to procuring the supplies I needed, to sharing your experience with me, your role cannot be overstated. I strive to be as integral a part of my future workplace as you were to our lab. I would like to acknowledge Lexi Bunda. Thank you for your work maintaining the mouse colony and sharing your expertise in genotyping and behavior with me. Your work ethic and dedication are enormously admirable. I would like to acknowledge Zachary Tepper and Sumeet Panesar. I learned a great deal from you both, and your friendship was tremendously helpful when I first began. Your continued support gave me confidence as I took on my own projects, and your assistance in those projects helped me to succeed. I would like to acknowledge Julian Brown. Working with you last summer helped me become a better mentor, and since then your knowledgeability has surpassed mine. I look forward to hearing about your many future accomplishments. I would also like to acknowledge the NIH for funding the research contained in this thesis (R00-MH099405).

LIST OF FIGURES AND TABLES

INTRODUCTION

Figure 1| Regions of the mouse medial prefrontal cortex

Figure 2| Regions of the mouse amygdala

Figure 3| Regions of the mouse hippocampus

Figure 4| Perisomatic inhibition

Figure 5| Basic neural connections implicated in fear

Figure 6| Schematic of a voltage-gated calcium channel complex

Figure 7| Proposed mechanism of Cav2.2-mediated anxiogenic signaling

Figure 8| eCB-mediated feedback inhibition system in CA3

CHAPTER 1

Figure 9| Breeding schematics for triple-transgenic mouse models

Table 1| Primer sequences and band sizes for mouse genotyping

Figure 10| CCK expression in *CCK-tdT* mice and GABAergic CCK expression in *CCK-Dlx5/6-tdT* mice

Figure 11| Channelrhodopsin expression in the BLA of *CCK-ChR2* and *CCK-Dlx5/6-ReaChR* mice

Figure 12| Morphophysiology and postsynaptic currents in CCK+IN/P-cell synapses in the BLA

Figure 13| Cav2.2 antagonism reduces IPSC peak amplitude in CCK+IN/P-cell synapses in the BLA

CHAPTER 2

Figure 14| GABAergic CCK and CB₁ expression in the BLA and HPC

Figure 15| Effects of CB₁ modulation in CCK+IN/P-cell synapses in the BLA

CHAPTER 3

Figure 16| Effects of Ca_v2.2 antagonism on IPSCs in GABAergic/P-cell synapses in the IL

Figure 17| GABAergic CCK expression in the IL

Figure 18| Effects of Ca_v2.2 antagonism on IPSCs in CCK+IN/P-cell synapses in the IL

Figure 19| Effects of Ca_v2.2 antagonism on P-cell intrinsic firing pattern and spike frequency in the IL

ABSTRACT

REGULATION OF GABA RELEASE BY PRESYNAPTIC $Ca_v2.2$ IN THE BASOLATERAL AMYGDALA AND INFRA-LIMBIC CORTEX

by

Maxwell Robert Blazon

University of New Hampshire, May, 2018

Anxiety is linked to dysregulation of neuronal activity in several brain regions including the infralimbic (IL) area of the medial prefrontal cortex (mPFC) and the basolateral nucleus of the amygdala (BLA). Disruptions to the balance of excitatory and inhibitory signaling in these regions are implicated in anxiety-like behaviors in animals and anxiety disorders in humans. The neuronal circuitry between excitatory neurons, known as pyramidal cells (P-cells), and inhibitory neurons, known as interneurons (INs), is a primary target for anxiety modulation at the cellular level. INs, particularly the subtype that contain the neuropeptide cholecystinin (CCK+INs), form inhibitory synapses around P-cells. Through GABAergic neurotransmitter release, CCK+INs regulate P-cell activity and subsequent anxiety-related neuronal output. Two protein complexes, the N-type calcium channel ($Ca_v2.2$) and the type-1 cannabinoid receptor (CB_1), are expressed in the presynaptic terminal of CCK+INs. $Ca_v2.2$ and CB_1 have been shown to regulate neurotransmitter release from CCK+INs in the hippocampus, but it is not known if this role is conserved in the anxiety-related neuronal circuits of the BLA and IL. $Ca_v2.2$ has also been shown to regulate the intrinsic firing properties of P-cells in the hippocampus and deep cerebellar nuclei, but this role has not been assessed in the IL. To investigate these neuronal circuits, I used a combination of transgenic mouse models, confocal microscopy, patch-clamp electrophysiology, optogenetics, and

pharmacology. In the first chapter of my thesis, I investigated the role of Cav2.2 in CCK+IN/P-cell synapses in the BLA. In the second chapter of my thesis, I investigated the role of CB₁ in regulating GABA release from CCK+INs in the BLA. In the third chapter of my thesis, I assessed the regulation of GABA release and intrinsic firing by Cav2.2 in the IL. I present electrophysiology data which demonstrate GABA release from CCK+INs is partially Cav2.2-dependent in the BLA. I obtained preliminary electrophysiology recordings which suggest CB₁ receptors modulate GABA release in CCK+IN/P-cell synapses in the BLA. I found that neurotransmitter release from GABAergic INs is partially Cav2.2-dependent in the IL. However, I found that GABA release from CCK+INs is not Cav2.2-dependent in this region. Lastly, I observed that Cav2.2 plays a minimal role in the intrinsic firing properties of P-cells in the IL. My findings suggest that Cav2.2 differentially regulates GABA release and intrinsic firing properties across brain regions, suggesting there are region-specific implications of Cav2.2 modulation in anxiety-related neuronal output.

INTRODUCTION

Overview

Fear and anxiety are normal experiences in day-to-day life. Fear often results from an apparent external danger, while anxiety is a widespread response to an unknown or non-specific threat. Both trigger appropriate and adaptive responses to risks, be they physical, mental, or societal (Steimer, 2002). When fear and anxiety become pathological, they can manifest as an anxiety disorder. Anxiety disorders include panic disorder, generalized anxiety disorder, agoraphobia, specific phobias, social anxiety disorder, post-traumatic stress disorder, obsessive-compulsive disorder, and separation anxiety disorder. In these conditions, an individual's ability to cope with various stressors is compromised, meaning non-threatening stimuli can cause severe distress. Anxiety disorders alter numerous physiological processes, facilitating poor physical health outcomes over time (Kroenke, Spitzer, Williams, Monahan, & Löwe, 2007). The National Institute of Mental Health reports a 19.1% past-year prevalence of anxiety disorders in U.S. adults (Harvard Medical School National Comorbidity Survey, 2017). Current medications used to treat anxiety disorders (benzodiazepines, selective serotonin reuptake inhibitors) cause several adverse effects (impaired cognition, addiction), thus many patients withdraw from treatment (Baldwin, Woods, Lawson, & Taylor, 2011). A greater understanding of the neurobiology behind anxiety disorders is required to produce more effective treatments.

Anxiety is a highly integrated emotional component of cognitive processing facilitated by the thalamus, locus coeruleus, hypothalamus, hippocampus, amygdalar nuclei, and the prefrontal, sensory, entorhinal, and association cortices (Steimer, 2002). Classically, these brain areas are defined as components of the limbic system or 'emotional brain.' In animal models, their connections are implicated in emotional learning and conduct, including fear-conditioning and

anxiety-like behaviors (Steimer, 2002). Of particular importance for their role in modulating anxiety are the medial prefrontal cortex (mPFC) and the basolateral amygdala (BLA). The mPFC processes the cognitive components of anxiety (i.e. rumination) and mediates sympathetic nervous system responses (fight-or-flight). The behavioral responses related to anxiety (i.e. avoidance) are modulated by the BLA (Johansen, Cain, Ostroff, & Ledoux, 2011). While each area has independent roles in anxiety, their interconnections are involved in fear expression and the extinction of conditioned fear (Ferreira, Yousuf, Dalton, & Sheets, 2015; Milad & Quirk, 2002; Phelps, Delgado, Nearing, & Ledoux, 2004). Research targeting the neural circuits involved in this disruption may provide insight as to how anxiety is regulated at the cellular level.

The balance between excitatory and inhibitory activity in the mPFC and BLA is disrupted in anxiety disorders (Ehrlich et al., 2009). Pyramidal neurons (P-cells) are the primary excitatory cell type in the mPFC and BLA. P-cells receive excitatory inputs through projections from other brain areas and inhibitory inputs from local interneurons (INs) (Freund, 2003). Multiple types of INs exist, and the cholecystinin-containing subtype (CCK+INs) are strongly linked to anxiety-related behaviors (Truitt, Johnson, Dietrich, Fitz, & Shekhar, 2009). The inhibitory neurotransmitter gamma-aminobutyric acid (GABA) is released from CCK+INs onto P-cells, decreasing their excitability (Freund & Katona, 2007). Membrane proteins like voltage-gated calcium channels (Cavs) and cannabinoid receptors modulate neurotransmitter release (Guo & Ikeda, 2004). Ca_v s permit calcium ions to enter the presynaptic terminal which facilitate vesicular fusion and neurotransmitter exocytosis. Cannabinoid receptors are coupled to Ca_v s and downregulate calcium ion entry when activated by cannabinoids (Zamponi & Currie, 2013). Additionally, Ca_v s modulate the intrinsic firing properties of P-cells by coupling to calcium-activated potassium channels (Loane, Lima, & Marrion, 2007). There are multiple Ca_v and

cannabinoid receptor subtypes; the N-type calcium channel (Ca_v2.2) and the type-1 cannabinoid receptor (CB₁) are known to regulate neurotransmitter release from CCK+INs in the hippocampus (Szabo et al., 2014). However, the role of Ca_v2.2 and CB₁ in CCK+INs of the BLA and mPFC has not been described. In my master's thesis, I aim to elucidate the role of Ca_v2.2 in CCK+IN/P-cell synapses in the BLA (**CHAPTER 1**) and determine if CB₁ regulates neurotransmitter release in this system (**CHAPTER 2**). Additionally, I will assess the role of Ca_v2.2 in regulating GABA release and intrinsic firing properties in the infralimbic region of the mPFC (**CHAPTER 3**).

The Role of Fear and Anxiety in Survival

Emotions are thought to be the result of natural selection, as they prompt behavioral responses important for survival (Darwin, 1998). A critical emotion for survival, fear, is defined as a motivational state that promotes either defensive or escaping behaviors (Gherardi, McFarland, & Tinbergen, 1988). Exposure to fearful stimuli often correlates with learning. Animals (including humans) adapt behavioral changes to avoid repeat exposure to fear, particularly if the fearful stimuli are associated with pain or stress. Fear-related learning can manifest through a closely related emotion; anxiety (Steimer, 2002). Anxiety involves behavioral and physiological responses including avoidance, vigilance, and arousal, all intended to protect the animal from danger. While fear is focused on known dangerous stimuli, anxiety is often a directionless response to an unknown danger or internal conflict (Ritu, Sandeep, Mamta, & Nirja, 2013).

Fear and Anxiety are Related to the Limbic System

The limbic system, also known as the 'emotional brain,' was largely defined by James Papez (1937) and Paul MacLean (1955). Papez related brain areas like the cingulate cortex,

thalamus, hypothalamus, hippocampus, and with emotional patterns observed in human experiments. MacLean refined Papez's work, highlighting the role of the prefrontal cortex and subcortical areas like the amygdala and septum in emotional experiences (J. LeDoux, 1996; Roxo, Franceschini, Zubarán, Kleber, & Sander, 2011). More than a series of brain structures, limbic areas form a functional system. Feelings of fear and anxiety are complex, involving more than just emotional components. For example, fear and/or anxiety-related stimuli are processed by the prefrontal cortex (PFC), which modulates physiological and behavioral responses (via the amygdala). The amygdala assimilates sensory, contextual, and cognitive information to influence fear extinction, anxiety-related behavior, and selective attention (J. E. LeDoux, 2009; Steimer, 2002). The integration of cognitive, physiological, and sensory information in the BLA and PFC illustrates the complexity of fear and anxiety (J. E. LeDoux, 2009).

The Role of the Medial Prefrontal Cortex in Anxiety

The PFC is believed to influence the conscious experiences and thoughts related to anxiety (J. LeDoux, 1996; Steimer, 2002) as well as module anxiety-like behaviors (Sierra-Mercado, Padilla-Coreano, & Quirk, 2011). fMRI studies show changes in PFC activity in patients with anxiety disorders (generalized and post-traumatic), which are behaviorally characterized by the inability to control fear responses (Sierra-Mercado et al., 2011). Deficient recruitment of the PFC (ventromedial region) during fear inhibition is observed in patients with generalized anxiety disorder (Greenberg, Carlson, Cha, Hajcak, & Mujica-Parodi, 2013). Similarly, decreased activation of the PFC (ventromedial region) in response to trauma-related cues is present in patients with post-traumatic stress disorder (PTSD) (Shin et al., 2004). In animal research, similar observations have been made. Lesions to the rat PFC (right infralimbic region) were shown to have

anxiolytic effects and suppress autonomic nervous system responses (Sullivan & Gratton, 2002). In mouse models, the PFC is associated with fear-related learning and fear expression, both of which can be impaired with selective inactivation of PFC sub-regions (Sierra-Mercado, Corcoran, Lebrón-Milad, & Quirk, 2006; Sierra-Mercado et al., 2011)

The rodent PFC is comprised of multiple sub-regions with specialized functions including the medial, lateral, and orbitofrontal cortices. The medial prefrontal cortex (mPFC) is the target of extensive anxiety research (Duvarci & Pare, 2014; Morgan, Romanski, & LeDoux, 1993; Sullivan & Gratton, 2002). Further divided, the mPFC is comprised into the anterior cingulate cortex (AC), the prelimbic cortex (PL), and the infralimbic cortex (IL) (**Figure 1**) (Paxinos & Watson, 2007). The IL and PL play unique roles in anxiety-related processing and differentially connect to the amygdala. The IL facilitates the storage of extinction learning in target structures (Do-Monte, Manzano-Nieves, Quinones-Laracuate, Ramos-Medina, & Quirk, 2015). IL-BLA connections are involved in the extinction of conditioned fear (Ferreira et al., 2015; Sierra-Mercado et al., 2011). Excitatory neurons in the PL project to the BLA and are involved in the expression of fear (Sierra-Mercado et al., 2011; Wang et al., 2015). In rodents, fear is expressed by behaviors like freezing. An animal that displays reduced explorative behaviors or excessive grooming is

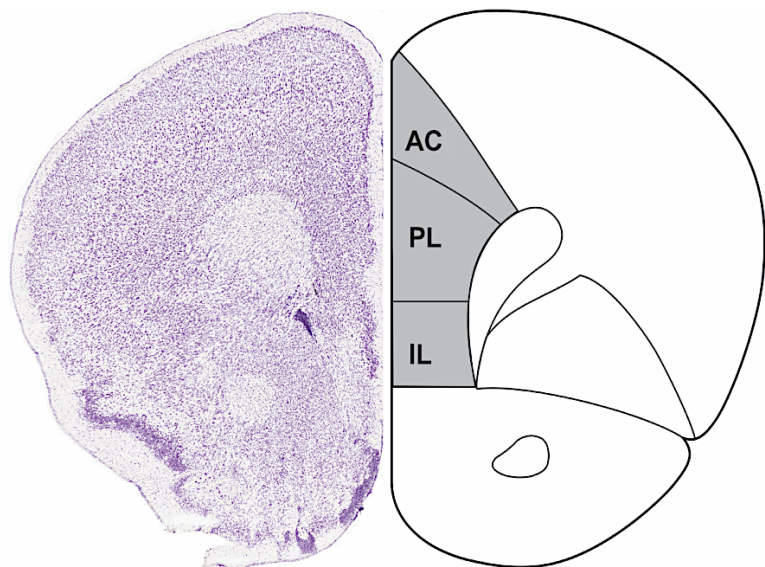


Figure 1| Regions of the mouse medial prefrontal cortex. A Nissl stained coronal section of the mouse brain containing the PFC is paired with a stereotaxic atlas depiction of the subdivisions of the mPFC. AC, anterior cingulate; PL, prelimbic; IL, infralimbic. Adapted from Michelsen et al., 2007; Paxinos & Watson, 1998; Allen Mouse Brain Atlas.

considered to be exhibiting anxiety-like behavior. Stressful stimuli activate the PL and increase fear expression and anxiety-like behaviors (Hurley, Herbert, Moga, & Saper, 1991; Sullivan & Gratton, 2002), while selective inactivation of the PL reduces them (Sierra-Mercado et al., 2011). Abnormal activity in the connections from the PL and IL to the BLA can prompt inappropriate or deficient response to fear (Greenberg et al., 2013), a characteristic common to anxiety disorders.

The Role of the Amygdala in Processing Fear and Anxiety

The amygdala is an almond-shaped, highly interconnected limbic system structure implicated in the behavioral output of anxiety. Amygdalar functions and connections are conserved across many species, suggesting that research findings in animal models like the mouse (*Mus musculus*) may have human implications (Janak & Tye, 2015). For non-human primates, lesions to the amygdala impair their ability to associate a stimulus with positive/non-harmful or negative/potentially harmful outcomes (Weiskrantz, 1956) and lead to hypo-emotionality (Aggleton & Passingham, 1981). In rodents, the amygdala facilitates behavioral responses (i.e. freezing/playing dead in front of predator) by integrating rapid sensory input (i.e. visualization of a predator) from the thalamus and slower sensory input (i.e. motivation to escape the predator) from the prefrontal cortex (Steimer, 2002). Furthermore, the amygdala influences cognition, perception, and associative learning (J. E. LeDoux, 2009; Steimer, 2002). In associative learning, an animal relates a new response to a particular stimulus, or one stimulus to a second stimulus (Janak & Tye, 2015). In humans, (Anderson & Phelps, 2001) and rats (Blanchard & Blanchard, 1972), damage to the amygdala hinders the ability to recognize fearful stimuli. Amygdalar dysfunction is also caused by disruptions in the balance of excitatory and inhibitory signaling.

These disruptions are observable in anxiety disorders (Etkin, Prater, Schatzberg, Menon, & Greicius, 2009).

The amygdala is composed of several nuclei, including the basolateral amygdala (BLA) and the central amygdala (CeA) (**Figure 2**). The BLA is further comprised of the basal amygdala (BA) and lateral amygdala (LA), and is the main source of excitatory output to other brain regions involved in fear and anxiety. Thalamic and cortical sensory signals project to the LA, which connects to the BA and CeA (Keifer, Hurt, Ressler, & Marvar, 2015). Direct stimulation of the BLA is correlated with anxiety-like behavior (Johansen et al., 2010). The BLA can both upregulate and downregulate freezing behaviors through projections to the PL and IL, respectively, and is involved in anxiety-related memories via hippocampal connections (Sierra-Mercado et al., 2011).

Opposite of the BLA, the CeA is mainly composed of inhibitory interneurons. Divided into the centromedial (CEm) and centrolateral (CEl) amygdala (CEl), the CeA is involved in the translation of BLA signals to behavioral output (Janak & Tye, 2015). It has been demonstrated that inhibition of BLA-CeA connections increases anxiety-related behaviors while direct stimulation decreases them (Tye et al., 2011).

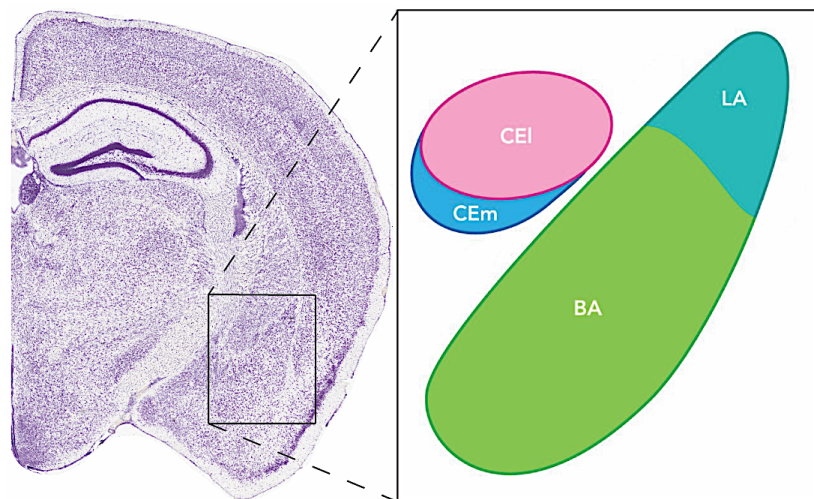


Figure 2| Regions of the mouse amygdala. A Nissl stained coronal section of the mouse brain is paired with a diagram representing the amygdala nuclei. The basal (BA) and lateral (LA) nuclei comprise the basolateral amygdala (BLA) while the centromedial (CEm) and centrolateral (CEl) nuclei comprise the central amygdala (CeA). Adapted from Allen Mouse Brain Atlas; Keifer et al., 2015.

The Role of the Hippocampus in Anxiety-related Learning and Memory

The HPC is divided into ventral and dorsal regions, each of which contains Cornu Ammonis (CA) regions (CA1 - CA4). Additionally, the CA regions contain a system of laminar organization (**Figure 3**). The stratum oriens (SO), stratum pyramidale (SP), stratum radiatum (SR), and stratum lacunosum-moleculare (slm) possess different cells, circuit organization, and functions in hippocampal processes. The ventral portion of the hippocampus (vHPC) is implicated in fear conditioning and anxiety-like behavior through its connections with the mPFC and BLA. BLA-vHPC connections are necessary for forming memories of environmental context (Goosens, 2001; Maren & Fanselow, 1995), while vHPC-mPFC connections are required for retrieving memories when presented with specific context (Sierra-Mercado et al., 2011). Contextual memory and the memory retrieval process are important for the survival of a species, especially when the context involves perceived danger or negative emotions (Goosens, 2001). Chronic stress, fear, and anxiety

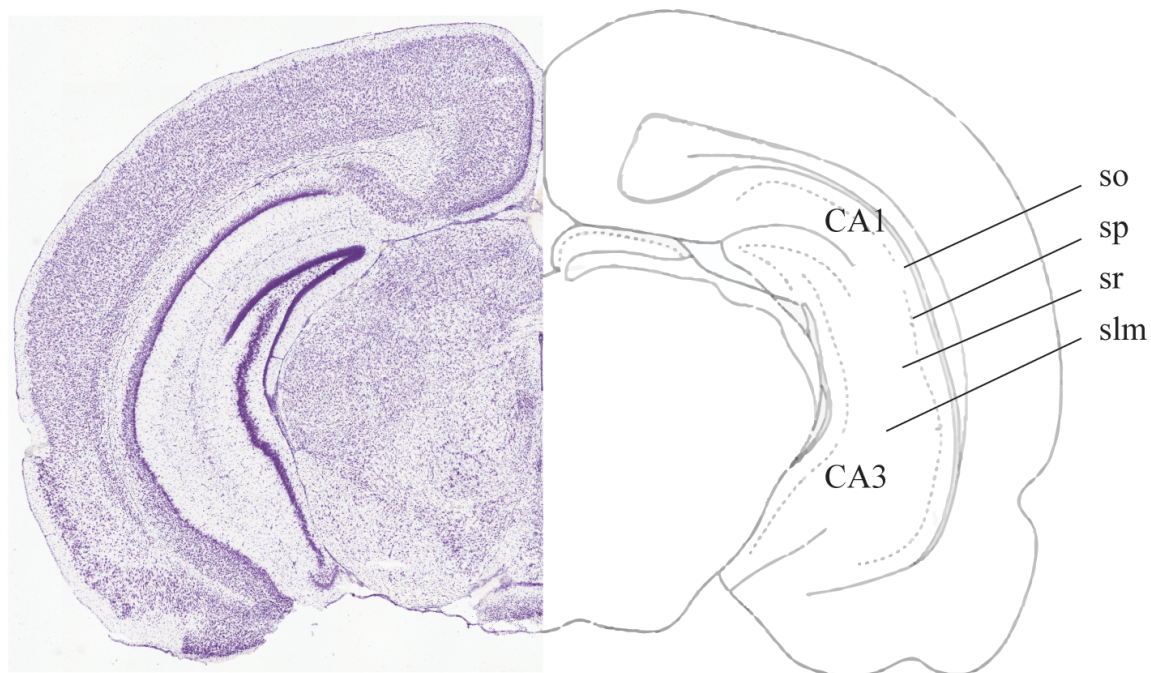


Figure 3| Regions of the mouse hippocampus. A Nissl stained coronal section of the mouse brain is paired with a diagram detailing the regions and layers of the vHPC. CA, Cornu Ammonis; so, stratum oriens; sp, stratum pyramidale; sr, stratum radiatum; slm, stratum lacunosum-moleculare. Adapted from Allen Mouse Brain Atlas; Silva-Gómez, 2013; Paxinos & Watson, 1998.

can disrupt these processes and result in a state of hippocampal dysfunction. There is evidence that hippocampal dysfunction is both a risk factor for developing and complication of anxiety disorders (Cominski, Jiao, Catuzzi, Stewart, & Pang, 2014).

Cells and Circuits in Anxiety-related Brain Areas

New and developing pharmacological treatments for anxiety disorders must aim to decrease activity in the neural circuits that influence anxiety and increase activity in those that reduce anxiety. Fundamental to these objectives is research which provides a more complete understanding of the molecular neuroanatomy of the limbic system and the functional neurophysiology of anxiety disorders. Communication between and within limbic system areas is facilitated by complex and highly organized neuronal circuits. Similar cell types and circuitry are thought to exist across limbic regions like the mPFC, BLA, and vHPC (Jinno, 2009). However, it is not understood if there are underlying functional differences in these circuits, nor what implications they might have in the neuronal processes of anxiety.

The mPFC, BLA, and vHPC contain a mixture of excitatory (glutamatergic) pyramidal cells (P-cells) and inhibitory (GABAergic) interneurons (INs). P-cells are characterized by their piriform morphology, apical dendrites, and long axons which allow for communication across brain regions. INs innervate local P-cells and are classified by the domain in which they target. INs that target P-cell bodies (somas/somatas) are termed basket cells (BCs), those that target the axon initial segments are termed chandelier cells, and those that target dendrites are termed dendritic inhibitory cells (Freund, 2003). INs can be further categorized by identifying their intrinsic firing properties and neuropeptide content. Intrinsic firing properties, including action potential spike frequency and firing pattern, indicate how an IN behaves in a neuronal circuit

(Benda & Herz, 2003). Neuropeptide contents are used as a marker of IN subtypes, and indicate the neurotransmitters, receptors, and functions likely associated with a particular subtype. In the mPFC, BLA, and HPC, several subtypes of BCs have been identified for their unique roles in influencing P-cell activity (Barsy, Szabó, Andrási, Vikór, & Hájos, 2017; Freund, 2003; Whissell, Cajanding, Fogel, & Kim, 2015). BCs containing the neuropeptide parvalbumin (PV+BCs) process multiple converging stimuli and display fast, non-adapting firing patterns (Nyíri, Stephenson, Freund, & Somogyi, 2003). Cholecystokinin-containing BCs (CCK+BCs) respond to slow, asynchronous inputs and display moderate, adapting firing patterns (Bartos & Elgueta, 2012; Veres, Nagy, & Hájos, 2017). Understanding functional specifics about INs within limbic structures may help elucidate their complex role in mediating fear and anxiety.

Descriptions of the wiring, innervation, and postsynaptic targets of INs requires a description of how IN/P-cell networks operate. Across P-cells and IN subtypes, there are variations in intrinsic firing and synaptic properties (Kullmann, 2011). In general, the synaptic events which excite INs are faster than those that excite P-cells. This is advantageous for controlling anxiogenic pathways, as excitation is under strict regulation by INs, particularly BCs (Deleuze, Paziéti, & Bacci, 2014). This regulation comes in multiple forms including feedforward inhibition. In feedforward inhibition, a local IN, excited by an afferent projection, delivers an inhibitory signal to a P-cell. Depending on the cellular properties of the IN, feedforward inhibition can limit the window for action potential generation or cancel out P-cell excitation (Jasnow, Ressler, Hammack, Chhatwal, & Rainnie, 2009). In addition to feedforward inhibition, there is feedback inhibition. The firing of P-cells activates INs, which in turn inhibit P-cells (Freund & Katona, 2007). Once

feedback and feedforward inhibition decline, P-cells are able to fire again. The combination of feedforward and feedback inhibition establish a neuronal oscillation, also known as a brainwave (Möhler, 2002). A prominent form of inhibition in the BLA and mPFC is known as perisomatic inhibition (**Figure 4**), wherein CCK+BCs and PV+BCs synchronize the activity of local P-cells (Freund & Katona, 2007). The synapses made in perisomatic inhibitory are highly modifiable by ion

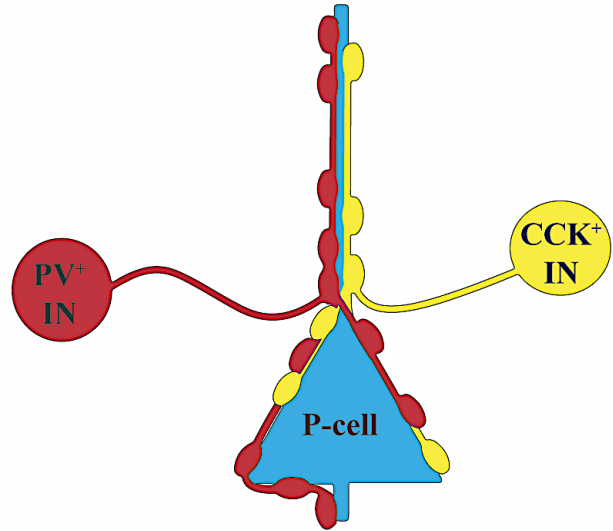


Figure 4| Perisomatic inhibition. Simplified circuit diagram depicting perisomatic inhibition of a pyramidal cell by parvalbumin (PV+) and cholecystokinin (CCK+) containing basket cell interneurons (INs). Adapted from Deleuze et al., 2014.

channels, neurotransmitters, and additional extracellular messengers, prompting a closer review of their underlying molecular components of in anxiety-implicated circuits of the vHPC, mPFC, and BLA.

In the vHPC, excitatory signaling is transmitted through P-cell projections from CA3 to CA1. Anxiety research often targets CA3 and CA1, as these sub-regions are major output pathways to other limbic areas. Several networks of INs exist within these output pathways which can modulate P-cell activity (Kullmann, 2011). These include fast-spiking PV+BCs, regular-spiking CCK+BCs, chandelier INs, and Schaffer collateral-associated (SCA) INs (Kullmann, 2011). Research has shown that while PV+BCs are more abundant overall, CCK+BCs outnumber PV+BCs in several sub-regions of the hippocampus (Whissell et al., 2015). The most superior layer of the vHPC, the SO, contains BC bodies and the basal dendrites of P-cells, whose cell bodies are located the second-most superior layer, the SP (Lacaille & Williams, 1990). The SP is

recognizable by its dense P-cell composition and role in hippocampal output. BCs can be found in the SP as well; their proximity to P-cells illustrates their known role in perisomatic inhibition (Neu, Földy, & Soltesz, 2007; Whissell et al., 2015). The layer immediately following the SP, the SR, contains P-cell projections from CA3 to CA1, termed the Schaffer collaterals. Schaffer collaterals are the topic of extensive neuropsychiatric research, as they are critical for long-term potentiation and emotional memory (Kumar, 2011; Stanton, Winterer, Zhang, & Müller, 2005). BCs in CA1 are innervated by Schaffer collaterals, while the dendrites of Schaffer collaterals themselves are innervated by SCA INs (Kullmann, 2011).

Similar to the SP layer of the vHPC, the mPFC contains mostly P-cells (80-90%) with a minority of INs (10-20%) spread heterogeneously across a system of laminar organization. In the human brain, there are six layers (L1-L6) while in rodents there are only five (rodents do not possess L4) (Heidbreder & Groenewegen, 2003). Across layers, composition and connectivity vary, but functional characteristics of IN/P-cell connections are relatively conserved. INs wield strong, differential control over local circuitry and are able to synchronize P-cell spiking throughout the mPFC (Sparta et al., 2014). In rodents, cells located in L1 are thought to be exclusively GABAergic INs (Riga et al., 2014). L1 INs receive excitatory input from the thalamus and facilitate dendritic inhibition of L2/3 P-cells (Cruikshank et al., 2012). BC/P-cell perisomatic inhibitory networks are seen in L2/3 and L5. P-cells in L2/3 and L5 receive excitatory inputs from the thalamus, the contralateral mPFC, the vHPC, and the BLA. These P-cells project to various brain areas depending their location within the mPFC. In the PL, L2/3 P-cells projects to the BLA, while in the IL, L2/3 and L5 P-cells project to the BLA (Ferreira et al., 2015; Zaitsev, Povysheva, Gonzalez-Burgos, & Lewis, 2012). P-cells in L2/3 of the PL are involved in fear expression while P-cells in L2/3 and L5 of the IL are involved in the extinction of conditioned fear (**Figure 5**) (Sierra-Mercado

et al., 2011). It is vital to make these distinctions, as they demonstrate that even within L2/3 of the mPFC, IN/P-cell connections mediate different anxiety-related processes.

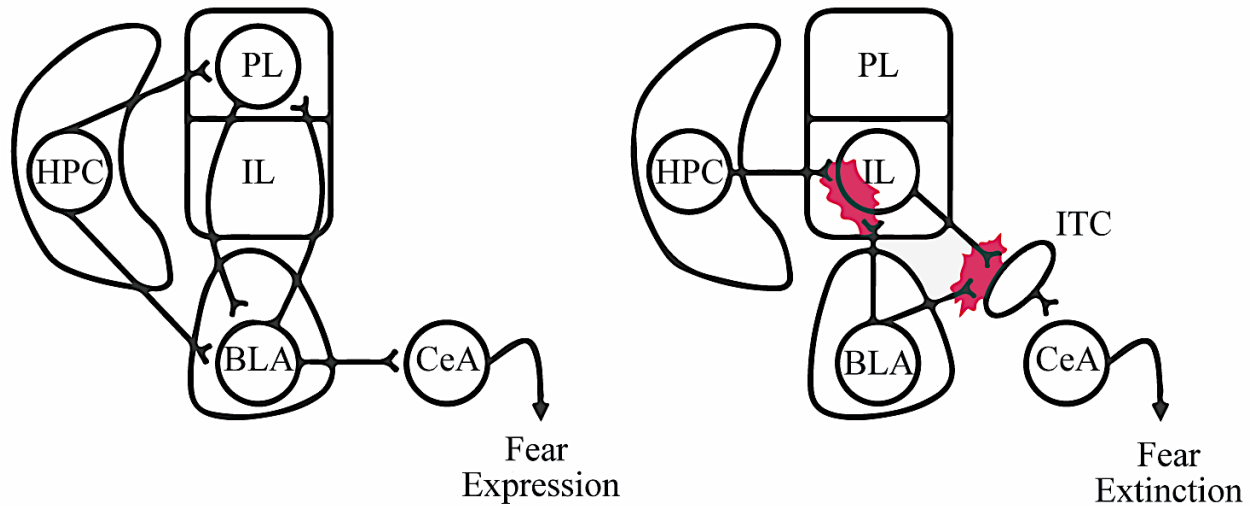


Figure 5| Basic neural connections implicated in fear. Left: The circuitry involved in fear expression. Emotional memories from the hippocampus (HPC) interact with the prelimbic cortex (PL) which regulates behavioral output via the amygdala (BLA and CeA). Right: The circuitry involved in fear extinction. The HPC and basolateral amygdala (BLA) interact with the infralimbic cortex (IL) to facilitate fear extinction. Behaviors reflective of fear extinction are produced by the IL via the extended amygdala (ITC) and central amygdala (CeA). Neuronal plasticity associated with extinction learning is represented in pink. Adapted from Sierra-Mercado et al., 2011.

The BLA is comprised of P-cells and multiple IN subtypes including PV+BCs and CCK+BCs (Ehrlich et al., 2009; Freese & Amaral, 2005). P-cells receive inhibitory input from local BCs and excitatory input from cortical areas via the external capsule (EC), a white matter fiber tract containing clusters of P-cell axons (Little & Carter, 2013). Excitation of P-cells in the BLA correlates with anxiety-like behavior (Johansen et al., 2010). Perisomatic inhibition, facilitated by CCK+BCs and PV+BCs, has been observed in electrophysiology recordings from P-cells in the BLA (Freund, 2003). PV+BCs and CCK+BCs receive excitatory signals from local and distant P-cells (via the EC) and inhibitory signals from local INs (Faber, Callister, & Sah, 2001; Rainnie, Asproдини, & Shinnick-Gallagher, 1993). Studies have been performed on the

underlying molecular components of perisomatic inhibitory synapses in the vHPC, however less is known regarding similar circuits in the BLA (Barsy et al., 2017; Freund & Katona, 2007; Trouche, Sasaki, Tu, & Reijmers, 2013). Functional studies on neurotransmitter release in BC/P-cell synapses are needed to understand how behavioral output associated with anxiety is regulated in the BLA.

The Neurochemical Correlates of Anxiety - GABA and Glutamate

Neuronal circuits in the BLA, mPFC, and vHPC possess extensive γ -aminobutyric acid (GABA) and glutamate neurotransmitter systems (Bystritsky, Khalsa, Cameron, & Schiffman, 2013). GABA is the principle inhibitory neurotransmitter in the brain while glutamate is the principle excitatory neurotransmitter. Balance between GABAergic and glutamatergic activity is critical for normal fear and anxiety-related processing (Möhler, 2002). Excess GABAergic activity can be anxiolytic but can also impair cognition. Insufficient GABAergic activity can result in increased anxiety (Möhler, 2002). Chronic deficits in GABAergic activity contribute to the pathophysiology of anxiety disorders; anti-anxiety medications including benzodiazepines and gabapentinoids enhance GABAergic activity (Sills, 2006). Alterations to glutamate transmission have also been shown to be effective in augmenting anxiety disorders (Dawson & Watson, 2009), as glutamate is involved in the pathways underlying normal and pathological anxiety states (Bystritsky et al., 2013).

The effects of neuronal inhibition differ across cell types, circuits, and brain areas. When P-cells are inhibited, they no longer release glutamate onto their projection targets. On the contrary, inhibition of INs prevents IN-mediated inhibition; resulting in P-cell disinhibition (Andrási et al., 2017). Accordingly, it is important to examine neuronal inhibition at the cellular and circuit level

to more readily understand its implications in anxiety. GABA binds to the GABA_A receptor, a ligand-gated ion channel. Upon binding, the channel opens and chloride (Cl⁻) anions flow inward (U. Rudolph & Antkowiak, 2004). Chloride influx induces electrical events known as inhibitory postsynaptic currents and potentials (IPSCs and IPSPs). As a result, hyperpolarization, action potential inhibition, and decreased neurotransmitter release occur (Amir, Michaelis, & Devor, 1999). GABA_A receptors are widespread, expressed in multiple cellular domains (i.e. terminals, somas, and axons) and cell types not exclusively involved in anxiety (Freund, 2003; Freund & Katona, 2007). In addition to the GABAergic system, the glutamatergic system regulates anxiety-related neuronal output from P-cells.

Proper glutamatergic transmission is required for anxiety states (Bystritsky et al., 2013). The glutamate receptors most pertinent to anxiety-related circuits are the AMPA and NMDA subtypes. As a whole, glutamatergic activity shows cell-type specific dynamics in modulating anxiety-related neuronal output (Nyíri et al., 2003). For example, long-term potentiation, implicated in storage of traumatic memories, relies on the NMDA receptors within Schaffer collaterals of the hippocampus (Harris & Cotman, 1986). Additionally, AMPA receptors on P-cells in the BLA are redistributed from dendritic stores into spines following severe stress (Hubert, Li, Rainnie, & Muly, 2014).

Molecular Components of GABAergic and Glutamatergic Neurotransmission

GABA and glutamate neurotransmission are modulated by G protein-coupled receptors (GPCRs) and voltage-gated calcium channels (Cavs). Located in the transmembrane domain, GPCRs are signal transduction proteins which interact with molecules in the extracellular and intracellular environment, as well as other transmembrane receptors (Trzaskowski et al., 2012).

There are numerous families and subtypes of GPCRs which couple to different subunits. GPCRs in the mPFC, vHPC, and BLA are coupled to the G_i alpha subunit ($G_{\alpha i}$), including metabotropic GABA and glutamate receptors (Lee et al., 2015; Lenkey et al., 2015; Talani & Lovinger, 2015; Zoppi et al., 2011). These GPCRs are involved in a variety of anxiety-related physiological processes including behavior and mood regulation (Swanson et al., 2005). For this reason, $G_{\alpha i}$ receptors are the target of several pharmaceutical anxiety treatments. $G_{\alpha i}$ receptors are activated by ligand binding (whether endogenous or synthetic) and exert an inhibitory effect on cAMP and calcium, two major internal signaling molecules. As a result, calcium-mediated processes and cAMP-dependent signal transduction pathways are inactivated (Scotter, Graham, & Glass, 2009).

Fundamentally, Cav_s are protein complexes consisting of several subunits (α_1 , β , $\alpha_2\delta$, and γ) which mediate calcium ion entry into a cell (**Figure 6**). There are two distinct classes of Cav_s based on their voltage-gating properties; high voltage-activated (HVA) and low voltage-activated (LVA). The phrase ‘voltage-gated’ is derived from the closed state of these channels under resting membrane potential conditions.

Only a strong enough membrane depolarization (i.e. an action potential) will release this voltage-gate (Stotz, 2001). Within each class of Cav_s, subtypes are determined by the α_1 subunit. The importance of the α_1 subunit cannot be stressed enough, as it forms the calcium-selective ion channel

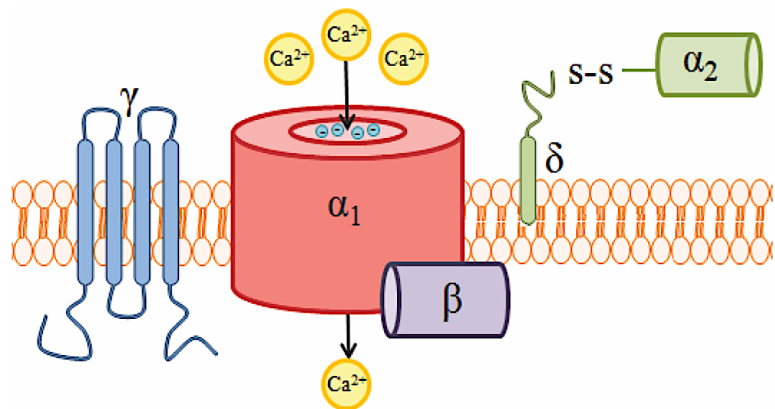


Figure 6| Schematic of a voltage-gated calcium channel complex. Cav_s are composed of a pore-forming subunit (α_1) and several ancillary subunits. The α_1 subunit functions as a voltage sensor, binding site, and permeable ion channel. The β subunit provides stability and modulates activation of α_1 . The $\alpha_2\delta$ subunit enhances expression and regulation of α_1 . The γ subunit is not well understood but does not appear to regulate channel function. Adapted from Marrero-Rosado et al., 2014; Hannon & Atchison, 2013.

through which calcium enters the cell (Williams et al., 1992). The α_1 subunit can detect changes in membrane potential and contains binding sites for pharmaceutical antagonists (Catterall, 2011; Zamponi, 2016). From ten known α_1 subunits there are five known Cav isoforms. The isoforms and their respective α_1 subunit encoding genes (in parenthesis) are as follows: L-type (Cav1.1, Cav1.2, Cav1.3, Cav1.4), P/Q-type (Cav2.1), N-type (Cav2.2), R-type (Cav2.3), and T-type (Cav3.1, Cav3.2, Cav3.3) (Catterall, 2011). The remaining Cav subunits serve α_1 ; enhancing its expression (δ), stabilizing its conformation (β), and regulating its activation and inactivation kinetics (β , $\alpha_2\delta$) (Hannon & Atchison, 2013).

Of the numerous α_1 subunits, those encoded by Cav2.1, Cav2.2, and Cav2.3 (P/Q-, N-, and R-type channels) are most involved in mediating signal transduction in GABAergic and glutamatergic cells (Catterall, 2011; Zamponi, 2003). Additionally, Cav2 channels have been shown to modulate neuronal firing through coupling to calcium-activated potassium channels (Alviña & Khodakhah, 2008; Loane et al., 2007). During membrane depolarization, Cav2 opens and allows calcium entry into the neuron, which induces numerous physiological events. For

instance, calcium interacts with SNARE proteins to fuse neurotransmitter vesicles to the presynaptic terminal, where subsequent exocytosis leads to synaptic transmission (Südhof, 2012). It has been demonstrated that calcium

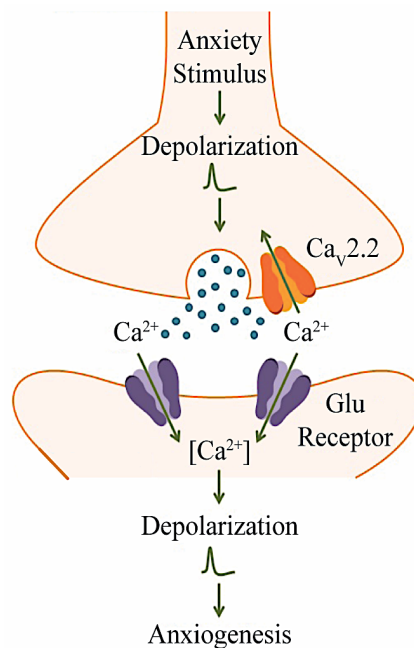


Figure 7 | Proposed mechanism of Cav2.2-mediated anxiogenic signaling. Anxiety-related signaling is propagated by excitatory pathways in areas like the vHPC and BLA. Action potentials travel down the presynaptic axon and into the terminal, whereby Cav2.2 is activated and calcium (Ca²⁺) enters the cell. Neurotransmitters (blue circles) are released into the synapse and activate Ca²⁺ entry through postsynaptic glutamate (Glu) receptors. Increased Ca²⁺ concentration further propagates anxiogenic signaling through the postsynaptic cell and beyond. Adapted from Schmidtko et al., 2010; Hannon & Atchison, 2013.

entry through Cav2.1 and Cav2.2 channels initiates the release of glutamate and GABA in fast synapses. More specifically, it has been discovered that Cav2.2 channels regulate GABA release from presynaptic CCK+INs in the vHPC (Szabo et al., 2014). Given the role of CCK+INs in perisomatic inhibition of P-cells, and the role of excess P-cell activity in anxiety-related behaviors (**Figure 7**), Cav2.2 channels are a critical research target for anxiety disorders (Kurihara & Tanabe, 2003; Lee et al., 2015; Lee, 2013; Szabo et al., 2014).

Modulation of the N-type Channel and Anxiety Implications

Ca_v2.2 modulation is a current target for treating neuropathic pain (Hannon & Atchison, 2013) and has emerged as a possible means of treating anxiety (Newton & Messing, 2009). Previous studies have found that mice lacking Ca_v2.2 display reduced anxiety levels (Saegusa, 2001), and current research aims to dissect the role Ca_v2.2 blockers play in anxiety. In nature, a highly-specific Ca_v2.2 blocker is found in the venom of the cone snail, *Conus magus*. Known as ‘ ω -Conotoxin GIVA’ when isolated, this peptide neurotoxin show affinity only for Ca_v2.2 (McCleskey et al., 1987). Zinconotide and Leconotide, synthetic ω -Conotoxins used to treat neuropathic pain, have strong yet poorly-understood anxiety correlates (Kolosov, Aurini, Williams, Cooke, & Goodchild, 2011; Schmidtko, Löttsch, Freynhagen, & Geisslinger, 2010; Scott, Wright, & Angus, 2002). The GABA analogue drugs Gabapentin and Pregabalin have seen increasing off-label use to treat anxiety disorders. Typically used to treat seizures and nerve pain, Gabapentin and Pregabalin target the $\alpha_2\delta$ subunit, indirectly modulating Ca_v2.2 (Sills, 2006). By modulating Ca_v2.2, the side effects associated with GABA modulation (i.e. benzodiazepines) can be bypassed. It is important to state that these drugs are not approved as a primary treatment for anxiety disorders. However, the increasing and successful use of Ca_v2.2 modulators in treating anxiety disorders

prompts research into their functional role in anxiety-related neuronal circuits (Lee, 2013; Lotarski et al., 2011).

Ca_v2.2 channels are modulated by a variety of GPCRs. One form of modulation is voltage-dependent inhibition facilitated by the binding of the G beta-gamma complex (G_{βγ}) to the pore-forming subunit of Ca_v2.2 channels (Ikeda, 1996). Two inhibitory mechanisms can occur as a result. In one mechanism, G_{βγ} induces a shift in the voltage-dependent activation properties of Ca_v2.2 channels, which then require larger-than-normal depolarizations to open (Zamponi & Currie, 2013). Alternatively, GPCRs can inactivate Ca_v2.2 through a ‘hinged lid’ mechanism, closing the ion channel-forming subunit, α₁ (Stotz, 2001). In either mechanism, calcium entry through Ca_v2.2 is limited or blocked, and subsequent neurotransmitter release from presynaptic terminals is inhibited. There are a wide variety of GPCRs that exhibit inhibitory effects on Cav_s, but a specific family has been shown to extensively couple with Ca_v2.2 in anxiety-related brain areas. Cannabinoid receptors, part of the endocannabinoid system, are a specific family of primarily G_{oi} GPCRs heavily implicated in anxiety (Haller, Bakos, Szirmay, Ledent, & Freund, 2002).

The Endocannabinoid System and Anxiety

The endocannabinoid (eCB) system is a network of primarily G_{oi} GPCRs and ligands known to modulate synaptic transmission throughout the brain. Of the two cannabinoid receptor types (CB₁ and CB₂), CB₁ is the major synaptic constituent of the eCB system, heavily expressed in CCK+INs (Lutz, Marsicano, Maldonado, & Hillard, 2015). CB₁ is activated by endogenous cannabinoid molecules like anandamide (AEA) and 2-arachidonoylglycerol (2-AG), as well as exogenous cannabinoids like THC (Pagotto, Marsicano, Cota, Lutz, & Pasquali, 2006).

Cannabinoids act as retrograde feedback inhibition messengers; postsynaptic cells synthesize 2-AG/AEA, which bind to CB₁ receptors on the presynaptic terminal, suppressing neurotransmitter release (Figure 8). CB₁-mediated inhibition occurs in two general forms; phasic and tonic. Phasic inhibition occurs as a result of postsynaptic depolarization, thus is generated in response to specific postsynaptic signals. Tonic inhibition is the result of basal CB₁ activity, and occurs

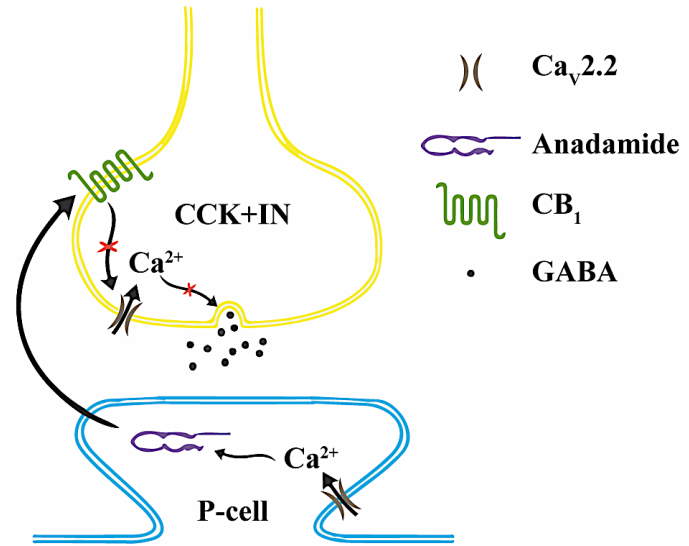


Figure 8 | eCB-mediated feedback inhibition system in CA3. Calcium (Ca²⁺) entry through Cav_v2.2 in the postsynaptic P-cell induces anandamide synthesis. Anandamide binds to cannabinoid receptor 1 (CB₁) on the presynaptic cholecystokinin interneuron (CCK+IN) terminal. Ca²⁺ entry through Cav_v2.2 is then inhibited, preventing GABA release. Adapted from Sharkey & Pittman, 2005.

irrespective of postsynaptic signals (Lee et al., 2015; Soltesz et al., 2015). Mechanistically, CB₁ modulates neurotransmitter release by coupling to and downregulating Cav_s (Wilson, Kunos, & Nicoll, 2001). By inhibiting calcium entry through Cav_s, processes like vesicular fusion are prevented (Catterall, 2011). In the CA3 region of the vHPC, CB₁ was shown to specifically couple to Cav_v2.2, but it is not known if this coupling is conserved in the BLA.

The eCB system has been shown to differentially modulate synaptic transmission across different brain regions, cell types, and synapses. Heavy integration of the eCB system has been observed in the HPC, PFC, and amygdala, where it is thought to have modulatory effects on fear and anxiety processing (Lutz et al., 2015). At GABAergic synapses, eCB-mediated inhibition is known as depolarization-induced suppression of inhibition (DSI), and in glutamatergic synapses, it is known as depolarization-induced suppression of excitation (DSE) (Ramikie & Patel, 2012).

DSI and DSE are short-term effects, as eCB-mediated synaptic modulation follows a negative-feedback loop. Neurons containing CB₁ are classified into two groups; high CB₁-expressing cells, which are sparsely distributed in the BLA and cortical areas, and low CB₁-expressing cells, which are more evenly dispersed (Marsicano & Lutz, 1999; Yoshida et al., 2011). Research on cell-specific CB₁ expression has revealed high selectivity for CCK+INs over other INs. In the BLA, 95% of high CB₁-expressing cells and 90% of low CB₁-expressing cells were CCK+INs (Marsicano & Lutz, 1999). Contrarily, CB₁ expression is largely absent from PV+INs. In addition to CCK+IN selectivity, CB₁ has been shown to couple with Cav2.2. In rat sympathetic neurons, N-type calcium currents were inhibited by CB₁ agonists, inhibition which was then reversed by CB₁ antagonists (Guo & Ikeda, 2004). Furthermore, CB₁-Cav2.2 coupling appears to be prevalent in CCK+INs. In the CA3 region of the vHPC, Cav2.2-dependent GABA release from CCK+IN terminals was shown to be inhibited with CB₁ agonists (Szabo et al., 2014).

It is widely accepted that there is a strong correlation between the eCB system and anxiety, but this correlation is not fully understood (Lutz et al., 2015). eCB system modulation shows potential for treating anxiety disorders, a well-known example of which being the anxiolytic properties of THC (Onaivi, Green, & Martin, 1990). In both humans and rodents, it has been shown that cannabinoids can influence anxiety-like symptoms in a biphasic manner; low doses produce anxiolytic effects while high doses produce anxiogenic effects (Moreira, Grieb, & Lutz, 2009; Rey, Purrio, Viveros, & Lutz, 2012). Research suggests that CB₁ modulation has opposite effects on anxiety-like behavioral output in glutamatergic and GABAergic cells. Knockout mice lacking CB₁ in all glutamatergic cells show increased anxiety-like behaviors, while knockout mice lacking CB₁ in all GABAergic cells show reduced anxiety-like behaviors (Häring, Kaiser, Monory, & Lutz, 2011). CB₁-mediated anxiety effects are not confined to GABAergic and glutamatergic activity

however, and are different when isolating specific brain regions (Rovira-Esteban et al., 2017; Szabo et al., 2014). Accordingly, more detailed neurophysiological research must be conducted on the role of CB₁ in cell populations and brain regions implicated in anxiety.

Implications of CCK and CCK+INs in Anxiety

CCK and CCK+INs have well-established links to anxiety which originate from their role in neuronal circuits. CCK, the CCK receptor (CCK_B), and CCK+INs are highly expressed in the limbic system (Vanderhaeghen, Signeau, & Gepts, 1975). As a neuropeptide, CCK is found in vesicles and displays synaptic properties similar to classical neurotransmitters (Emson, Lee, & Rehfeld, 1980). CCK is associated with anxiety through its interactions with CCK_B. In healthy patients, CCK administration induces panic attacks (Montigny, 1989) while CCK_B antagonists block these panicogenic effects (Bradwejn, Koszycki, Couetoux du Tertre, van Megen, & et al., 1994). In rodents, CCK agonists produce anxiety-like behaviors (Frankland, Josselyn, Bradwejn, Vaccarino, & Yeomans, 1996) while CCK_B antagonists attenuate them (Josselyn et al., 1995). Binding of CCK to CCK_B has been shown to modulate the neuronal properties of classical neurotransmitters (Altar & Boyar, 1989). Interactions exist between CCK and GABA, dopamine, and endocannabinoid neurotransmission (Altar & Boyar, 1989; Chhatwal et al., 2009; Lanza & Makovec, 2000). While these interactions remain relatively understudied, they represent potential underlying mechanisms by which CCK is linked to anxiety.

CCK+INs display a distinct regulatory role over anxiety-like behaviors. Along with PV+INs, CCK+INs establish GABAergic connections onto the soma of P-cells in several brain regions including the BLA, HPC, and PFC (Freund & Katona, 2007; Sparta et al., 2014). In the BLA, CCK+INs innervate up to eight hundred P-cells each (Vereczki et al., 2016), and are thought

to prevent anxiety-like responses from occurring in non-threatening situations (Freund, 2003; Mascagni & McDonald, 2003; Truitt et al., 2009). When CCK+INs in the BLA are lesioned, rats display increased anxiety-like behaviors (Truitt et al., 2009), a phenotype thought to be the result of lost GABAergic and CCKergic activity. Additionally, it has been proposed that by acting with the eCB system, CCK+INs modulate fear inhibition and extinction (Bowers, Choi, & Ressler, 2012). CCK+INs likely modulate fear extinction at the level of the BLA by inhibiting ‘extinction’ neurons (Duvarci & Pare, 2014). CCK+IN synapses are remodeled by fear extinction, displaying increased CB₁ expression and thus decreased inhibition of extinction neurons (Duvarci & Pare, 2014; Trouche et al., 2013). Given their expression of Cav2.2 and CB₁, role in perisomatic inhibition, as well as integration in limbic system structures, CCK+INs are essential targets for anxiety research.

Master’s Thesis Research

Research Motivations

We are motivated to determine the role of Cav2.2 in GABA release from CCK+INs onto P-cells in the BLA. It has been demonstrated in the CA3 region of the HPC that GABA release in CCK+IN/P-cell synapses is eliminated by blocking Cav2.2 (Szabo et al., 2014). If conserved, Cav2.2 may be a potential target for mediating anxiety at the level of the amygdala. Additionally, we are motivated to determine the role of CB₁ in CCK+IN/P-cell synapses in the BLA. Given findings which indicate CB₁ inhibits Cav2.2 and subsequently GABA release from CCK+INs onto P-cells in the HPC (Szabo et al., 2014), we are interested in examining this system in the BLA. CB₁ shows promise in the development of novel anxiety treatments, but a greater understanding of its role in anxiety-related circuits is needed. Research describing the role of the IL in fear

extinction and its connections to the BLA motivates us to determine if Cav2.2 regulates presynaptic transmitter release and intrinsic firing properties in this region of the mPFC. P-cells in the mPFC receive dendritic inhibition from INs in superficial layers and perisomatic inhibition from proximal BCs (Riga et al., 2014). However, little is known about the role of Cav2.2 in regulating GABA release in these inhibitory synapses.

Research Questions

Chapter 1: *Is GABA release in CCK+IN/P-cell synapses in the BLA Cav2.2-dependent?*

P-cells carry the bulk of information from the BLA to other brain areas implicated in anxiety. Previous research shows that excitation of P-cells in the BLA increases anxiety-like behaviors (Johansen et al., 2010). Local INs expressing the peptide cholecystokinin (CCK+INs) synapse onto the soma of P-cells, forming a system of perisomatic inhibition (Freund, 2003). Previous studies in the CA3 region of the HPC have shown that the GABA release from CCK+INs onto P-cells is dependent on Cav2.2 (Szabo et al., 2014). If this circuitry is conserved in the amygdala, Cav2.2 could be a potential pharmacological target for regulating anxiety at the level of the BLA.

Chapter 2: *What is the role of CB₁ in CCK+IN/P-cell synapses in the BLA? Does CB₁ exhibit tonic and/or phasic inhibition of GABA release?* The eCB system and anxiety-like behavior are strongly correlated (Lutz et al., 2015). Similarly, P-cell excitability in the BLA is correlated with anxiety-like behavior (Davis, Rainnie, & Cassell, 1994). CB₁ has been shown to inhibit neurotransmitter release in both glutamatergic and GABAergic synapses (Azad, 2003) in both ligand dependent (tonic) and independent (phasic) manners (Farrant & Nusser, 2005; Neu et al., 2007; Roberto et al., 2010). When GABA release is suppressed, P-cells are disinhibited and more excitable. In the hippocampus, CB₁ is present in and regulates transmitter release in CCK+IN/P-

cell synapses (Yoshida et al., 2011). We are interested if this circuitry is conserved in the amygdala, and by what means (phasic and/or tonic) CB₁ mediates GABA release from CCK+INs onto P-cells in the BLA.

Chapter 3: *Is transmitter release in IN/P-cell synapses in the IL Cav2.2-dependent? Is GABA release in CCK+IN/P-cell synapses in the IL Cav2.2-dependent? Are intrinsic firing properties of P-cells in the IL regulated by Cav2.2?* Calcium channel physiology is relatively understudied in the infralimbic area of the mPFC. Our initial goal is to determine if, and to what degree, Cav2.2 is present in presynaptic IN inputs onto P-cells in the IL. Upon determining the role of Cav2.2 in IN terminals, we will specifically target Cav2.2 in CCK+INs. Comparisons can be drawn about the properties of this IL circuit to those in the BLA and HPC. We are also interested in determining if Cav2.2 modulates the intrinsic firing properties of P-cells in the IL. Cav2.2 makes a significant contribution to intrinsic firing properties of P-cells in the cerebellum (Alviña & Khodakhah, 2008), and couples to calcium-activated potassium channels in the HPC to modulate the after-hyperpolarization phase of action potentials (Loane et al., 2007).

Summary of Findings

Chapter 1: I present fluorescence images depicting CCK+IN expression in the BLA as well as electrophysiological data on the role of Cav2.2 in CCK+IN/P-cell synapses. Cells were exposed to a Cav2.2 antagonist (ω -Conotoxin GIVA), following which IPSC peak amplitude decreased by an average of 51%. Results demonstrate that the release of GABA in CCK+IN/P-cell synapses in the BLA is partially Cav2.2-dependent.

Chapter 2: I present immunofluorescence images depicting CCK+IN and CB₁ expression in the BLA and HPC, quantifying the level colocalization in each area. Second, I present

electrophysiology data on the sensitivity of GABA release in CCK+IN/P-cell synapses to phasic and tonic inhibition. A total of two cells were exposed to a CB₁ agonist (2-AG) and antagonist (AM251). IPSC peak amplitude decreased by 26% following exposure to 2-AG and increased 34% following exposure to AM251. Results can be used to confirm the findings of Rovira-Esteban and colleagues (2017), who describe tonic and phasic CB₁-mediated inhibition of transmitter release in CCK+IN/P-cell synapses in the BLA.

Chapter 3: I present electrophysiological data on the role of Cav2.2 in regulating GABA release from general INs, GABA release from specifically CCK+INs, and in P-cell intrinsic firing properties in the IL. Following exposure to ω -Conotoxin GIVA, IPSC peak amplitude in IN/P-cell synapses decreased an average of 46% across six cellular recordings. In CCK+IN/P-cell synapses, IPSC peak amplitude decreased an average of 9% over eight cellular recordings in response to ω -Conotoxin GIVA. Additionally, ω -Conotoxin GIVA did not significantly affect the firing pattern and spike frequency of P-cells. These results can be used to demonstrate that 1) GABA release from INs in the IL is partially Cav2.2-dependent, 2) GABA release from CCK+INs in the IL is not significantly Cav2.2-dependent, and 3) P-cell firing properties are not significantly modulated by Cav2.2 in the IL.

CHAPTER 1: CA_v2.2-MEDIATED GABA RELEASE FROM CCK+ INTERNEURONS ONTO PYRAMIDAL CELLS IN THE BASOLATERAL AMYGDALA

Abstract

The basolateral nucleus of the amygdala (BLA) is an interconnected limbic system structure implicated in anxiety. Normal function of the BLA relies on a balance between excitatory and inhibitory signaling, which is known to be disrupted in anxiety disorders like post-traumatic stress. Excitatory activity in the BLA is facilitated by glutamatergic pyramidal cells (P-cells), which when directly stimulated produce anxiety-like behavior. P-cells are regulated by inhibitory signaling from local interneurons (INs) including those that contain the neuropeptide cholecystokinin (CCK+). It has been demonstrated that CCK+INs regulate anxiety-like behavior at the level of the BLA, likely due to their inhibitory control over local neuronal circuits. The release of inhibitory neurotransmitter (GABA) from CCK+INs is regulated by voltage-gated calcium channels (Cav_s), of which there are multiple subtypes. In the hippocampus, GABA release from CCK+INs is entirely dependent on the N-type calcium channel (Cav_v2.2). It is not known if this role of Cav_v2.2 is conserved in the BLA, representing a potential target by which inhibition of anxiety-related output from the BLA is regulated. In this study, we determined the role of Cav_v2.2 in GABA release in CCK+IN/P-cell synapses in the BLA. To visualize the neuroanatomy of CCK+INs, a triple transgenic mouse model (*CCK-Dlx5/6-tdT*) was generated which labelled CCK+INs with red fluoresce (via the tdTomato fluorophore). To evoke GABA release from CCK+INs, a second triple transgenic mouse model (*CCK-Dlx5/6-ReaChR*) was generated in which CCK+INs express red-activatable channelrhodopsins. Following optogenetic stimulation, inhibitory postsynaptic currents (IPSCs) were recorded in P-cells. The sensitivity of GABA release to Cav_v2.2 block was determined through bath addition of ω -Conotoxin GIVA (CTX). Following Cav_v2.2 block, average IPSC peak amplitude decreased by 51% (n = 7 cells, SD = 14%, SEM = 5%) compared to control conditions, which was determined to be statistically significant (p = 0.0046, one-tailed paired t-Test). Our results indicate that GABA release from CCK+INs in the BLA is partially Cav_v2.2-dependent, contrasting total Cav_v2.2-dependency reported in the hippocampus. We propose that CCK+IN/P-cell synapses are differentially regulated by Cav_v2.2 in the BLA and hippocampus. As a result, Cav_v2.2 modulation likely has region-specific implications in anxiety.

Introduction

Fear is the result of an immediate, recognizable threat while anxiety is the result of perceived, imprecise threats (Steimer, 2002). Both fear and anxiety produce emotional, physiological, and behavioral changes intended for survival and are products of similar neurological activity. Anxiety can become dysfunctional however, occurring in inappropriate situations and causing disruptions to normal stimulus processing. This can manifest as anxiety

disorders in humans and anxiety-like behaviors in animal models. Common in both stations is abnormal activity in brain regions like the amygdala (Ritu et al., 2013). The amygdala is a critical brain region for fear-related learning and memory as well as anxiety-related behavioral output (Phelps et al., 2004; Roozendaal, McEwen, & Chattarji, 2009). Proper function of the amygdala requires balance between excitatory and inhibitory signaling. This balance is known to be disrupted by chronic anxiety and is observable in anxiety disorders like post-traumatic stress (PTSD) (Milad et al., 2009). The molecular components which regulate the balance between excitatory and inhibitory activity in the amygdala are not fully understood but serve as vital targets for anxiety research.

The amygdala is composed of multiple nuclei with diverse functions and connections. The central amygdala (CeA), composed of the lateral nucleus (CeL) and medial nucleus (CeM), is considered an inhibitory mediator of the basolateral amygdala (BLA) (Capogna, 2014; Janak & Tye, 2015). The BLA, composed of the lateral nucleus (LA) and basal nucleus (BA), is considered the main source of excitatory neuronal output from the amygdala to brain regions involved in anxiety like the hippocampus (HPC) and prefrontal cortex (PFC) (Gale, 2004). The CeA is predominantly composed of GABAergic cells, containing both local and projection interneurons (INs). The cytoarchitecture of the BLA is similar to that of the PFC, as a majority (approximately 80%) of neurons are glutamatergic pyramidal cells (P-cells) while a minority (approximately 20%) are GABAergic INs (Spampanato, Polepalli, & Sah, 2011). It is within the connections established between these two cell types that neuronal output is modulated.

P-cells are known for their distinct piriform morphology, lengthy apical dendrites, and far-reaching axonal projections. Within the BLA and PFC, P-cells display similar intrinsic properties including regular spiking, non-adapting firing patterns and moderate spike frequency (Rainnie et

al., 1993). P-cells are targeted by several IN types (Freund, 2003); those which synapse onto the body of P-cells (soma) are termed basket cells (BCs) (Armstrong & Soltesz, 2012). BCs have a round morphology and branching dendrites that are involved in perisomatic inhibition in brain regions like the BLA, PFC, and HPC (Ferreira et al., 2015; Neu et al., 2007; Veres et al., 2017). Perisomatic inhibition is a form of feedback inhibition wherein P-cell activation stimulates the release of GABA from presynaptic BC terminals onto the P-cell body, suppressing excitatory activity (Freund & Katona, 2007). Subtypes of BCs, distinguishable by their firing patterns and neurochemical markers, differentially regulate P-cells through unique synaptic properties (Duvarci & Pare, 2014). Of particular interest to anxiety research are cholecystokinin-containing (CCK+) BCs.

CCK is a neuropeptide with profound anxiogenic and panicogenic properties (Montigny, 1989; Frankland et al., 1996; Rotzinger & Vaccarino, 2003). CCK+INs have been shown to regulate anxiety-like behavior at the level of the BLA, likely due to their role in neuronal circuits (Truitt et al., 2009). In the HPC and PFC, it has been demonstrated that CCK+BCs regulate the activity of P-cells through perisomatic inhibition (Freund & Katona, 2007; Whissell et al., 2015), however less functional data is available on their connectivity within the BLA (Duvarci & Pare, 2014). It has been suggested that CCK+BCs in the BLA are analogous with cortical CCK+BCs, as both have relatively slow, adapting spiking patterns and are likely to respond to slow, asynchronous inputs (Bartos & Elgueta, 2012; Jasnow et al., 2009). However, there are multiple subtypes of CCK+INs across brain regions with different intrinsic properties (Jasnow et al., 2009). These differences are thought to be the result of specific ion channel variations (Jasnow et al., 2009).

In multiple brain regions, CCK+INs have been found to express N-type calcium channels (Cav2.2) (Freund & Katona, 2007; Katona et al., 2001; McDonald & Mascagni, 2001; Szabo et al.,

2014). Cav2.2 is a voltage-gated calcium channel (Cav) subtype critically involved in neurotransmitter release (Szabo et al., 2014). Located in the transmembrane domain, the ion channel-forming subunit of Cav2.2 (α_{1B}) opens in response to membrane depolarization (Loane et al., 2007; Williams et al., 1992). Subsequently, calcium ions enter the neuron and interact with the SNARE protein complex to facilitate synaptic vesicle fusion and neurotransmitter exocytosis (Südhof, 2012). Functional studies have revealed that in the HPC, GABA release from CCK+IN is entirely dependent upon Cav2.2. However, the role of Cav2.2 role in regulating neurotransmitter release from CCK+INs has not been functionally described in the BLA.

Currently, Cav2.2 is a target for treating neuropathic pain (Scott et al., 2002), but shows promise as a novel target for anxiety disorders (Newton & Messing, 2009). It has been proposed that the anxiolytic effects of Gabapentin (Lotarski et al., 2011) may be due to $\alpha_2\delta$ -dependent effects on Cav2.2 channels (Cassidy, Ferron, Kadurin, Pratt, & Dolphin, 2014; Zamponi, 2016), wherein neurotransmitter release is suppressed and excitatory synapses are downregulated throughout the brain (Eroglu et al., 2009). Cav2.2 antagonists have been found to be anxiogenic; administration of Zinconotide (Prialt) can produce anxiety and panic attacks (McCleskey et al., 1987; Scott et al., 2002). While it has been shown Cav2.2 is implicated in anxiety-related neurotransmission, the underlying molecular mechanics are poorly understood and deserve further investigation. Here, I propose a comprehensive study combining transgenic mouse models, fluorescence microscopy, brain slice electrophysiology, and pharmacology to test the hypothesis that GABA release in CCK+IN/P-cell synapses in the BLA is Cav2.2-dependent.

Methods

Animal Models

All procedures were approved by the Institutional Animal Care and Use Committee at the University of New Hampshire (**APPENDIX**). To visualize the neuroanatomy of CCK+INs in the amygdala, we performed intersectional labeling using two molecular markers: CCK and Dlx5/6. CCK is expressed in both GABAergic and glutamatergic neurons, whereas Dlx5/6 is only expressed in GABAergic INs. We obtained a triple transgenic mouse line via the breeding schematic in **Figure 9A**. Initially, *Cck-IRES-Cre* mice (012706; The Jackson Laboratory) were crossed with *Dlx5/6-Flpe* mice (010815; The Jackson Laboratory). Cre and Flpe are recombinases expressed under the control of the CCK promoter and the Dlx5/6 promoter, respectively. Progeny from this initial cross, *Cck-IRES-Cre; Dlx5/6-Flpe* (abbreviated *CCK-Dlx5/6*), were dual transgenic mice with both alleles. Because the Dlx5/6 mutation could not be bred to homozygosity, we selected for *CCK-Dlx5/6* mice that were homozygous for CCK-Cre and heterozygous for Dlx5/6-Flpe. To optimize the recombination efficiency, male *CCK-Dlx5/6* mice were bred to female reporter mice (*Ai65(RCFL-tdT)-D*; 021875; The Jackson Laboratory) which contained the fluorescent protein tdTomato behind two recombinase target-flanked STOP cassettes. The first STOP cassette was flanked by loxP sites (recognized by Cre) and the second was flanked by FRT sites (recognized by Flpe). Progeny from this cross were triple-transgenic mice with the genotype *Cck-IRES-Cre; Dlx5/6-Flpe; Ai65(RCFL-tdT)-D* (abbreviated *CCK-Dlx5/6-tdT*). In these mice, Cre-Lox and Flpe-FRT recombination removed the two STOP cassettes, resulting in tdTomato fluorescence in tissues that expressed both CCK and Dlx5/6, i.e. GABAergic CCK+INs (abbreviated CCK+INs). Bright-red fluorescence is observable in the cell bodies and neuronal processes of CCK+INs throughout the BLA (**Figure 10B**).

CCK is contained in glutamatergic cells in addition to GABAergic INs (Ma, Dankulich-Nagrudny, & Lowe, 2013). This was evidenced when we bred dual-transgenic mice in which all

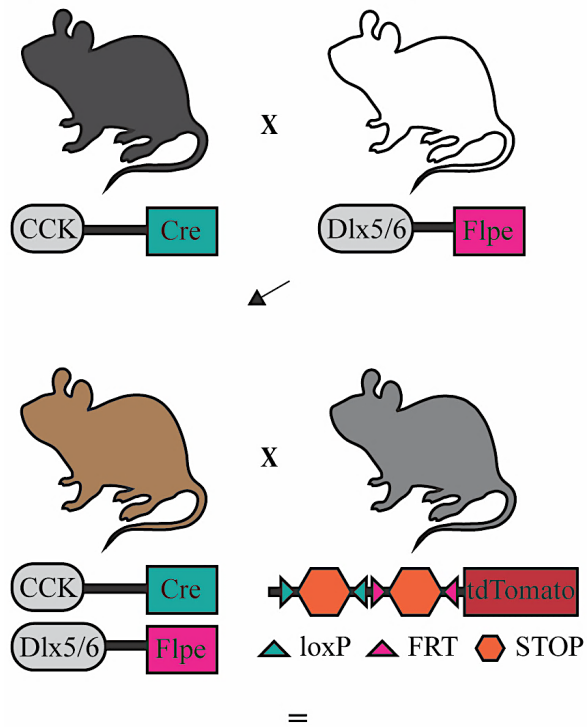
CCK+ cells/tissue were labeled. *Cck-IRES-Cre* mice were crossed with a Cre reporter mouse line (007914; The Jackson Laboratory) which contain the fluorescent protein tdTomato behind a single loxP-flanked STOP cassette (*Ail4(RCL-tdT)-D*). The resultant progeny, *Cck-IRES-Cre; Ail4(RCL-tdT)-D* (abbreviated *CCK-tdT*), show widespread, non-specific fluorescence in both glutamatergic and GABAergic CCK+ cells/tissue in the BLA (**Figure 10A**).

To perform electrophysiological studies of CCK+IN/P-cell synapses, we used optogenetics. Optogenetics allow for the precise study of specific cell populations related to anxiety-like behavior (Tye & Deisseroth, 2012). The specific optogenetic tool we used was derived from channelrhodopsin (ChR), a cation-permeable channel that opens in response to a specific wavelength of light to cause membrane depolarization, action potentials, and neurotransmitter release (Britt, McDevitt, & Bonci, 2012; Lin, Knutsen, Muller, Kleinfeld, & Tsien, 2013). By embedding light-activatable cation channels in GABAergic CCK+ cells/tissue, we are able to selectively activate presynaptic GABA release from CCK+IN terminals. To accomplish this, we bred a second triple transgenic mouse line.

CCK-Dlx5/6 mice were bred to a mouse strain that contains an allele that codes for red-activatable channelrhodopsin (ReaChR) (**Figure 9B**). This mouse strain (*R26 LSL FSF ReaChR-mCitrine*; 024846; The Jackson Laboratory) contained ReaChR and two STOP cassettes (loxP- and FRT-flanked). mCitrine, a yellow-fluorescent protein, was bound to the C-terminus of ReaChR, allowing for mapping of ReaChR expression. Progeny from this cross are triple-transgenic mice with the genotype *Cck-IRES-Cre; Dlx5/6-Flpe; R26 LSL FSF ReaChR-mCitrine* (abbreviated *CCK-Dlx5/6-ReaChR*). In these mice, Cre-loxP and Flpe-FRT recombination removed the two STOP cassettes, resulting in the expression of ReaChR in CCK+INs. This strategy allowed for stimulation of only GABAergic CCK+INs. To visualize channelrhodopsin expression both

glutamatergic and GABAergic CCK⁺ cells, *Cck-IRES-Cre* mice were crossed with mice that expressed a loxP-flanked STOP cassette and fluorescence-tagged (EYFP, yellow) Channelrhodopsin 2 (ChR2) cation channels (*Ai32(RCL-ChR2(H134R)/EYFP*); 024109; The Jackson Laboratory). Progeny from this cross were *Cck-IRES-Cre; Ai32(RCL-ChR2(H134R)/EYFP*) mice (abbreviated *CCK-ChR2*) which displayed widespread EYFP fluorescence in the transmembrane domain of CCK⁺ cells/tissue.

A) CCK-Dlx5/6-tdTomato Breeding Scheme



B) CCK-Dlx5/6-ReaChR Breeding Scheme

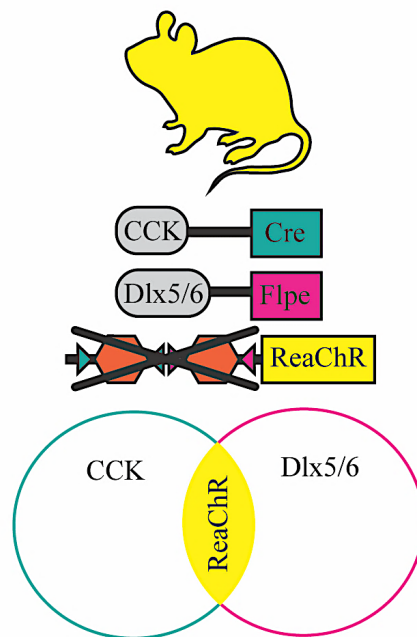
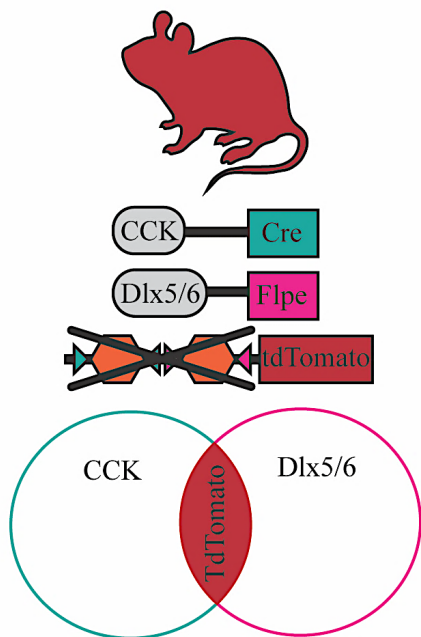
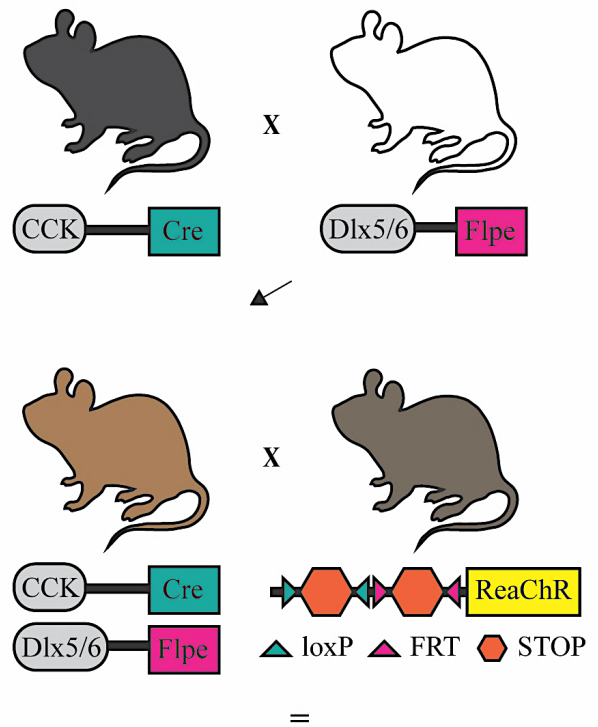


Figure 9 | Breeding schematics for triple-transgenic mouse models. Genotypes are depicted under each mouse; oval, promoter/marker; rectangle, recombinase; triangle, recombinase target; hexagon, STOP cassette. **A)** CCK-Dlx5/6-tdTomato breeding scheme. Top: Initial mating between Cck-IRES-Cre (black) and Dlx5/6-Flpe (white) mouse lines gave rise to CCK-Dlx5/6 progeny (brown). Middle: Second mating of CCK-Dlx5/6 mouse to Ai65(RCFL-tdT)-D mouse (grey) gave rise to CCK-Dlx5/6-tdT progeny (red). Combined action of Cre-loxP and Flpe-FRT recombination removed both STOP cassettes. Bottom: tdTomato is expressed in GABAergic CCK+ cells, represented in an intersectional breeding diagram. **B)**

CCK-Dlx5/6-ReaChR breeding scheme. Top: Initial cross between Cck-IRES-Cre (black) and Dlx5/6-Flpe (white) mice produced CCK-Dlx5/6 offspring (brown). Middle: Second cross between CCK-Dlx5/6 and R26 LSL FSF ReaChR-mCitrine mice (ash) produced CCK-Dlx5/6-ReaChR progeny (yellow). Cre-loxP and Flpe-FRT recombination removed both STOP cassettes. Bottom: Red-activatable channelrhodopsin (ReaChR) was expressed in CCK+ GABAergic cells, represented in an intersectional breeding diagram.

Genotyping

To confirm the presence of alleles in a given mouse, we performed genotyping using tail biopsy. Tail biopsy was performed in P7-P9 pups. Genomic DNA was extracted using the Phire Animal Tissue Direct PCT kit (F140WH; ThermoFisher) according to manufacturer instructions. PCR was then performed with AmpliTaq Gold 360 (4398813; ThermoFisher) under the following conditions: a hot-start of 95°C for 10 min, followed by 35 cycles of 95°C for 30 sec, 60°C for 30 sec, 72°C for 1 min, and a final step of 72°C for 7 min. Primer sequences and band size are located in **Table 1**.

Mouse Line	Primers	Expected Products
<i>Cck-IRES-Cre</i>	F-MT: 5'-TGGTTTGTCCAAACTCATCAA F-WT: 5'-GGGAGGCAGATAGGATCACA R-CM: 5'-GAGGGGTCGTATGTGTGGTT	Hom: 215 bp Het: 215 and 468 bp WT: 468 bp
<i>Dlx5/6-Flpe</i>	F-TG: 5'- CAGAATTGATCCTGGGGAGCTACG R-TG: 5'- CCAGGACCTTAGGTGGTGTTTTAC F-IC: 5'-CAAATGTTGCTTGTCTGGTG R-IC: 5'-GTCAGTCGAGTGCACAGTTT	TG: 406 bp IC: 200 bp *PCR does not differentiate Hom and Het mice
<i>Ai65(RCFL-tdT)-D</i> and <i>Ai14(RCL-tdT)-D</i>	F-MT: 5'-CTGTTCTGTACGGCATGG R-MT: 5'-GGCATTAAAGCAGCGTATCC F-WT: 5'-AAGGGAGCTGCAGTGGAGTA R-WT: 5'-CCGAAAATCTGTGGGAAGTC	Hom: 196 Het: 196 and 297 WT: 297
<i>R26 LSL FSF</i> <i>ReaChR-mCitrine</i>	R-MT: 5'-CGGGCCATTTACCGTAAGTTAT F-IC: 5'-AAGGGAGCTGCAGTGGAGTA R-WT: 5'-CCGAAAATCTGTGGGAAGTC	Hom: 284 bp Het: 284 bp and 297 bp WT: 297 bp
<i>Ai32(RCL- ChR2(H134R)/EYFP)</i>	F-WT: 5'-AAGGGAGCTGCAGTGGAGTA R-WT: 5'-CCGAAAATCTGTGGGAAGTC F-MT: 5'-ACATGGTCTGTGGAGTTC R-MT: 5'-GGCATTAAAGCAGCGTATCC	Hom: 253 bp Het: 253 bp and 297 bp WT: 297 bp

Table 1 | Primer sequences and band sizes for mouse genotyping. Information on the primer sequences and expected PCR products for each mouse line used. F, forward primer sequence; R, reverse primer

sequence; MT, mutant; WT, wild-type; CM, common; Hom, homozygous; Het, heterozygous; TG, transgene; IC, internal control.

Fluorescence Stainings

Adult *CCK-tdT* and *CCK-Dlx5/6-tdT* mice ($30 \leq P < 120$) were deeply anesthetized with isoflurane (07-893-1389; Patterson Veterinary). Proper levels of anesthesia were confirmed through the absence of a rear-foot reflex. Intraperitoneal injections (0.05 mL for females and 0.07 mL for males) of Euthasol euthanasia solution (710101; Virbac Co.) were delivered to the lower-right abdomen with a 26-gauge needle. Cardiac perfusions were performed using formalin solution (HT501128; Sigma-Aldrich) to attain brain fixation. Brains were rapidly dissected and stored at 4°C in formalin solution for 24-72 hours for further fixation. 100 µm coronal brain slices were prepared using a vibratome (VT1000 S; Leica) and transferred to a 12-well plate (Greiner Bio-One). Slices were washed for ten minutes three times in PBT (0.2% Triton X (T8787; Sigma-Aldrich) in PBS (P3813; Sigma-Aldrich)) on an orbital rocker (SK-O180-S; Scilogex). To stain nucleic acids and identify cell bodies, slices were incubated for one hour at room temperature in a 1:10000 dilution of SYTO-13 in PBT. SYTO-13 is a green fluorescent nucleic acid stain (S7575; ThermoFisher). Following incubation, slices were washed twice in PBT and once in PBS before mounting onto micro slides (48311-703; VWR) with Vectashield medium (H-1400; Vector Laboratories) and micro cover glass (48393-221; VWR). Slides were stored at 4°C for a minimum of 24 hours before confocal imaging.

Fluorescence stainings for *CCK-Dlx5/6-ReaChR* mice followed the protocol described above, with a modification to the incubation step. *CCK-Dlx5/6-ReaChR* mice express the fluorophore mCitrine rather than tdTomato. mCitrine and SYTO-13 have partially overlapping emission spectra, so TO-PRO-3, another nucleic acid stain (T3605; Thermo-Fischer), was used

instead (1:4000 dilution). Fluorescence studies in *CCK-ChR2* mice examined the native EYFP fluorophore, so sections were not incubated in a nucleic acid stain. Brains were sliced, washed, and mounted in the same manner as described above.

Confocal Microscopy

Following fluorescence stainings, brain slices were imaged on one of two confocal systems. *CCK-Dlx5/6-ReaChR* sections were imaged on a Leica SP8 confocal using HyVolution super-resolution imaging (Huygens Software). *CCK-tdT*, *CCK-Dlx5/6-tdT*, and *CCK-ChR2* slices were imaged on a Zeiss LSM 510 Meta using accompanying LSM imaging software. A combination of argon and helium-neon lasers were used to excite fluorophores at 488 nm, 514 nm, 543 nm, and 633 nm. For brain slices with multiple fluorescent proteins, multi-track acquisition was implemented to avoid excitation cross-talk. A series of band- and long-pass filters were applied to isolate emission peaks from individual fluorophores and prevent emission cross-talk. Fluorophores and their spectra were as follows (excitation/emission (nm)): SYTO-13 (488/509), EYFP (513/529), mCitrine (514/529), tdTomato (554/581), and TO-PRO-3 (642/661). Images were set to either a 1024 x 1024 or 2048 x 2048 frame size. A left-to-right scan with line averaging was used, each line being scanned eight times. The camera pinhole was kept at 1 airy unit across all imaging. The Zeiss range indication tool was used to adjust the amplifier offset and detector gain, preventing over/under saturation of signals. A combination of tile-scans, z-scans, and single-plane images of the BLA were taken at 5x, 10x, 20x, 40x, and 63x. Our primary objectives were to confirm the specificity to which our triple transgenic mouse models labelled CCK+INs and identify the neuroanatomy of CCK+INs in the BLA.

In Vitro Brain Slice Preparation

No less than three adult male and three adult female *CCK-Dlx5/6-ReaChR* mice were deeply anaesthetized with isoflurane and decapitated. Brains were rapidly removed from the skull and placed into chilled and oxygenated artificial cerebral spinal fluid ('cutting' aCSF) containing (in mM): NaCl (130), KCl (3.5), KH₂PO₄ (1.1), MgCl₂ (6), CaCl₂ (1), dextrose (10), kynurenic acid (2), NaHCO₃ (30), ascorbate (.4), thiourea (.8), and sodium pyruvate (2) at pH 7.35 and 310 mOsm. 300 µm coronal slices containing the amygdala were prepared after mounting the brain in a vibratome. A scalpel was used to cut the corpus callosum and obtain hemi-coronal sections. Slices were transferred from the vibratome to a brain slice chamber (BSKH; Digitimer) containing oxygenated cutting aCSF and kept at 37°C for 15 minutes before transferring to a second slice chamber containing oxygenated room temperature 'regular' aCSF. Regular aCSF was composed of (in mM) NaCl (130), KCl (3.5), KH₂PO₄ (1.1), MgCl₂ (1.3), CaCl₂ (2.5), dextrose (10), NaHCO₃ (30), ascorbate (.4), thiourea (.8), and sodium pyruvate (2) at pH 7.35 and 300 mOsm. Slices were allowed to stabilize for one hour before transferring to the recording chamber where they remained for no more than two hours during patch-clamp recordings.

Electrophysiology

Our electrophysiology rig was housed on a nitrogen-fed workstation (Vision IsoStation; Newport). On the workstation was an upright microscope (BX51WI; Olympus) equipped with halogen (TH4-100; Olympus) and LED (Lumen 300; Prior Scientific) light sources. A CMOS microscopy camera (01-ROL-BOLT-M-12; QImaging) and 38mm c-mount (DC50NN; Qioptiq) were used in conjunction with capture software (Q-Capture Pro; QImaging) to perform differential interference contrast (DIC) microscopy. DIC microscopy was used to identify brain regions under

a 4x objective and P-cells under a 40x objective. The microscope was also equipped with an electrophysiology system consisting of a fixed-stage platform with manual x-y translator and a micromanipulator with a precision controller (1078-325-Y51; Sutter Instruments). Attached to the micromanipulator was a grounding electrode (E242; Warner Instruments) and headstage (CV-7B; Axon Instruments) connected to an amplifier (700B; Molecular Devices) and digitizer (1550A; Molecular Devices). Data from the digitizer was processed and recorded with the Axon pCLAMP 10 software suite (Molecular Devices).

Brain slices were held under the microscope in a rectangular slice chamber (RC-27LD; Warner Instruments) and anchored with a harp (64-0257; Warner Instruments). The slice chamber was housed in a magnetic platform (PM-7D; Warner Instruments) mounted to the microscope staging. Slices were kept healthy through a bath perfusion of 'regular' aCSF. aCSF was contained in a 60 mL syringe (BD Instruments) mounted above the microscope and oxygenated with 95 % O₂/CO₂. The perfusion was driven by a peristaltic pump (13-876; Fisher Scientific) which cycled regular aCSF from the 60 mL syringe to the slice chamber and back through laboratory-grade tubing (07407-71; Cole Palmer) and tubing connectors (64-1565; Warner Instruments). An IV flow regulator (ISGRF1001; Invacare Supply) was used to control the rate of the perfusion and a valve controller (VC-6; Warner Instruments) was used to start and stop aCSF flow.

For patch-clamp electrophysiology experiments, borosilicate glass micropipettes with tip resistances between 4-7 mOhms were prepared using a micropipette puller (P-1000; Sutter Instruments) and filled with intracellular solution. Recordings involving action potentials and/or cellular firing properties utilized a potassium-based internal solution consisting of (in mM): K-gluconate (140), HEPES (10), MgCl₂ (3), K-ATP (2), Na₂GTP (0.4), and phosphocreatine (5) at pH 7.4 and 290 mOsm. Recordings involving inhibitory postsynaptic currents (IPSCs) utilized a

cesium-based intracellular solution consisting of (in mM): Cs-gluconate (140), HEPES (10), MgCl₂ (3), K-ATP (2), Na₂GTP (0.4), and phosphocreatine (5) at pH 7.4 and 290 mOsm.

Whole-cell patches were performed on P-cells in the BLA. P-cells were identified by their morphology and intrinsic firing properties (**Figure 12A**). P-cells characteristically display ‘non-adapting’ firing patterns at a moderate frequency while CCK+INs display ‘adapting’ firing patterns at a much slower frequency (Freund & Katona, 2007; Rainnie et al., 1993). To evoke and characterize firing patterns, suspected P-cells were patched using the current-clamp technique and a supra-threshold square-pulse current was injected for three seconds as to elicit an action potential spike train. For IPSC recordings, P-cells were patched and held at 0 mV using the voltage-clamp technique. LED flashes passed through a Texas Red filter, out of the 40x objective, and onto the slice, inducing IPSCs via optogenetic activation of ReaChR. As ReaChR expression is variable, LED intensity was adjusted for each cell to ensure baseline IPSCs had a peak amplitude large enough for pharmacologically-induced changes to be observed, but small enough to avoid exhausting or damaging tissue. IPSC protocols were programmed in pCLAMP 10 software and consisted of stimulation and recording components. A single stimulation (0.1 ms LED application) occurred 10 ms into a 1000 ms recording window, also called a trace or sweep. Patches in which sweeps displayed polysynaptic input (multiple peaks) were discarded. Sweeps began every 10 or 15 seconds depending on the individual P-cell’s ability to tolerate and recover from repeat stimulation and were continuously evoked for 45-60 minutes during pharmacology experiments.

To confirm our recordings were strictly due to GABAergic activity, we performed two control experiments. A variable holding-potential protocol was used to determine if IPSCs displayed reversal potential and driving force properties characteristic of chloride. By altering the voltage-clamp, IPSCs were recorded at different P-cell membrane potentials. In 10 mV increments,

IPSCs were evoked at holding potentials of 20 mV through -90 mV for a total of twelve sweeps. After examining reversal potential and driving force, we performed a pharmacological test to confirm that our postsynaptic currents were produced through GABA binding to the GABA_A receptor. P-cells were held at 0 mV and IPSCs were evoked for several minutes to establish a baseline peak amplitude. Bicuculline (BIC), a GABA_A antagonist, was then added by pipette to the 60 mL syringe of aCSF. IPSCs were continually evoked until IPSC peak amplitude was eliminated. After the recording session was finished, the 60 mL syringe, tubing, ground electrode, 40x objective, slice chamber, and harp were washed thoroughly with hydrogen peroxide and MilliQ water to avoid pre-exposing future tissue to residue from pharmacological agents. Following confirmation of GABAergic activity, we determined the sensitivity of IPSC peak amplitude to Ca_v2.2 block via ω -Conotoxin GVIA (CTX). In the same manner as with BIC, a baseline IPSC peak amplitude was established under control conditions. Afterwards, CTX was added to the bath perfusion and sweeps were continually evoked until no further changes in peak amplitude were observable. At this point, BIC was added to the bath perfusion to demonstrate that the brain slice was indeed being exposed to pharmacological agents.

Pharmacology

Drug dosing (working concentration) was determined by multiplying the EC₅₀/IC₅₀ of a given compound by twenty, ensuring full effects would be observable in-perfusion. Stock concentrations were made at 1000x working concentrations and stored at -20°C. BIC (ab120107; Abcam) and CGP (ab120167; Abcam), GABA_A and GABA_B antagonists, respectively, were added to the bath perfusion (100 μ M and 2 μ M, respectively) to confirm that IPSCs were due to GABA_A receptor activity. CTX (ab120215; Abcam), a specific Ca_v2.2 antagonist, was added to the bath

perfusion (1 μ M) to study the role Cav2.2 in GABA release from CCK+INs onto P-cells in the BLA. Of note, we later determined that 1 μ M CTX was a much higher dose than required. Equivalent effects were observable using 300 nM, and we used this dose in future experiments (**CHAPTERS 2/3**). Smaller lipophilic compounds took considerably less time to display full effects on peak amplitude compared to larger lipophobic compounds. BIC permeated the slice and blocked IPSCs typically within five minutes, whereas CTX typically took fifteen minutes.

Data Analysis

After electrophysiology experiments were recorded, IPSC data was analyzed in Clampfit software and plotted in Origin 6.1 (OriginLab). Sweeps were selected to represent the changes that occurred to IPSCs under various holding voltages and pharmacological conditions. For pharmacological studies, we used IPSC peak amplitude (in pA) as a quantitative measure of the amount of GABA released from CCK+INs onto P-cells. Peak amplitudes were calculated by subtracting baseline sweep current (pre-IPSC) from the maximum positive-going current of the sweep, which occurred just milliseconds after LED stimulation. The time at which each sweep began was converted into minutes, to create a timescale. For recordings in which sweeps occurred in 15 second intervals, sweep 1 = 0 min, sweep 2 = 0.25 min, sweep 3 = 0.5 min, etc. The peak amplitude and time values for each sweep were plotted in Origin 6.1. A time-course line plot was created from this data for each cellular recording (n = 7). IPSC peak amplitude (pA) was assigned to the y-axis and time (min) to the x-axis.

A two-point segment graph was created to compare mean IPSC peak amplitude under control and CTX conditions across multiple cells (**Figure 13 - bottom right**). Recordings from male and female *CCK-Dlx5/6-ReaChR* mice were pooled in this plot, as there was no significant

association between sex and CTX effects (see details in results). The mean control conditions IPSC peak amplitude was calculated by averaging peak amplitude values from sweeps prior to CTX addition to the bath perfusion. CTX-dependent effects were examined only after the point in the time-course plot at which peak amplitude no longer decreased, i.e. the ‘plateau’ phase. From this time point forward, peak amplitudes across sweeps were averaged to obtain the mean peak amplitude under CTX conditions. For within-animal analysis, a one-tailed paired t-Test was performed in Microsoft Excel 2016 to determine if there was a significance to the changes in peak amplitude when moving from control to CTX conditions. For cross-animal analysis, control and CTX condition peak amplitudes were averaged for the seven recordings and plotted as grey circles in the two-point segment plot. The standard deviation (SD) and standard error of the mean (SEM) were calculated for both conditions as both numerical values (in pA) and percentages. Vertical black bars attached to the gray average peak amplitude circles on the two-point segment plot represent the SEM (in pA).

Results

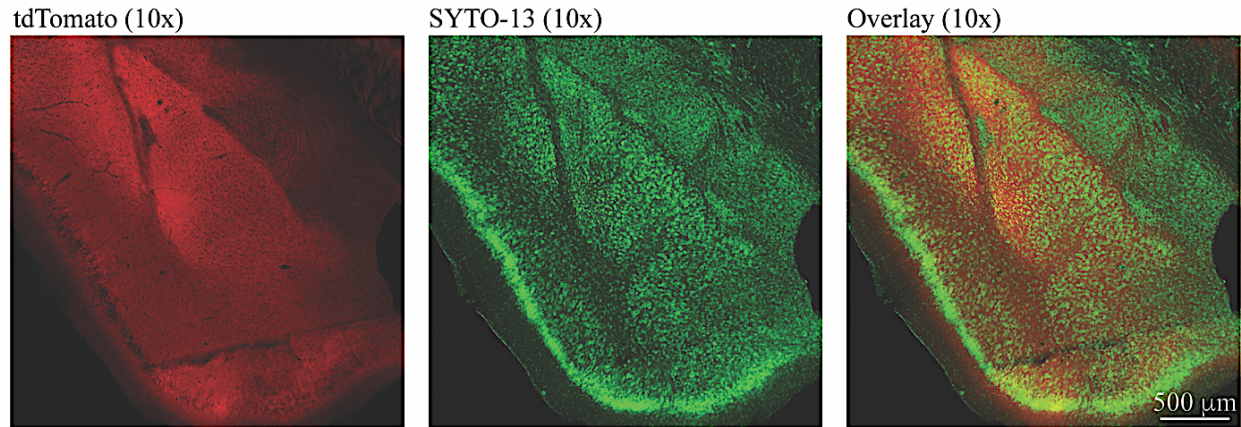
Histological Characterization in CCK-tdT and CCK-Dlx5/6-tdT Mice

Fluorescence experiments in *CCK-tdT* mice labelled CCK+ cell/tissues with tdTomato and cell bodies with SYTO-13 (**Figure 10A**). Confocal microscopy images display widespread CCK expression with notable regions of concentrated signal. CCK fluorescence is particularly intense in the BLA, layer 2 of the piriform area, the piriform-amygdalar area, and the endopiriform nucleus (**Figure 10A - left**). CCK expression is weak in the CeA and layer 1 of the piriform area. Like CCK, SYTO-13 signaling is also low in the thalamus and layer 1 of the piriform area, as well as the external capsule (**Figure 10A - middle**). Colocalization of CCK and SYTO-13 signal,

represented by yellow fluorescence, indicates a CCK+ cell (**Figure 10A - right**). Groups of CCK+ cells appear in the medial portion of the BLA, the LA, and the dorsal endopiriform nucleus.

Fluorescence experiments in *CCK-Dlx5/6-tdT* mice labelled CCK+INs with tdTomato and cell bodies with SYTO-13 (**Figure 10B**). Confocal images show that tdTomato expression is restricted to a fewer number of cells than in the *CCK-tdT* mouse. CCK+ signaling is constrained to GABAergic INs and their projections. Cell bodies strongly express tdTomato while expression in what appear to be neuronal projections is much milder and variable. Based on morphology, thicker projections (i.e. primary dendrites) can contain more CCK expression and higher levels of fluorescence than thinner projections (i.e. secondary/tertiary dendrites). Thin, faint networks of CCK+ projections can be seen in the center of the BLA. CCK+INs are mostly absent in the external and amygdalar capsules but are prevalent in the ventral/dorsal endopiriform nucleus and the BLA (**Figure 10B - left**). SYTO-13 signaling appears prevalent and uniform in the BLA, absent in the external/amygdalar capsules, and sparse in the ventral endopiriform nucleus (**Figure 10B - middle**). Since *CCK-Dlx5/6-tdT* mice possess the Dlx5/6 promoter, colocalization of CCK and SYTO-13 signal is indicative of GABAergic CCK+INs (**Figure 10B - right**). Compared to the *CCK-tdT* mouse (**Figure 10A - right**), there is very little colocalization signal in the *CCK-Dlx5/6-tdT* model. Colocalization distribution appears more uniform however, and the clustering of highly concentrated yellow signal in **Figure 10A - left** is not present. Web-like tdTomato signaling (**Figure 10B - left**) surrounds cell bodies (**Figure 10B - right**), a characteristic pattern of perisomatic inhibitory networks.

A| CCK Expression in the BLA (*CCK-tdT*)



B| GABAergic CCK Expression in the BLA (*CCK-Dlx5/6-tdT*)

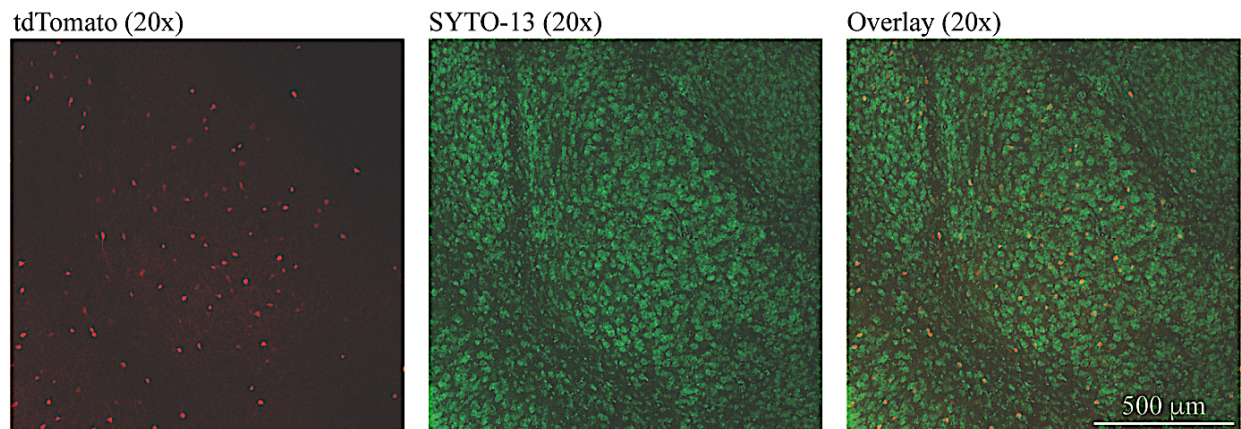


Figure 10| CCK expression in *CCK-tdT* mice and GABAergic CCK expression in *CCK-Dlx5/6-tdT* mice. **A|** Fluorescence images of coronal brain slices containing the BLA from an adult *CCK-tdT* mouse (10x magnification). Left: tdTomato (red) is expressed in all CCK+ cells/tissue. Middle: SYTO-13 nucleic acid stain (green) labels cell bodies. Right: In an overlay of the two channels, cell bodies that express CCK appear yellow due to colocalization of SYTO-13 and tdTomato signal. **B|** Fluorescence images of coronal brain slices containing the BLA from an adult *CCK-Dlx5/6-tdT* mouse (20x magnification). Left: Cells/tissue that contain both CCK+ and Dlx5/6 promoters express tdTomato. Middle: Cells bodies are stained with SYTO-13. Right: In an overlay of the two channels, CCK+INs appear yellow due to colocalization of tdTomato and SYTO-13 signal.

Characterization of Fluorescence in CCK-ChR2 and CCK-Dlx5/6-ReaChR Mice

CCK-ChR2 mice express EYFP-tagged ChR2 in CCK+ cells/tissue (**Figure 11A**). The BLA, CeA, and cortical tissue display weak EYFP signaling while the piriform area and the endopiriform nucleus display stronger signaling (**Figure 11A - left**). At 40x magnification, ChR2 expression is absent in what appear to be cell bodies and blood vessels (**Figure 11A - right**).

Overall fluorescence levels are moderate, but strong EYFP signaling in what morphologically appear to be neuronal projections can be distinguished from the background in the lower right-hand side of **Figure 11A - right**. Focusing on the small bulbous structures containing strong EYFP signal throughout the tissue, it looks as if ChR2 is expressed in CCK+ synaptic terminals.

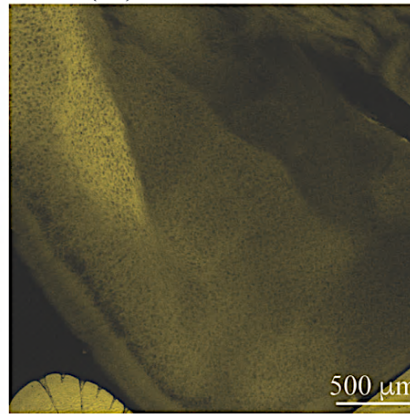
CCK-Dlx5/6-ReaChR mice express mCitrine-tagged ReaChR in CCK+INs. Confocal images of fluorescence in these mice contain strikingly specific and distinguishable mCitrine expression (**Figure 11B - left**). Since ReaChR expression is confined to GABAergic CCK+INs, cell and their projections are far easier to distinguish from the background than in **Figure 11A - right**. ReaChR is embedded in the transmembrane domain and fluorescence is restricted to the C-terminus of these cation channels, thus mCitrine signal is not as robust as tdTomato signal under the microscopy conditions that we used for imaging. Based on morphology, the thin, rod-like projections with high fluorescence could represent ReaChR in CCK+IN dendrites while the small, bulbous areas of high fluorescence could represent ReaChR in CCK+IN synaptic terminals (**Figure 11B - right**). Some CCK-negative cells, represented by empty/black circles, appear to be isolated from CCK+IN innervation in the lower right-hand side of **Figure 11B - left**. Other CCK-negative cells are surrounded by mCitrine fluorescence in what appear to be patterns of perisomatic inhibition by CCK+INs (**Figure 11B - left**). A CCK+IN with extensive ReaChR expression is observable in **Figure 11B - right** along with its highly-fluorescent projections.

Figure 11| Channelrhodopsin expression in the BLA of CCK-ChR2 and CCK-Dlx5/6-ReaChR mice.

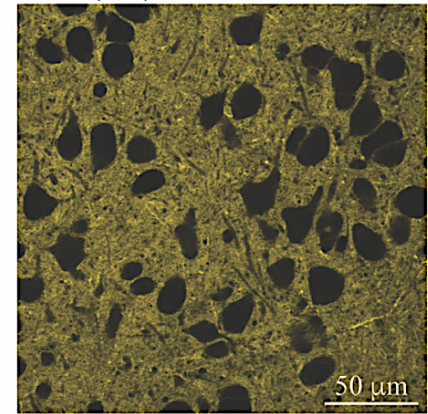
A| Confocal images of fluorescence in coronal brain slices containing the BLA from an adult CCK-ChR2 mouse. EYFP (yellow) is bound to the C-terminus of channelrhodopsin-2 and expressed in CCK+ cells/tissue. Left: Widespread EYFP expression can be seen in and around the BLA. Right: EYFP can be seen in what appear to be dendrites and synaptic terminals, but not in cell bodies. **B|** Confocal images of fluorescence in coronal brain slices containing the BLA from an adult CCK-Dlx5/6-ReaChR mouse. mCitrine (yellow) is bound to the C-terminus of Red-activatable channelrhodopsin (ReaChR) and expressed in GABAergic CCK+INs. Left: Non-fluorescent cell bodies are heavily innervated by ReaChR-mCitrine, indicating postsynaptic currents can be recorded from these cells using optogenetics. Right: ReaChR can be seen in a CCK+IN and its projections. Some surrounding cells are innervated by the CCK+IN in patterns characteristic of perisomatic inhibition, while others receive no innervation.

A| ChR Expression in CCK+ Cells (CCK-ChR2)

EYFP (5x)

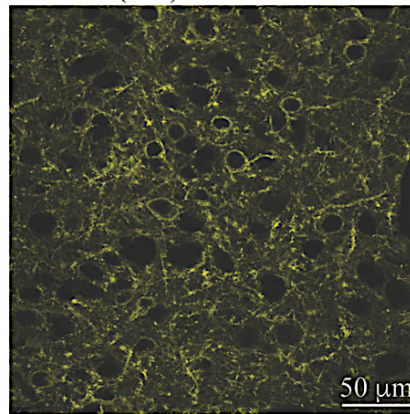


EYFP (40x)

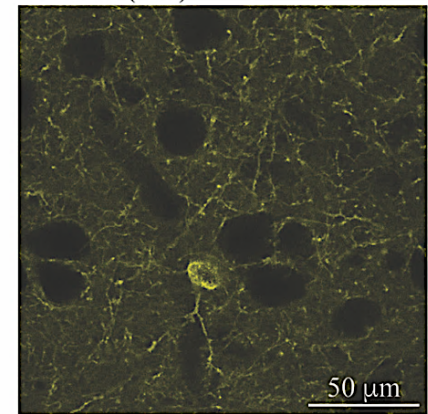


B| ChR Expression in GABAergic CCK+ Cells (CCK-Dlx5/6-ReaChR)

mCitrine (20x)



mCitrine (40x)

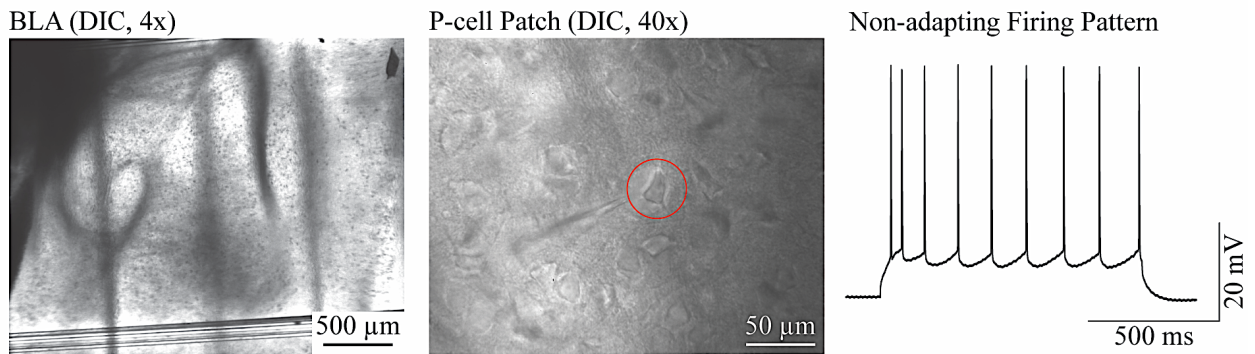


Light-evoked IPSCs in CCK+IN/P-cell Synapses in the BLA

The BLA (**Figure 12A - left**) contains P-cells with piriform morphology and projections on their apical and basal ends (red circle in **Figure 12A - middle**). P-cell displayed non-adapting firing patterns when stimulated by a supra-threshold square-pulse current injection (**Figure 12A - right**). When P-cells were held at 0 mV, a positive-going inhibitory postsynaptic current (IPSC) was produced (black trace in **Figure 12B - left**). The driving force for Cl⁻ was strong and inwards when the membrane potential was clamped at 0 mV (the equilibrium potential for chloride is -70

mV). When P-cells were held at -70 mV, there was no IPSC following optogenetic stimulation, as there was no driving force for Cl⁻ at this membrane potential (mint trace in **Figure 12B - left**). When P-cells were held at -90 mV, a negative-going reverse IPSC was produced (purple trace in **Figure 12B - left**). At this membrane potential, the driving force for Cl⁻ was small and outwards, into the extracellular space. Exposing P-cells to BIC lead to an elimination of control-condition IPSCs (**Figure 12B - middle**). BIC swiftly, totally, and irreversibly blocked optogenetically-evoked IPSCs in CCK+IN/P-cell synapses in the BLA of *CCK-Dlx5/6-ReaChR* mice (**Figure 12B - right**).

A| Morphophysiology of P-cells in the BLA (*CCK-Dlx5/6-ReaChR*)



B| IPSCs in CCK+IN/P-cell Synapses in the BLA (*CCK-Dlx5/6-ReaChR*)

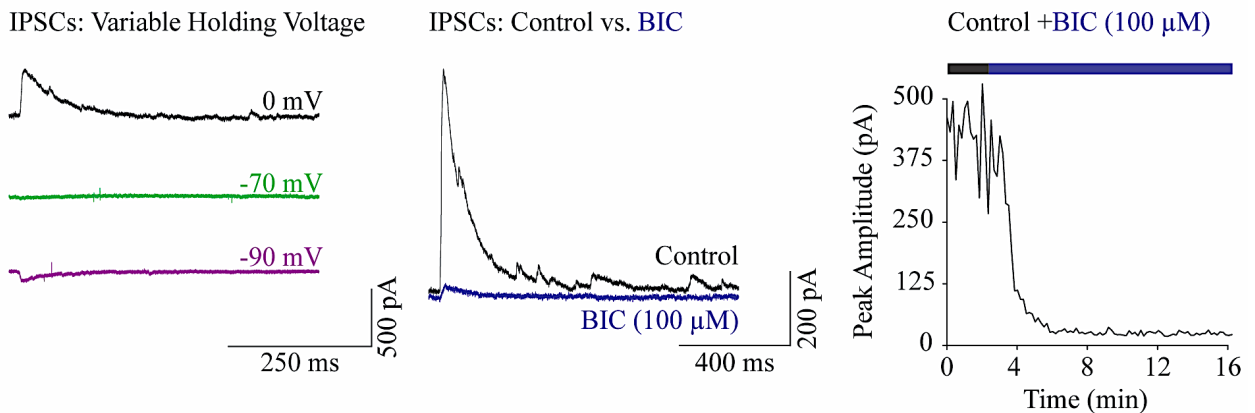


Figure 12| Morphophysiology and postsynaptic currents in CCK+IN/P-cell synapses in the BLA. Scale bars represent size in DIC images and time/current in IPSC traces. **A|** Identifying P-cells in the BLA of adult *CCK-Dlx5/6-ReaChR* mice. Left: DIC microscopy of the BLA contained in the brain slice chamber (4x magnification). Middle: Micropipette performing a whole-cell patch on a P-cell in the BLA (red circle).

Distinct piriform morphology and projections are observable. Right: A non-adapting firing pattern characteristic of P-cell intrinsic firing properties was produced by a supra-threshold square-pulse current injection. **B**| Confirming GABAergic activity of IPSC in CCK+IN/P-cell synapses. Left: IPSCs evoked at variable holding potentials display patterns representative of the driving force of Cl⁻. A positive-going peak is produced when the P-cell is held at 0 mV (top, black). No peak is produced at -70 mV (middle, mint), and a negative-going peak is produced at -90 mV (bottom, purple). Middle: IPSC traces under control and bicuculline (BIC) conditions. BIC (100 μM) eliminates IPSCs. Right: Time-course plot of IPSC peak amplitude under control and BIC conditions (indicated in the color-coded timeline). BIC added to the bath perfusion after 3 min rapidly eliminates IPSCs. Peaks are initially 400 pA and reduce to <10 pA after 8 min. There is no IPSC recovery upon continued stimulation.

Ca_v2.2 Block Reduced IPSC Peak Amplitude in CCK+IN/P-Cell Synapses in the BLA

CTX reduced IPSC peak amplitude in CCK+IN/P-cell synapses in the BLA of *CCK-Dlx5/6-ReaChR* mice (**Figure 13 - top right**). A cellular recording is represented in a time-course plot wherein average IPSC peak amplitude drops from 230 pA to 66 pA following CTX conditions (**Figure 13 - left**). It took about fifteen minutes for CTX to decrease peak amplitude to a new stable baseline, and five additional minutes for BIC to eliminate the remaining IPSCs (**Figure 13 - left**). These two drugs have different pharmacokinetics and pharmacodynamics, thus permeate the slice and act upon their targets at different rates. A total of seven cells were treated with CTX and their average peak amplitudes under control and CTX conditions are represented in a two-point segment plot (**Figure 13 - bottom right**). Each pair of circles represents the average IPSC peak amplitude before and after CTX treatment for one cellular recording. Comparisons across cells were made by calculating the percentage change in IPSC peak amplitude for each recording. The mean IPSC peak amplitude decrease for all seven cells was 51% (SD = 14%, SEM= 7%), with an average amplitude of 211 pA (SD = 103 pA, SEM = 39 pA) under control conditions and 97 pA (SD = 40 pA, SEM = 15 pA) under CTX conditions. There was no association between sex and CTX effects (51.87% mean peak amplitude decrease for males vs. 49.56% for females). A one-tailed paired t-Test on average control and CTX peak amplitudes produces a p-value of 0.0046. We conclude that

there was a significant effect of CTX on IPSC peak amplitude, and that GABA release from CCK+INs in the BLA is partially $Ca_v2.2$ -dependent.

$Ca_v2.2$ Antagonism in CCK+IN/P-cell Synapses in the BLA (*CCK-Dlx5/6-ReaChR*)

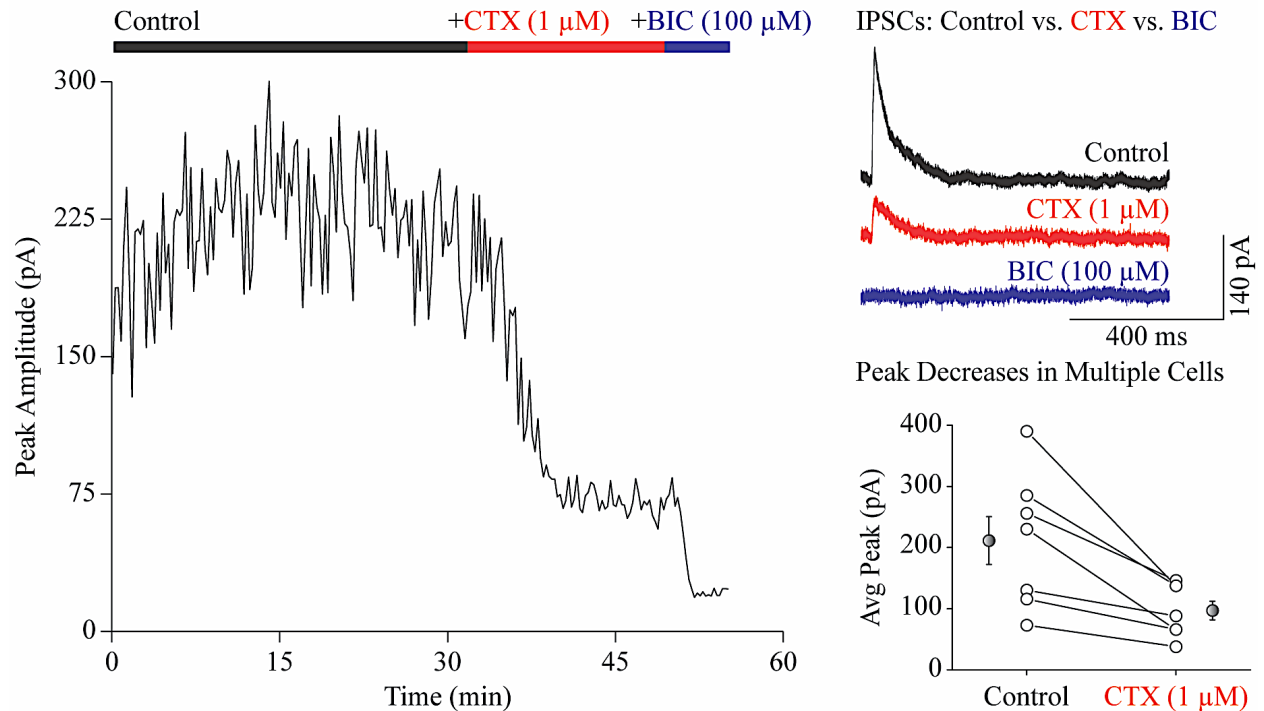


Figure 13| $Ca_v2.2$ antagonism reduces IPSC peak amplitude in CCK+IN/P-cell synapses in the BLA. Optogenetically-evoked IPSC were recorded in adult CCK-Dlx5/6-ReaChR brain slices. Left: Time-course plot of IPSC peak amplitude under three pharmacological conditions (indicated in color-coded timeline). ω -Conotoxin GVIA (CTX, 1 μ M) and bicuculline (BIC, 100 μ M) were added to the bath perfusion at 30 and 49 min, respectively. Peak amplitude was initially 230 pA but reduced to 66 pA following CTX addition. Blockade stabilized at 41 mins. BIC addition eliminated remaining IPSCs. Top right: Representative IPSCs traces from each of the three pharmacological conditions. The top IPSC (black) is a control trace. The middle (red) and bottom (blue) IPSCs are traces under CTX and BIC conditions, respectively. Scale bars represent time and current values. Bottom right: Two-point segment plot of average IPSC peak amplitude under control and CTX conditions for multiple recordings. Each pair of circles represents one cell ($n = 7$). CTX significantly decreased peak amplitude ($p = 0.0046$, one-tailed paired t-Test) by an average of 51% compared to control conditions (SD = 14%, SEM = 5%). Grey circles represent the mean IPSC peak under control (211 pA) and CTX (97 pA) conditions. Vertical black lines represent the SEM (39 pA and 15 pA, respectively).

Discussion

Connections between CCK+INs and P-cells have been described in the cerebral cortex (Freund, 2003), hippocampus (Whissell et al., 2015), and amygdala (Andrási et al., 2017; Freund & Katona, 2007). Additionally, the role of $Ca_v2.2$ in CCK+IN/P-cell synapses has been described for the hippocampus (Szabo et al., 2014). This is the first study to demonstrate the role of $Ca_v2.2$ in CCK+IN/P-cell synapses in the BLA. GABA release from CCK+INs onto P-cells in the CA3 region of the hippocampus was shown to be entirely blocked by CTX (Szabo et al., 2014). We found that in the BLA, GABA release is only partially blocked (51%). Our findings suggest that CCK+IN/P-cell are functionally distinct in the BLA and the hippocampus.

Specificity of CCK-Dlx5/6-ReaChR Mouse Model

Optogenetics allows for a level of precision in circuit-level research unattainable with traditional methods like electrical stimulation (Tye & Deisseroth, 2012). Electrical stimulation is a longstanding means of inducing neurotransmitter release and studying neurophysiology. While there are many appropriate applications of electrical stimulation, it is impractical to try to isolate specific cell circuitry using this technique. Investigations are limited because electrical stimulation excites all of the cells in proximity of the microelectrode. Accordingly, postsynaptic currents are the result of cumulative neurotransmitter release from multiple inputs, some of which may not be the target of study. Optogenetic stimulation induces transmitter release by opening light-gated ion channels and depolarizing the membrane of a genetically targeted neuronal population, thus the power of optogenetics lies in its cell specificity.

Critical to our research interests, genetic targeting of GABAergic INs has been made possible in recent years. Taniguchi and colleagues (2011) used *Cck-IRES-Cre*, *Dlx5/6-Flp*, and dual

recombinase-expressing mice to label GABAergic CCK+INs with GFP. Our *CCK-Dlx5/6-tdT* mouse model followed similar intersectional breeding framework, and as a result we are confident in our specific labelling of CCK+INs with tdTomato. Also critical to our research interests, optogenetic techniques have successfully been used to study perisomatic inhibitory circuits in the amygdala. Andrási and colleagues (2017) present electrophysiological data demonstrating potent inhibition of P-cells by local CCK+INs, as well as ChR2-mediated excitation of P-cells. Accordingly, our *CCK-Dlx5/6-ReaChR* mouse model aligns with prior models and can be used to make conclusions regarding CCK+IN/P-cell neurophysiology in the BLA.

Expression of tdTomato and ChR in CCK+ Cells in the BLA

Confocal microscopy images of fluorescence in *CCK-tdT* mice demonstrate widespread tdTomato expression throughout the brain slice (**Figure 10A - left**). This is to be expected, as the amygdala and surrounding cortical regions are known to contain high levels of CCK, both as a marker for excitatory and inhibitory cells (Beinfeld, Meyer, Eskay, Jensen, & Brownstein, 1981). Accordingly, the widespread expression of ChR2 in CCK+ cells from *CCK-ChR2* mice is also to be expected (**Figure 11A**). We observe similar patterns of tdTomato and EYFP fluorescence in CCK+ cells (**Figure 10A/11A - left**). Of note, the structures with intense fluorescence are related to the limbic system. Fluorescence is particularly concentrated in the LA and medial BLA, as well as the cortical piriform area, the piriform-amygdalar area, and the endopiriform nucleus. The latter three brain areas are part of the piriform cortex, a structure which is thought to be implicated in olfactory-based learning (Krettek & Price, 1977; Majak, Pikkarainen, Kemppainen, Jolkkonen, & Pitkänen, 2002). High expression of CCK+ cells has been reported in the piriform-amygdalar area and the endopiriform nucleus previously (Ingram, Krause, Baldino, Skeen, & Lewis, 1989). The

role of CCK in olfactory structures has been identified (Ma et al., 2013), and it continues to be a neurotransmitter of interest for sensory-limbic integration. Therefore, our observations of CCK expression and tdTomato/EYFP fluorescence in *CCK-tdT* and *CCK-ChR2* mice support previous findings.

Fluorescence experiments in *CCK-Dlx5/6-tdT* mice illustrate that CCK expression is far more refined when restricted to GABAergic IN populations (**Figure 10B - left** vs **Figure 10A - left**). Additionally, there are far fewer light-gated ion channels expressed in *CCK-Dlx5/6-ReaChR* mice (**Figure 11B - right**) when compared to *CCK-ChR2* mice (**Figure 11A - right**). By incorporating *Dlx5/6-Flpe* into our *CCK-Dlx5/6-tdT* and *CCK-Dlx5/6-ReaChR* triple transgenic mouse models, tdTomato/mCitrine fluorescence is only expressed in GABAergic CCK+INs (Taniguchi et al., 2011). As described by Freund (2007), CCK+IN innervation exerts heavy control over P-cells in the BLA. This innervation appears to be isolated in both triple transgenic mouse models and visualized in **Figure 10B - left** and **Figure 11B - right**. CCK+INs sit atop web-like patterns of low-level tdTomato fluorescence (**Figure 10B - left**) and mCitrine fluorescence encircling empty cell bodies (**Figure 11B - right**). Both patterns likely indicate perisomatic inhibitory connections with local P-cells. Strikingly similar images are presented by Rovira-Esteban and colleagues (2017), who selectively targeted GABAergic CCK+INs using a *BAC-CCK-DsRed* mouse line (adapted from Máté et al., 2013). These patterns are not observable in *CCK-tdT* mice (**Figure 10A**) or *CCK-ChR2* mice (**Figure 11A**), as glutamatergic and GABAergic CCK+ expression are homogenized in these lines.

GABA Release from CCK+INs onto P-cells in the BLA is Partially Ca_v2.2-dependent

When analyzing neurotransmitter release, IPSCs are a useful quantitative measurement as they allow for direct insight into fast-synaptic activity. The amplitude of an IPSC is reflective of the degree of inward anion (Cl^-) flow, which is the product of GABA binding to GABA receptors. Greater amounts of neurotransmitter binding will produce stronger IPSCs with higher peak amplitudes. Reduced neurotransmitter binding will produce weaker IPSCs with lower peak amplitudes.

We observe decreases in IPSC peak amplitude following CTX addition in all patch-clamp recordings (**Figure 13 - bottom right**). This consistency suggests that $\text{Cav}2.2$ -dependent GABA release from CCK+INs is pervasive and present to some degree around most P-cells in the BLA. While pervasive, it does not appear uniform. Neither total IPSC block nor zero IPSC block was observed in any of our recordings; decreases in peak amplitude ranged from 32% to 71%. There is likely variation in the degree to which $\text{Cav}2.2$ is expressed in presynaptic CCK+IN terminals. The remaining peak amplitude suggests that there are additional $\text{Cav}2$ subtypes which mediating neurotransmitter release. P/Q-type channels facilitate GABA release from PV+INs onto P-cells, and CCK+INs are closely paired with PV+INs in perisomatic inhibitory circuits (Sparta et al., 2014; Zamponi & Currie, 2013). Accordingly, P/Q-type channels may also play a role in transmitter release from CCK+IN terminals in the BLA. It has been demonstrated previously that there is a degree of functional compensation between P/Q-type channels and N-type channels in the presynaptic terminal (Inchauspe, 2004). Another possible $\text{Cav}2$ subtype, the R-type calcium channel, has been shown to partially contribute to action potentiation in presynaptic P-cell inputs (Wu, Borst, & Sakmann, 1998). R-type blockers (i.e. Lamictal) are used as mood-stabilizing drugs and in the treatment of affective disorders (Zamponi, 2016), thus may have some role in anxiety-related neuronal output from the BLA. As the functional roles of many presynaptic calcium

channels in regulating neurotransmitter release across brain regions remain unidentified, further pharmacological testing is required to determine which Cav subtypes regulate GABA release in CCK+IN/P-cell synapses in the BLA.

Observations of partial Cav2.2-dependency in CCK+IN/P-cell synapses suggest that Cav2.2 differentially regulates neurotransmitter release in the BLA compared to other brain regions. Szabó and colleagues (2014) report complete IPSC blockade in response to CTX (i.e. total Cav2.2-dependency) in CCK+IN/P-cell synapses in the hippocampus (CA3). Partial reduction of IPSC peak amplitude in the BLA is not likely due to of insufficient CTX dosing. Szabó and colleagues (2014) saw complete block with a 50 nM dose while we used 1 μ M. Moreover, we incrementally increased CTX concentration after decreases in IPSC peak amplitude had plateaued and no further effects were observable (**Figure 13 - left**).

Overall, our findings are an important contribution to the growing understanding of the molecular mechanisms involved in anxiety. We demonstrate that although CCK+IN/P-cell synapses are also found in the HPC and PFC, these circuits are differentially regulated by Cav2.2 in the BLA. Additionally, our results challenge the notion that Cav2.2 is the only Cav2 subtype involved in regulating neurotransmitter release from CCK+INs. These two concepts are important when considering the conflicting anxiogenic and anxiolytic properties reportedly caused by Cav2.2 antagonists. Anxiety-related neuronal activity and ultimately the experience of anxiety-like symptoms are likely differentially modulated by Cav2.2 in different brain regions. As a result, novel Cav2.2-based pharmacological treatments for anxiety disorders should consider region-specific effects and target precise anxiogenic circuits.

Additional Considerations for Future Research

$Ca_v2.2$ blockade partially reduced IPSC peak amplitude in CCK+IN/P-cell synapses in the BLA. By blocking additional Ca_v s, we may be able to determine which additional subtypes are behind the remaining peak amplitude. Following a similar electrophysiology protocol, additional Ca_v antagonists could be added to the bath perfusion following ω -Conotoxin GVIA. There are pharmacological agents that specifically target other Ca_v subtypes; Nimodipine is an L-type blocker, ω -Agatoxin IVA is a P/Q-type blocker, and SNX 482 is an R-type blocker. By blocking Ca_v subtypes in succession, we can fully eliminate IPSCs. If this process of multiple drug conditions prolongs recordings to the point at which they become detrimental to slice health, multichannel blockers could be used instead. Drugs like cilnidipine (N- and L-type blocker) or ω -Conotoxin MVIIC (N- and P/Q-type blocker) may eliminate IPSCs in our system.

The *CCK-Dlx5/6-ReaChR* mouse model we have developed has incredible potential for studying CCK+INs. These studies do not have to be limited to circuits in the BLA, or even to electrophysiology experiments. ReaChR has been shown to enable transcranial optogenetic activation of neurons in deep brain structures (Lin et al., 2013). Therefore, the role of CCK+INs in behavior could be examined. Local injections, toxins, and other genetic manipulations would allow us to target the underlying components behind CCK+IN-related behaviors. Fluorescence experiments in our *CCK-Dlx5/6-tdT* mouse line have shown extensive CCK+IN expression throughout the brain and spinal cord. There are major CCK+IN-mediated properties left unexplored at the behavioral and cellular level. For example, CCK+INs have been shown to innervate other CCK+INs, parvalbumin-expressing basket cells (PV+BCs), and even themselves via autapses (Freund, 2003; Fukudome et al., 2004; Rainnie et al., 1993). We have demonstrated

that we can distinguish between P-cells and INs in patch-clamp recordings; additional research could study the role of $Ca_v2.2$ in CCK+IN/CCK+IN synapses.

In addition to CCK+INs, PV+INs synapse onto the soma of P-cells to form a system of perisomatic inhibition. This type of inhibition has been well studied in the hippocampus and cerebral cortex (Freund, 2003), however less is known about its role in the BLA. PV+INs have firing properties distinct from CCK+INs, indicating they process inputs differently. PV+INs fire fast non-adapting spiking patterns, allowing them to process multiple converging stimuli (Bartos & Elgueta, 2012). Despite the relevance of spiking frequencies on PV+IN function, the ion channel composition underlying these distinctive properties has not been fully described in the BLA. Spiking frequency depends on the concerted activity of various ion channels, including Ca_v s and calcium-activated potassium channels (K_{Ca} s). Generally, Ca_v s provide calcium for the activation of K_{Ca} s; a form of selective coupling that then hyperpolarizes neurons and reduces spiking frequency (Womack, 2004). In the future, we can propose a comprehensive study that combines *in vitro* electrophysiology, transgenic mouse models, and pharmacology to compare Ca_v s and K_{Ca} s in CCK+INs and PV+INs in the BLA, to determine which channels underlie higher spiking frequency patterns in PV+INs.

CHAPTER 2: CB₁-MEDIATED MODULATION OF GABA RELEASE FROM CCK+ INTERNEURONS ONTO PYRAMIDAL CELLS IN THE BASOLATERAL AMYGDALA

Abstract

The endocannabinoid (eCB) system is a network of receptors and ligands throughout the mammalian brain implicated in anxiety. The type-1 cannabinoid receptor (CB₁) is expressed at high levels in the basolateral amygdala (BLA), a brain region involved in regulating anxiety-like behaviors. The BLA is the main source of excitatory neuronal output from the amygdala to brain regions like the prefrontal cortex and hippocampus. This output is facilitated by pyramidal cells (P-cells) and regulated by local inhibitory interneurons (INs). INs that express the neuropeptide cholecystinin (CCK+) are known to co-express CB₁. CB₁ regulates neurotransmitter release from CCK+INs by downregulating voltage-gated calcium channels (Cav_s) in the presynaptic terminal. P-cells disinhibition in the BLA may contribute to increased anxiety-like behaviors. CB₁-mediated inhibition can occur in a ligand-dependent (phasic) and ligand-independent (tonic) manner. It has been demonstrated that CB₁ is expressed in CCK+INs in the BLA, however the underlying molecular mechanisms of these channels is not well understood. Using a combination of transgenic mouse models, immunofluorescence, electrophysiology, and pharmacology, we aimed to determine if/how CB₁ modulates CCK+IN/P-cell synapses in the BLA. Our confocal microscopy experiments revealed heavy colocalization of CB₁ and CCK+IN signal in both the BLA and hippocampus. Using optogenetic stimulation and whole-cell patch clamp electrophysiology in our transgenic mouse model (*CCK-Dlx5/6-ReaChR*), we evoked GABA release from CCK+INs and recorded inhibitory postsynaptic currents (IPSCs) in P-cells. We then determined how sensitive GABA release was to CB₁ modulation by observing IPSC peak amplitude under control condition and following bath addition of a CB₁-agonist (2-AG) and a CB₁-antagonist (AM251). Our initial recordings suggests there is both phasic and tonic CB₁-mediated inhibition of GABA release from CCK+INs in the BLA. IPSC peak amplitude decreased by 26% from control to 2-AG conditions and increased by 34% from control to AM251 conditions. Following the publication of a comprehensive study on CCK/CB₁-expressing INs in the BLA by Rovira-Esteban and colleagues (2017), we decided to discontinue electrophysiology recordings and reallocate our mice to focus on novel experiments. Our preliminary data serves to confirm the findings presented by Rovira-Esteban and colleagues (2017), and our model transgenic mouse model serves as a tool for future studies on the molecular components underlying CB₁-mediated inhibition in the BLA.

Introduction

The endocannabinoid (eCB) system is a series of ligands and receptors integral for regulating synaptic transmission in brain areas like the prefrontal cortex (PFC), hippocampus (HPC), and basolateral amygdala (BLA). Circuit-level modulation of the eCB system can have large impacts on emotion and behavior, particularly in areas involved in anxiety (Lutz et al., 2015).

In the brain regions implicated in anxiety, type-1 cannabinoid receptors (CB₁) are located in presynaptic terminals. CB₁ is activated by the eCBs 2-Arachidonoylglycerol (2-AG) and anandamide (AEA), as well as exogenous cannabinoids (CBs) like tetrahydrocannabinol (THC) and cannabidiol (CBD) (Katona et al., 2001; Lee et al., 2015). Upon eCB/CB binding, CB₁ downregulates voltage-gated calcium channels (Cav_s), preventing calcium entry, vesicular fusion, and neurotransmitter release (Guo & Ikeda, 2004). CB₁ is believed to target and couple with Cav₂ channels, as they are also transmembrane proteins located in the presynaptic terminal (Alger, 2002; Wilson et al., 2001). CB₁ and Cav₂ are present in the excitatory cortical inputs to the amygdala (via the external capsule), and in inhibitory inputs from local INs (Azad, 2003). Dual expression in excitatory and inhibitory inputs suggests that eCBs can modulate output from the BLA and subsequently anxiety-related behaviors (Katona et al., 2001; Patel, Kingsley, MacKie, Marnett, & Winder, 2009; Yoshida et al., 2011). Additionally, it has been proposed that by acting with the eCB system, cholecystinin-containing (CCK+) interneurons (INs) modulate fear inhibition and extinction (Bowers et al., 2012).

CB₁ is selectively expressed in CCK+INs over other IN subtypes in the hippocampus (Katona et al., 2001). CCK+INs are known to regulate glutamatergic signaling of local pyramidal cells (P-cells), and are found in the neuronal output circuits of brain areas like the BLA, ventral HPC, and medial PFC (Freund & Katona, 2007). CCK+IN synapses can undergo CB₁-mediated depolarization-induced suppression of inhibition (DSI), a form of phasic, short-term inhibition (Zhu, 2005), as well as eCB-mediated long-term depression (LTD), a form of tonic, CB₁-independent inhibition (Marsicano et al., 2002). Both DSI and LTD are necessary for fear extinction (Chhatwal et al., 2009), a behavioral response facilitated by reciprocal connections from the infralimbic cortex (IL) of the medial PFC to the BLA (Sierra-Mercado et al., 2011). In the BLA,

CB₁ expression is found in the CCK+INs involved in perisomatic inhibition (basket cells (BCs)) (Mascagni & McDonald, 2003). These CCK+INs can be further grouped according to their level of CB₁ expression; so-called ‘high CB₁-expressing’ CCK+INs are sparsely distributed while ‘low CB₁-expressing’ CCK+INs are more evenly-distributed (Marsicano & Lutz, 1999; Yoshida et al., 2011).

While eCBs and CB₁ have been shown to modulate CCK+INs in multiple brain areas (Chhatwal et al., 2009; Szabo et al., 2014), the mechanisms by which they modulate neurotransmitter release and Cav_s is not completely understood (Lozovaya, Min, Tsintsadze, & Burnashev, 2009). N-type Cav_s (Cav_v2.2) and CB₁ are localized in CCK+INs and often found in regulatory nanodomains, indicating they have a strong functional linking (Dudok et al., 2015). Studies have revealed complex regulatory roles of CB₁ and eCBs on Cav_v2.2 in the HPC. Lenkey and colleagues (2015) observed that in the CA3 region of the HPC, tonic eCB-mediated activation in CCK+INs resulted in reduced Ca²⁺ entry through Cav_v2.2, independent of CB₁ content. Lenkey and colleagues (2015) also observed that only the CB₁ receptors located within 1 nm of Cav_v2.2 were responsible for eCB-mediated modulation of GABA release (Lenkey et al., 2015). Additionally, CCK+INs in the CA1 region of the HPC were reported to experience CB₁-mediated tonic inhibition of GABA release, disrupting perisomatic inhibition networks (Neu et al., 2007).

It is not known whether the eCB-dependent and eCB-independent mechanisms observed in the HPC are conserved in CCK+INs in the BLA. If conserved, CB₁ may modulate anxiety at the level of the BLA, indicating eCBs, CB₁, and Cav_v2.2 can possibly be targets of neuromodulators with anxiolytic properties. In this study, we aim to visualize CB₁ receptors in CCK+INs of the BLA and characterize their inhibition (phasic and/or tonic) of P-cells. If present, we aim to determine how Cav_v2.2 modulates eCB-mediated inhibition. We expect our experiments will reveal

more information on the contribution of eCBs and CB₁ to neurotransmitter release in CCK+IN/P-cell synapses in the BLA, which can be used to compare the role of CB₁ between the HPC and BLA.

Methods

Animal Models

Refer to **CHAPTER 1** for detailed information on the breeding, background, and research applications of our *CCK-Dlx5/6-tdT* and *CCK-Dlx5/6-ReaChR* mouse models. *CCK-Dlx5/6-tdT* mice were used in immunofluorescence experiments to visualize CCK+IN and CB₁ expression and colocalization in the BLA and HPC. *CCK-Dlx5/6-ReaChR* mice were used in electrophysiology experiments to study the role of CB₁ in CCK+IN/P-cell synapses in the BLA.

Immunofluorescence

Adult *CCK-Dlx5/6-tdT* mice were deeply anesthetized with isoflurane (07-893-1389; Patterson Veterinary) and given an intraperitoneal injection of Euthasol euthanasia solution (710101; Virbac Co.). Whole animal perfusion fixations were performed using formalin solution (HT501128; Sigma-Aldrich). Brains were rapidly dissected and stored at 4°C in formalin solution for 24-72 hours for further fixation. 80-100 µm coronal brain slices containing the amygdala and hippocampus were prepared using a vibratome (VT1000 S; Leica) and transferred to a 12-well plate (Greiner Bio-One). Slices were gently washed once in PBS and twice in 1% PBT (1% Triton X (T8787; Sigma-Aldrich) in PBS (P3813; Sigma-Aldrich)) for 10 minutes per wash on an orbital rocker (SK-O180-S; Scilogex). Slices were blocked in a 5% bovine serum albumin/PBT (5% BSA/PBT) solution for two hours at room temperature. After blocking, slices were washed three

times in 1% PBT before primary antibody incubation in a 1:200 dilution of anti-CB₁ antibody (ab23703; Abcam) and 5% BSA/PBT for 24-36 hours at 4°C. Following primary antibody incubation, slices were washed three times in 1% PBT and incubated in goat anti-rabbit Alexa 488 (ab150077; Abcam) secondary antibody for four hours at room temperature. After secondary antibody staining, slices were washed twice in 1% PBT and once in PBS before mounting onto micro slides (48311-703; VWR) with Vectashield medium (H-1400; Vector Laboratories) and micro cover glass (48393-221; VWR). Slides were stored at 4°C for a minimum of 24 hours before confocal imaging.

Confocal Imaging and Colocalization Quantification

Confocal microscopy on immunostained brain slices was completed using a Zeiss LSM 510 Meta. Multi-track acquisition with argon and helium-neon lasers was used to acquire images without excitation cross-talk. A series of band- and long-pass filters were applied to capture isolated emission peaks from individual fluorophores and prevent emission cross-talk. Fluorophores and their spectra (excitation/emission (nm)) were Alexa 488 (490/525) and tdTomato (554/581). Images were set to either a 1024 x 1024 or 2048 x 2048 frame size. A left-to-right scan with line averaging was used, each line being scanned eight times. The camera pinhole was kept at 1 airy unit across all imaging. Range indication was used to adjust the amplifier offset and detector gain, preventing over/under saturation of signals. A combination of tile-scans, z-scans, and single-plane images were taken at 5x, 10x, 20x, 40x, and 63x.

CB₁/CCK colocalization analysis was conducted with Carl Zeiss LSM Software (version 3.2). Single plane images of the BLA and the HPC were taken in the same brain slice using identical amplifier offset and detector gain settings to standardize fluorescence intensity. Intensity

thresholds were set using two different methods. First, intensity thresholds were manually set for green and red channels as to only include fluorescence in cell bodies/neuronal processes and exclude background signal. Second, intensity thresholds were automatically set using the Costes automated method, which computes the average intensity and standard deviation based off of a background ROI (an unlabeled cell body without observable CCK/CB₁ innervation). Of the two intensity threshold methods, our colocalization calculations were based off the Costes automated method as to prevent experimenter biases in threshold selection. Colocalization cut masks images were produced using this threshold in which only pixels containing colocalized CCK and CB₁ expression are displayed. The Mander's unweighted colocalization coefficient (MCC) and Pearson's correlation coefficient (PCC) were used to quantify colocalization and generated using the Costes automated method.

Electrophysiology

Refer to **CHAPTER 1** for specific details on *in vitro* brain slice preparation and electrophysiology, as we applied the same protocols up to the point of pharmacological additions. Briefly, whole-cell voltage-clamp electrophysiology was performed on P-cells in the BLA of an adult *CCK-Dlx5/6-ReaChR* female. GABA release was evoked from CCK+INs every fifteen seconds through optogenetic stimulation of ReaChR channels and IPSCs were recorded in proximal P-cells. A baseline IPSC peak amplitude was established over several minutes before pharmacological additions were performed. AM251 (1117; Tocris Bioscience), a potent CB₁ antagonist, was used to study the role of tonic inhibition in CCK+IN/P-cell synapses in the BLA. AM251 (10 μM) was added to the bath perfusion and IPSCs were continually evoked until no further changes in peak amplitude were observable. The brain slice was discarded, and equipment

was thoroughly cleaned. An additional brain slice was placed into the recording chamber with fresh aCSF. Baseline IPSC peak amplitude was again established before the addition of 2-AG (20 μ M) to the bath perfusion. 2-AG (53847-30-6; Tocris Bioscience) is an endogenous cannabinoid which we used to study the role of phasic inhibition in CCK+IN/P-cell synapses in the BLA. After recordings were finished, we determined if there were changes to average IPSC peak amplitude under control, 2-AG, and AM251 conditions.

Electrophysiology Data Analysis

The effects of CB₁ agonism and antagonism on IPSC peak amplitude in CCK+IN/P-cell synapses in the BLA were studied in two cells from a female *CCK-Dlx5/6-ReaChR* mouse. As described in **CHAPTER 1**, representative IPSC traces, time-course plots, and two-point segment plots were generated in Origin 6.1. Representative traces were plotted to compare control condition IPSCs to those under 2-AG and AM251 conditions. Peak amplitudes were used as a quantitative representation of the amount of GABA release from presynaptic CCK+INs and were calculated by subtracting baseline sweep current (pre-IPSC) from the maximum positive-going current of the sweep, which occurred just milliseconds after LED stimulation. Time-course plots were generated to illustrate the effects of 2-AG and AM251 on peak amplitude. Two-point segment plots were created to compare average IPSC peak amplitude under control, 2-AG, and AM251 conditions. Average peak amplitudes for the two pharmacological conditions were determined only after the point at which IPSCs had stabilized in the time-course plot, approximately ten minutes after addition to the bath perfusion.

Results

CB₁ Expression in CCK+INs in the BLA and Hippocampus

Confocal images of immunofluorescence in *CCK-Dlx5/6-tdT* brain slices display widespread CB₁ and CCK expression in the BLA and the HPC (CA3 region) (**Figure 14A - left/middle**). CB₁ is labelled with the Alexa 488 (green) fluorophore through secondary/indirect immunofluorescence while CCK+INs are labelled with tdTomato (red) through dual recombinase action (see **Figure 9A** for intersectional strategy). In **Figure 14A - left**, three CCK+INs are seen in the midst of several non-labelled cell bodies (black circles) in the BLA. Due to their bulbous morphology and dense fluorescence, it appears there are an abundance of GABAergic CCK+ terminals in peripheral tissue and around cell bodies. Several thick neuronal processes, likely primary dendrites, can be seen in the right-hand side of **Figure 14A - left**. Thinner neuronal processes, likely the secondary and tertiary dendrites of CCK+INs, are present throughout the tissue. Also seen throughout the tissue are CB₁-containing neuronal processes, which are especially prevalent encircling CCK+INs in **Figure 14A - left/middle**. CB₁ expression appears to be present in thinner projections, likely secondary/tertiary dendrites and terminals. There is no Alexa 488 fluorescence within cell bodies, as CB₁ is expressed in the transmembrane domain. There is minor colocalized signal around the center of the CCK+INs in **Figure 14A - left/middle** as well as in what appear to be the processes around non-labelled cell bodies. A cut mask image generated in Carl Zeiss LSM Software depicts colocalization of tdTomato and Alexa 488 fluorescence **Figure 14A - right**. Colocalization patterns suggest that synaptic terminals are areas of high combined CCK/CB₁ expression. Some neuronal processes, possibly secondary dendrites, also show colocalization, albeit at a lower level than synaptic terminals.

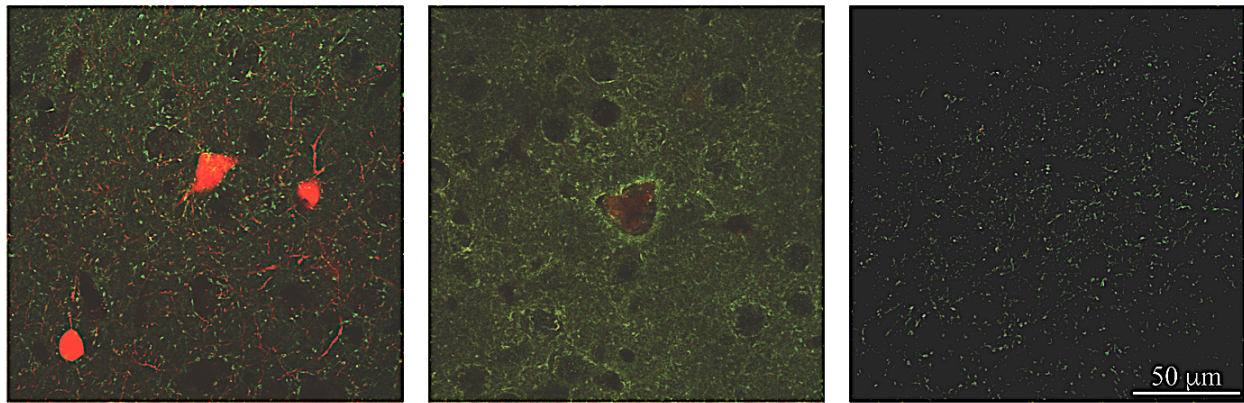
Figure 14B - left/middle depicts fluorescence representing CCK+IN and CB₁ expression in the CA3 region of the HPC in *CCK-Dlx5/6-tdT* brain slices. **Figure 14B - left** contains one CCK+IN with what appears to be high levels of innervation of cells in the stratum pyramidale (SP) layer. Many cells in the SP are innervated by CCK+IN projections. Additionally, CCK+IN projections are observable in the transition between the SP and the stratum lucidum (SL), and to a lesser extent in the larger SL layer. CB₁ expression patterns are similar here as in the SP, but with a greater degree of intensity. In the SP, CB₁ appears to be expressed in the synaptic terminals that comprise perisomatic inhibition patterns (**Figure 14B - left**). CB₁ is also expressed in neuronal processes which weave in and around cells. Based on morphology, there are many presynaptic terminals that express CB₁. Expression appears to be concentrated on either side of the SP. In the SL, CB₁ expression is weaker, as seen in the right-hand side of **Figure 14B - left**. Faint Alexa 488 fluorescence is observable in what are probably secondary/tertiary dendrites and synaptic terminals. **Figure 14B - middle** depicts a CCK+IN and CB₁ expression in the SL layer of CA3. Immediately visible are the thicker dendritic processes containing CB₁ expression. They run throughout the tissue but are noticeably denser in the top portion of **Figure 14B - middle**, close to the SP-SL transition. The cut mask in **Figure 14B - right** reveals that CCK/CB₁ colocalization is mild in the stratum oriens (SO), moderate in the SL, and strong in the SP. Not every cell in the SP is innervated by CCK+INs/CB₁, as some are indistinguishable from one another like in the lower center portion of **Figure 14B - right**.

Pearson's correlation coefficient (PCC) was used to measure overall colocalization (R) of CCK and CB₁ expression (**Figure 14A/B - right**). In the BLA, we obtained an R-value of 0.79 and in the HPC, an R-value of 0.84. We also calculated the Mander's unweighted colocalization

coefficient (MCC) for CCK/CB₁ signal in these two brain regions. We obtained an MCC of .783 in the BLA and .589 in the HPC.

A| GABAergic CCK and CB₁ Expression in the BLA (*CCK-Dlx5/6-tdT*)

CCK/CB₁ Innervation (63x) CCK+IN/CB₁ Colocalization (63x) Colocalization Cut Mask (63x)



B| GABAergic CCK and CB₁ Expression in the HPC (*CCK-Dlx5/6-tdT*)

CCK/CB₁ Innervation (63x) CCK+IN/CB₁ Colocalization (63x) Colocalization Cut Mask (63x)

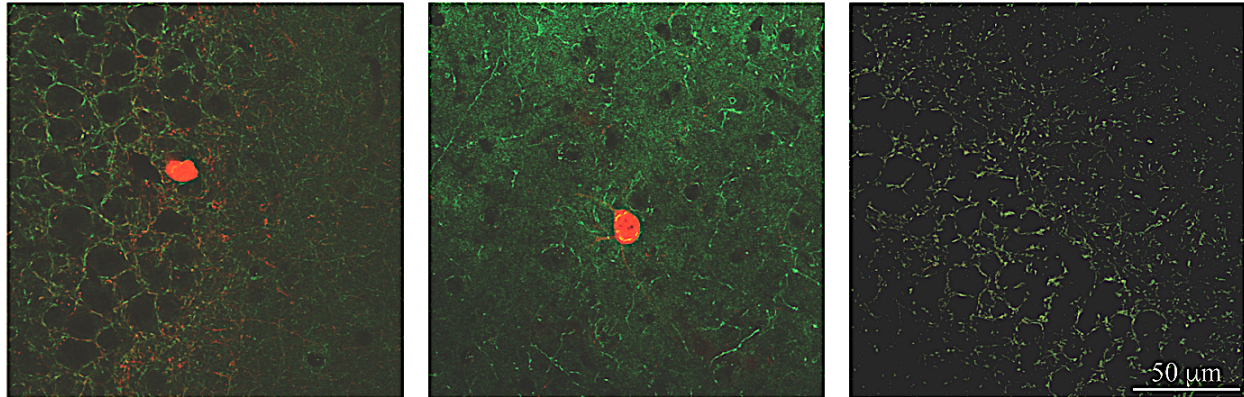


Figure 14| GABAergic CCK and CB₁ expression in the BLA and HPC. Confocal images taken of immunofluorescence in coronal brain slices from adult *CCK-Dlx5/6-tdT* mice. CCK+INs and their projections are tagged with tdTomato (red) while the type-1 cannabinoid receptor (CB₁) is tagged with Alexa 488 (green). Scale is applicable to every images within the figure, as identical settings were used to capture each image. **A|** GABAergic CCK and CB₁ expression in the basolateral amygdala. Left: CB₁ and GABAergic CCK are expressed in what appear to be synaptic terminals, indicated by small circular areas of high fluorescence. Fluorescence is also concentrated around cell bodies (black circles) in what appear to be perisomatic inhibition patterns. Areas of yellow signal contain both Alexa 488 and tdTomato fluorescence (colocalization). Middle: A CCK+IN is surrounded by what appear to be CB₁-containing terminals. Right: A colocalization cut mask displaying only pixels which contain colocalized GABAergic CCK and CB₁ expression. Non-colocalized pixels are set to zero intensity. **B|** GABAergic CCK and CB₁ expression in the CA3 region of the hippocampus (HPC). GABAergic CCK and CB₁-containing processes innervate many cells and colocalize around cell bodies. Left: In the HPC, what appear to be CB₁-containing

terminals innervate the stratum pyramidale, lucidum, and radiatum layers. Innervation by the CCK+IN displays similar patterns. Colocalization can be seen in multiple perisomatic inhibition-like circuits. Middle: A CCK+IN in the stratum radiatum layer of CA3 appears to be innervated by CB₁-containing terminals. Neuronal processes containing CB₁ are seen in the surrounding tissue. Right: A colocalization cut mask displaying only pixels which contain colocalized GABAergic CCK and CB₁ expression in CA3.

CB₁ Agonist (2-AG) Reduced IPSC Peak Amplitude in CCK+IN/P-cell Synapses in the BLA

We observed that the CB₁ agonist, 2-AG, reduced IPSC peak amplitude in CCK+IN/P-cell synapses in the BLA of an adult female *CCK-Dlx5/6-ReaChR* mouse. Addition of 2-AG to the bath perfusion decreased peak amplitude over a fifteen-minute recording (**Figure 15A**). A control-condition trace (black) and a 2-AG-condition trace (forest) are plotted in **Figure 15A - left** to represent the differences in peak amplitude. The gradual decrease in IPSC peak amplitude following addition of 2-AG (20 μM) to the bath perfusion is displayed in a time-course plot (**Figure 15A - middle**). 2-AG exerted its full effects eight minutes after addition. The change in average IPSC peak amplitude before and after 2-AG addition is represented by a two-point segment plot (**Figure 15A - right**). The pair of white circles represent the average peak amplitude before and after 2-AG addition. The average IPSC peak amplitude under control conditions is 225 pA and 167 pA after 2-AG addition (26% decrease).

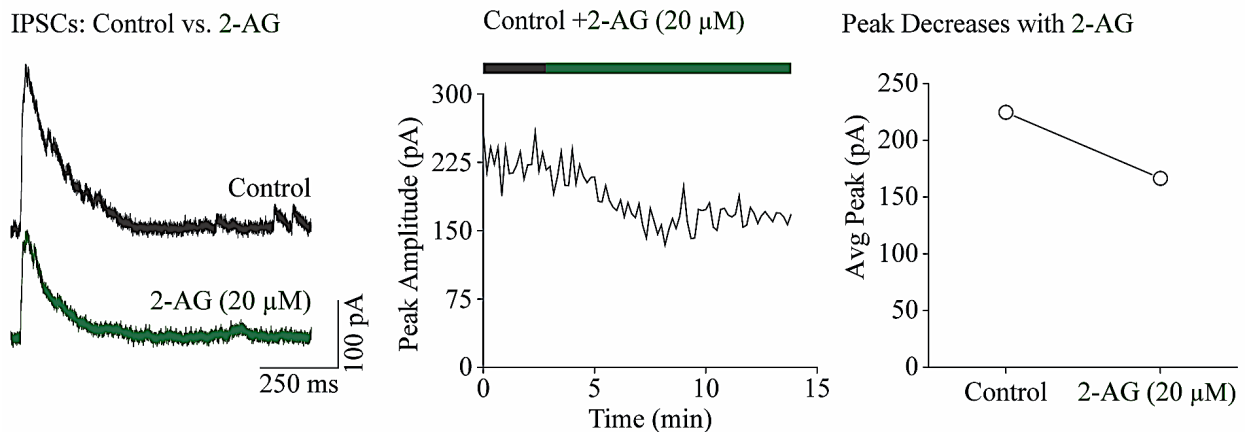
CB₁ Antagonist (AM251) Increased IPSC Peak Amplitude in CCK+IN/P-cell Synapses in the BLA

One P-cell was patched and recorded from the BLA of an adult female *CCK-Dlx5/6-ReaChR* mouse. AM251 applied to the bath perfusion (10 μM) increased IPSC peak amplitude in a CCK+IN/P-cell synapse in the BLA (**Figure 15B**). Representative traces depicting changes in IPSC peak amplitude are plotted in **Figure 15B - left**. The control trace (black) is 175 pA while the AM251 conditions trace (brown) is 225 pA. The gradual increase in IPSC peak amplitude following AM251 addition is displayed in a time-course plot (**Figure 15B - middle**). Stable IPSCs

were evoked for thirteen minutes before AM251 addition, after which peak amplitude began to increase, plateauing by minute twenty-three. The average IPSC peak amplitudes under control and AM251 conditions are represented in a two-point segment plot (**Figure 15B - right**). The first circle is the average peak amplitude under control conditions (170 pA), while the second circle is the average peak amplitude under AM251 conditions (229 pA).

A| CB₁ Agonism in CCK+IN/P-cell Synapses in the BLA (*CCK-Dlx5/6-ReaChR*)

IPSCs: Control vs. 2-AG



B| CB₁ Antagonism in CCK+IN/P-cell Synapses in the BLA (*CCK-Dlx5/6-ReaChR*)

IPSCs: Control vs. AM251

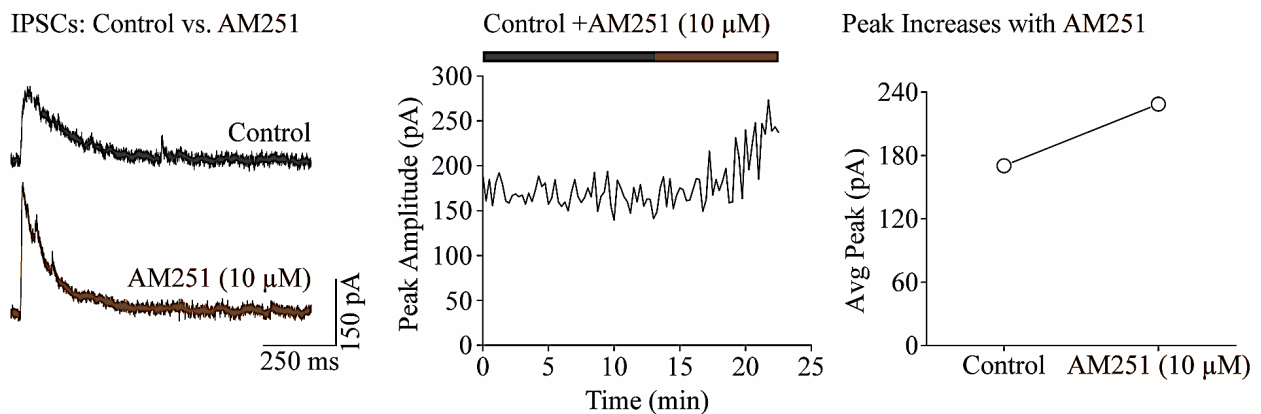


Figure 15| Effects of CB₁ modulation in CCK+IN/P-cell synapses in the BLA. Optogenetically-evoked IPSC were recorded in adult CCK-Dlx5/6-ReaChR brain slices. Scale bars indicate time and current values for IPSC traces. Drug conditions are indicated in the color-coded timelines. **A|** Effects of CB₁ agonism on IPSCs in CCK+IN/P-cell synapses. Left: Representative IPSC traces under control (black) and 2-AG (forest green) conditions. Middle: Time-course plot of IPSC peak amplitude in response to bath addition of 2-AG (20 μ M). 2-AG was added at 2 min and showed full effects by 10 min. Right: Average IPSC peak amplitude under control and 2-AG conditions. Peak amplitude decreased from 225 pA to 167 pA (-26%). **B|** Effects of CB₁ antagonism on IPSCs in CCK+IN/P-cell synapses. Left: Representative IPSC traces under control

(black) and AM251 (brown) conditions. Middle: Time-course plot of IPSC peak amplitude in response to bath addition of AM251 (10 μ M). AM251 was added at 13 min and showed full effects by 23 min. Right: Average IPSC peak amplitude under control and AM251 conditions. Peak amplitude increased from 170 pA to 229 pA (+34%).

Discussion

Expression of CB₁ in CCK+INs in the BLA and HPC

To quantify colocalization, we report both PCC and unweighted MCC values, each of which has strengths and shortcomings (Dunn, Kamocka, & McDonald, 2011). By obtaining the unweighted MCC values for tdTomato and Alexa 488 expression in the BLA and HPC, we acknowledge that the two fluorophores have different intrinsic brightness properties. Unweighted MCC values are based on pixel population rather than intensity (Adler & Parmryd, 2010), therefore they provide a better representation of the amount of CCK+IN/CB₁ content in tissue. We did not expect to find unweighted MCC values close or equal to one, as this would indicate every pixel containing tdTomato fluorescence also contains Alexa 488 fluorescence, represented by total colocalization (yellow signal) across the entire image. Additionally, a cut mask analysis would recreate the entire two-channel overlay image, converting red and green signals to yellow based on the intensity of their colocalization. In both the BLA and HPC we find areas of either no or sub-threshold colocalization, represented by black spaces in **Figure 14A/B - right**. Along similar lines, we did not expect to find unweighted MCC values approaching zero, indicative of perfectly opposite tdTomato and Alexa 488 patterns (no colocalization) (Everett, 2016). In addition to MCC values, we obtained PCC values with the Costes automated method (Costes et al., 2004). PCCs values are free of the influence of experimenter bias, as fluorescence threshold value cannot be manually set. If tdTomato and Alexa 488 fluorescence are perfectly linearly related, we would expect a PCC value of one, and if they perfectly inversely related, we would expect a PPC value of negative one.

While direct colocalization analysis has not been performed between CCK+INs and CB₁ in brain slices containing the BLA, previous mRNA and protein studies demonstrate a moderate-high degree (61-88%) of colocalization between CB₁ and CCK (Chhatwal et al., 2009; McDonald & Mascagni, 2001). We obtain a PCC value of 0.79 and an MCC value of 0.783, meaning 62% (PCC²) and 78% (MCC) of the variability in CB₁ (Alexa 488) fluorescence can be explained by the variability in GABAergic CCK (tdTomato) fluorescence. Despite being done in a novel system, these colocalization result falls within the range of reported CB₁ and CCK colocalization values for the BLA (Chhatwal et al., 2009; McDonald & Mascagni, 2001).

It has been previously reported that CB₁ is present in 82.7% of CCK+ terminals in the CA3 region of the HPC (Foldy, 2006). Furthermore, a majority of CB₁ terminals in the SP layer innervate P-cells while those in SO/SR layers target dendrites (Foldy, 2006). Our cut mask analysis appears to qualitatively reflect these finding (**Figure 14B - right**). In the HPC, we obtain a PCC of 0.84 and an MCC value of 0.589, meaning 71% (PCC²) and 59% (MCC) of the variability in CB₁ (Alexa 488) fluorescence can be explained by the variability in GABAergic CCK (tdTomato) fluorescence. I predict this variability to be due to the sensitivity of the MCC to the estimate of background. A decrease by just one gray level has been associated with a 2% decrease in the overall estimated overlap of signal in MCC analysis (Dunn et al., 2011). If considering PCC analysis only, then our R² value of 71% value is 12% percentage points lower than reported co-expression levels (Katona et al., 1999). This may be due to variations in technique (i.e. confocal vs electron microscopy, immunoperoxidase vs immunofluorescence), or suggest that CCK/CB₁ colocalization highly variable.

There are no direct comparisons of CCK/CB₁ colocalization between the BLA and HPC using brain slice immunofluorescence. However, across multiple studies with only minor

variations in reported expression value, it is clear that GABAergic CCK and CB₁ expression are highly linked in structures like the BLA, HPC, and PFC (Eggan, Melchitzky, Sesack, Fish, & Lewis, 2010; Katona et al., 1999; Shen, Piser, Seybold, & Thayer, 1996). Between our colocalization analysis of the BLA and HPC, PCC values are 9% apart while MCC values are 19% apart. As described above, MCC values are not ideal for our images, but could hold value if we had lower levels of background Alexa 488 expression. PCC values, while limited in their application, provide us with non-subjective background determinations. Given that both cut masks analyses in **Figure 14A/B - right** were performed using identical detection settings and in the same brain slice, PCC values present the most controlled measure of overall CCK/CB₁ colocalization.

Phasic CB₁-mediated Inhibition of GABA Release in CCK+IN/P-cell Synapses in the BLA

We observe a 26% decrease in IPSC peak amplitude (from 224 pA down to 167 pA) when CCK+IN/P-cell synapses in the BLA were exposed to 2-AG (**Figure 15A - right**). While our n-value is not large enough to determine significance, our preliminary finding aligns with what Rovira-Esteban and colleagues (2017) report. IPSC peak amplitude has been shown to be inhibited by application of synthetic CB₁ agonists in the BLA previously (Katona et al., 2001). Activity of 2-AG, the endogenous CB₁ agonist, can be studied by direct application of the agonist, or by stimulating the synthesis of the agonist in the postsynaptic cell (Yoshida et al., 2011). The latter method is used by Rovira-Esteban and colleagues (2017) to study transmission from CCK+INs in the basal amygdala. In order to draw comparisons between their study and ours, the differences in experimental design must be made apparent.

2-AG is synthesized in postsynaptic cells following depolarization, and retroactively binds to presynaptic terminals to suppress transmitter release in a system of negative feedback inhibition

(Zhu, 2005). The mechanism by which 2-AG is synthesized in P-cells and activates CB₁ in presynaptic terminals is known as depolarization-induced suppression of inhibition (DSI), while the manner in which CB₁ then inhibits transmitter release is known as phasic inhibition (Guo & Ikeda, 2004; Wilson et al., 2001). Rovira-Esteban and colleagues (2017) used DSI to study eCB-mediated inactivation of GABA release, whereas we used direct addition of 2-AG to the bath perfusion to study phasic inhibition in the same cellular circuit. Rovira-Esteban and colleagues (2017) demonstrate that the actions of 2-AG significantly reduce IPSC peak amplitude to 32% (+/- 7%) compared to baseline. Our 26% decrease is not as great in magnitude; however it is a preliminary indicator that eCB-dependent phasic CB₁ inhibition of transmitter release in CCK+IN/P-cell synapses of the BLA is a reproducible finding.

Tonic CB₁-mediated Inhibition of GABA Release in CCK+IN/P-cell Synapses in the BLA

We present a recording where IPSC peak amplitude increases by 34% in response to bath addition of AM251 (**Figure 15B - right**). As a CB₁ antagonist, AM251 blocks phasic, eCB-dependent inhibition of Cav_s (Lenkey et al., 2015). However, CB₁ does not require eCBs to downregulate Cav_s (tonic inhibition). AM251 also blocks tonic CB₁ inhibition of Cav_s, reducing the probability of GABA release onto postsynaptic P-cells (Biro, Holderith, & Nusser, 2006; Delaney, Crane, & Sah, 2007). In addition to blocking tonic CB₁-mediated inhibition of Cav_{2.2} and increasing GABA release probability, it has been proposed that AM251 increases the number of GABAergic exocytosis sites (Biro et al., 2006; Delaney et al., 2007; Rovira-Esteban et al., 2017). This would allow for a greater amount of GABA release from CCK+INs, represented by stronger chloride flow and subsequently greater IPSC peak amplitude in postsynaptic P-cells.

Similar to our observation of 34% increase, Rovira-Esteban and colleagues (2017) report a 45% increase in IPSC amplitude upon AM251 addition in CCK+IN/P-cell synapses in the BLA. The 11% discrepancy despite being from the same circuits can be potentially explained in several ways. Rovira-Esteban and colleagues (2017) have an n-value of 10, whereas we obtained an n-value of 1 before their paper was released. Additionally, a 34% increase falls within their reported standard deviations. We controlled for variables that could have given us false confirmation of their observations. For example, with too high a concentration of AM251, we may have observed a stronger increase in IPSC peak amplitude. The peak amplitude increase we observed with 10 μ M proved to be lower, but within deviation range, of the increase Rovira-Esteban and colleagues (2017) observed using a 5 μ M dose. Overall, our mouse line and initial experiments serve as a tool for further studies on the molecular components underlying CB₁-mediated inhibition in the BLA.

Additional Considerations for Future Research

Our future interests center on describing the regulatory role CB₁ exhibits on Cav2.2 channels in specific cell populations in the BLA (see NIH: R00-MH099405). Ideally, we aim to prove that CB₁ inhibits Cav2.2 channels to control transmission in CCK+IN/P-cell synapses. If present, CB₁-mediated inhibition of Cav2.2 would demonstrate tonic inhibition in the BLA, as it occurs independent of eCBs. To accomplish this, we would perform electrophysiology recordings from P-cells and quantify the component of IPSCs that is sensitive to ω -Conotoxin GVIA under the presence of AM 251. Additionally, we aim to show that eCBs acting through CB₁ are powerful anxiolytics via their inhibition of Cav2.2 channels in amygdala synapses. eCB-mediated modulation of Cav2.2 would be considered phasic inhibition, as it is ligand-dependent and short-

term, dissipating after eCBs have been cleared from the presynaptic terminal. This system can be studied through DSI experimentation as described by Ramikie and Patel (2012).

Additionally, we propose to study if CB₁-mediated inhibition of Cav2.2-dependent GABAergic release in the BLA is elevated during anxiety states. Behavioral studies like repetitive stress models, intended to induce anxiety-like behavior, have shown long-lasting changes to the eCB system in several brain areas including the BLA (M. N. Hill et al., 2010; Hill et al., 2009; Lafenêtre, Chaouloff, & Marsicano, 2007; Patel et al., 2009; Patel, Roelke, Rademacher, & Hillard, 2005; Qin et al., 2015; Viveros, Marco, & File, 2005). Additionally, anxiety is linked to reduced GABAergic transmission in the BLA (Ehrlich et al., 2009). Postsynaptic modulations have been observed during anxiety, but little has been shown regarding the impact of anxiogenic stimuli on effectors of CB₁, like Cav2.2 channels. It may be the case that that anxiety states cause enhanced CB₁ inhibition of Cav2.2 channels in CCK+INs. To determine this, we will put mice through an established anxiety-inducing behavioral paradigm and measure IPSCs in CCK+IN/P-cells synapses to assess the levels of phasic and tonic inhibition between anxious and non-anxious animal models.

CHAPTER 3: ASSESSING REGULATION OF GABA RELEASE AND INTRINSIC FIRING BY CA_v2.2 IN THE INFRA LIMBIC CORTEX

Abstract

The medial prefrontal cortex (mPFC) is an area of the brain involved in emotional processing. Rodent studies have demonstrated that neuronal output from the mPFC is crucial for the expression and conditioning of fear. Disruptions in the activity of the mPFC are associated with deficits in fear extinction, a process which is also disrupted by anxiety disorders like post-traumatic stress. Chronic and traumatic stress have been shown to negatively impact the mPFC at the cellular level; pyramidal cells (P-cells), the primary excitatory projections in the mPFC, become unstable and less responsive. In turn, the brain regions which are innervated by these P-cells are adversely affected. The resultant behavioral consequences vary depending upon the connection type. A sub-region of the mPFC known as the infralimbic cortex (IL) is involved in extinction memory. The IL is organized into multiple layers in which P-cells establish connections with the basolateral amygdala (BLA). The BLA is crucial for normal fear-related learning, particularly fear acquisition and fear extinction. Irregular activity in the connections between the IL and the BLA promote insufficient fear regulation and responses, however the underlying cellular physiology is not well understood. To help better understand the neurobiology of fear processing and anxiety disorders, we targeted the N-type calcium channel (Ca_v2.2) in this study. In limbic structures like the hippocampus, these channels have been shown to be expressed in the presynaptic terminal of cholecystokinin-positive interneurons (CCK+INs) and in P-cells, coupled to calcium-activated potassium channels. However, no data has been presented describing if these Ca_v2.2 roles are conserved within the IL. A series of electrophysiology and confocal microscopy experiments were conducted to study presynaptic and somatic Ca_v2.2 in the IL. We determined that inhibitory postsynaptic currents (IPSCs) in GABAergic/P-cell synapses are significantly reduced (46%) following Ca_v2.2 blockade ($p = .00015$). We found that Ca_v2.2 blockade had no significant effect on the firing properties of P-cells ($p = .204$). Confocal images depicted densely innervated P-cells in layers 2, 3, and 5. Electrophysiological studies revealed that the peak amplitude of IPSCs in CCK+IN/P-cell synapses is not significantly affected by Ca_v2.2 blockade ($p = .122$). We conclude that neurotransmitter release is partially Ca_v2.2-dependent in GABAergic/P-cell synapses and not significantly Ca_v2.2-dependent in CCK+IN/P-cell synapses in the IL, suggesting other voltage-gated calcium channel subtypes (Ca_vs) are involved. Our findings serve as a foundation for further research into the cellular mechanisms underlying anxiety-related circuits in the IL.

Introduction

The medial prefrontal cortex (mPFC) is involved in the processing and behavioral responses to fear and anxiety. Of the multiple sub-regions that comprise the mPFC, two areas in particular are of interest to researchers for their differentiable effects on anxiety-like behavior (Sierra-Mercado et al., 2011). The prelimbic region of the mPFC (PL) facilitates behavioral

responses to fearful stimuli (fear expression) through its interconnections with the basolateral amygdala (BLA) (Sullivan & Gratton, 2002). Ventral to the PL, the infralimbic region of the mPFC (IL) is involved in extinction of conditioned fear, a product of extinction-related neuronal plasticity in the hippocampus (HPC) and BLA (Do-Monte et al., 2015). Dysfunction in mPFC-amygdala pathways are observable in patients with anxiety disorders. Deficient recruitment of the mPFC is observed during the process of fear inhibition in patients with generalized anxiety disorder (GAD) (Greenberg et al., 2013). Patients with post-traumatic stress disorder (PTSD) exhibit decreased mPFC activation and increased amygdala activation in response to trauma-related cues (Shin et al., 2004). Additionally, reduced mPFC activity in PTSD has been associated with impaired fear extinction recall (Bremner et al., 2005) and greater symptom severity (Shin et al., 2005). In animal models, mPFC function has been associated with the expression of anxiety-like behaviors and the extinction of conditioned fear, both of which can be impaired with selective inactivation of the mPFC (Sierra-Mercado et al., 2006, 2011). Neuronal models of anxiety disorders have led to the belief that reduced mPFC function, in combination with over-excitation in the amygdala, mediate the dysregulation of fear responses (Rauch, Shin, & Wright, 2006). While the anxiety-related behavioral components of these connections have been extensively studied, their underlying neurobiology is less understood.

The process of fear extinction is of great concern for treating anxiety disorders like PTSD (Johansen et al., 2011; Shin et al., 2004) as sufferers are unable to extinguish anxiety-inducing memories developed in response to previous trauma. Accordingly, understanding the molecular mechanisms underlying IL-BLA connections may provide insight as how anxiety-related neuronal output is regulated (Johansen et al., 2011). In mice, the IL is divided into multiple layers (L1, L2/3, L5, and L6) based on cell types, projections, and local circuit organization (Allene, Lourenço, &

Bacci, 2015; Allen Mouse Brain Atlas). Across layers, a majority of neurons are excitatory P-cells (approximately 80%), while a minority are inhibitory interneurons (INs), including basket cells (BCs), dendritic cells, and axo-axonic cells (Allene et al., 2015; Riga et al., 2014). P-cells can be found in L2/3, L5, and L6 while INs are found within every layer (Cruikshank et al., 2012; Ma, Yao, Fu, & Yu, 2014; Riga et al., 2014). The projections from P-cells in L5/L6 are deep, generally targeting subcortical areas, while the projections from L2/3 are more superficial, generally targeting other cortical areas (Douglas & Martin, 2004). The intrinsic properties and circuit organization of these cells is of interest, as regulating their interactivity is required for normal fear and anxiety-related processing (Sierra-Mercado et al., 2006). P-cells in L2/3 and L5 are known to make reciprocal connections with the BLA (Allene et al., 2015; Ferreira et al., 2015). IL-BLA connections receive various excitatory inputs, primarily from the contralateral mPFC, midline thalamic nucleus, BLA, and ventral HPC (Riga et al., 2014). Additionally, IL-BLA connections receive various inhibitory inputs, which present themselves as targets for potentially mediating fear extinction at the level of the IL (Do-Monte et al., 2015).

Two major forms of inhibition are exerted upon IL-BLA projections (Allene et al., 2015). Dendritic inhibition of P-cells is facilitated by Martinotti cells and neurogliaform cells, two IN subtypes located in L2/3-L6 and L1, respectively (Palmer, Murayama, & Larkum, 2012; Y. Wang et al., 2004). Perisomatic inhibition is facilitated by parvalbumin-containing (PV+) and cholecystokinin-containing (CCK+) basket cells (BCs), two additional IN subtypes which synapse onto the soma of local P-cells (Freund, 2003; Freund & Katona, 2007). Dendritic inhibition can be evoked in a feed-forward manner by afferent projections. For example, thalamic input has been shown to excite dendritic INs in L1, which then inhibit P-cells in L2/3 (Cruikshank et al., 2012). Perisomatic inhibition is a form of feedback inhibition, where the firing of P-cells stimulates local

BCs to then regulate P-cell activity. Whereas the role of PV+BCs in perisomatic inhibition has been studied in L2/3, L5, and L6 (layers containing IL-BLA projections), the role of CCK+BCs in the same circuits has not (Allene et al., 2015; Armstrong & Soltesz, 2012; Freund, 2003).

Research suggests that in cortical regions, voltage-gated calcium channels (Ca_vs) are involved in regulating GABA release from INs and the intrinsic firing properties of P-cells (Ferreira et al., 2015; Freund, 2003; Jasnow et al., 2009; Kurihara & Tanabe, 2003; Loane et al., 2007). However, the role of Ca_vs in specifically the IL has not been functionally investigated, representing an important target by which anxiety may be regulated. Of the multiple Ca_v subtypes, N-type Ca_vs ($\text{Ca}_v2.2$) are distinguished for their anxiety correlation (Lotarski et al., 2011). GABA release from presynaptic INs was shown to be entirely dependent on $\text{Ca}_v2.2$ in the HPC (Szabo et al., 2014), but it is not known if this is conserved in the IL. Additionally in the HPC, $\text{Ca}_v2.2$ was shown to modulate the intrinsic firing of P-cells through coupling to calcium-activated potassium channels (Loane et al., 2007). $\text{Ca}_v2.2$ is also involved in the intrinsic firing of P-cells in the deep cerebellar nuclei, selectively regulating their spontaneous activity (Alviña & Khodakhah, 2008). As is the case for the presynaptic region, it has not been determined if these intrinsic roles of $\text{Ca}_v2.2$ are conserved in the IL.

The Ca_vs associated with GABA release from the multiple IN subtypes found in the IL have not been fully detailed. PV+BCs, Martinotti cells, and neurogliaform cells have been shown to express P/Q-type Ca_vs (Bartos & Elgueta, 2012), L-type Ca_vs (Wang et al., 2004), and further L-type Ca_vs (Li, Stewart, Canepari, & Capogna, 2014), respectively. On the other hand, the expression of $\text{Ca}_v2.2$ has been found in CCK+INs in the BLA, HPC, and mPFC (Ali, 2011; Eggan et al., 2010; Freund, 2003; Jasnow et al., 2009). GABA release from CCK+INs in the HPC was determined to be entirely-dependent on $\text{Ca}_v2.2$ (Szabo et al., 2014). This does not imply that

CCK+INs in the IL will function in the same manner however, as there are known variations in CCK+IN properties across brain regions, potentially due to ion channel variations (Kullmann, 2011). GABA release from two additional IN subtypes, chandelier and bipolar cells, has not been associated with any Cav subtype(s). In the IL, chandelier cells form inhibitory connections on the axon-initial segment of P-cells, while bipolar cells are thought to inhibit other INs (Allene et al., 2015). Little is known about the synaptic properties of these INs, and their Cav-dependency has yet to be determined for the IL.

Ultimately, there is a lack of direct functional studies on the role of Cav2.2 in the infralimbic cortex. Our goal is to determine this role, specifically in 1) GABA release from the general population of INs onto P-cells in L2/3, 2) GABA release from local CCK+INs onto P-cells in L2/3, and 3) the firing pattern and spike frequency of P-cells in L2/3. We hope this work will contribute to the overall understanding of the molecular mechanisms underlying P-cell regulation in the IL, regulation which is crucial for normal fear extinction processes and is disrupted in anxiety disorders.

Methods

Animal Models

Refer to **CHAPTER 1** for more detailed information on the breeding, background, and research applications of our *CCK-Dlx5/6-tdT* and *CCK-Dlx5/6-ReaChR* mouse models. *CCK-Dlx5/6-tdT* mice were used in fluorescence experiments to visualize CCK+INs in the IL and greater mPFC. *CCK-Dlx5/6-ReaChR* mice were used in electrophysiology experiments to study the role of Cav2.2 in CCK+IN/P-cell synapses in the IL. *Wild-type* mice were used in electrophysiology

experiments to study the role of Cav2.2 in GABAergic IN/P-cell connections as well as P-cell intrinsic firing properties.

In Vitro Brain Slice Preparation and Electrophysiology

Refer to **CHAPTER 1** for more detailed information on the preparation of live brain slices for electrophysiology experiments as well as a description of our electrophysiology rig. Protocols and equipment were conserved in this experiment with minor modifications. Slices containing the mPFC (rather than the BLA) were prepared from adult *wild-type* in addition to *CCK-Dlx5/6-ReaChR* mice.

Electrophysiology - Electrical Stimulation and Recording of GABAergic IN/P-cell Connections

To study the role of Cav2.2 in neurotransmitter release from GABAergic INs onto P-cells in the IL, we determined the sensitivity of electrically-evoked IPSCs to Cav2.2-blockade via addition of ω -Conotoxin GVIA (CTX) (ab120215; Abcam) to the bath perfusion. To stimulate neurotransmitter release from GABAergic INs, we used a concentric bipolar electrode (CBBPF100; FH-Co), which was connected to a stimulus isolator (A365; WPI) and mounted to a three-axis dovetail manipulator (MX130L, Siskiyou Co) attached to our microscope stage. Coronal brain slices containing the mPFC were prepared from adult *wild-type* mice and mounted in the recording chamber. **Figure 16 - top left** demonstrates our recording approach. The concentric bipolar electrode was placed in the Pia/L1 of the IL (**Figure 16 - top left**, yellow circle) where INs are exclusively GABAergic (Cruikshank et al., 2012). A micropipette was used to perform whole-cell patch-clamps on P-cells in layer 2/3 (**Figure 16 - top left**, red circle). Magnifying the patch, P-cells were distinguishable from other cell types by their piriform morphology and medial axonal

projections (**Figure 16** - top middle, red circle). P-cells were held at 0 mV and an electrically-evoked IPSC protocol was applied through pCLAMP 10 software. 1000 ms sweeps began every 15 seconds in which a .1 ms electrical stimulation was delivered to the brain slice via the concentric bipolar electrode. The stimulus isolator was used to adjust the amperage delivered by the electrode as a percentage of 1 mA, allowing us to alter the initial peak amplitude of the IPSCs. Initial peak amplitude was set to between 200-700 pA in order to be large enough for pharmacological changes to be observed while remaining small enough as to not exhaust neurotransmitter release or harm the brain slice.

Once satisfactory IPSCs were evoked, pharmacological recordings began. CPP (20 μ M) and DNQX (10 μ M), NDMA and AMPA/Kainate antagonists, respectively, were added to the bath perfusion to ensure we only recorded the GABAergic components of electrically-evoked neurotransmitter release. The initial few minutes of each recording was used to establish a baseline peak amplitude for control conditions, prior to the addition of pharmacological agents. CTX (400 nM) was added to the bath perfusion to observe if there were any significant effects of Cav2.2 blockade on peak amplitude. IPSCs were continually evoked until no further changes in peak amplitude were observable, i.e. a 'plateau' phase. CTX-dependent effects typically took fifteen-twenty minutes to fully present. Next, bicuculline (BIC) (ab120107; Abcam), a GABA_A antagonist, was added to the bath perfusion (100 μ M) to eliminate IPSCs and confirm the bath perfusion was delivering pharmacological agents to the brain slice. Recordings (n = 6 cells) were typically between 45-60 minutes in length. Once a recording was finished, brain slices were discarded and aCSF was replaced. Electrophysiology equipment was washed thoroughly with hydrogen peroxide and MilliQ water to avoid pre-exposing subsequent brain slices to pharmacological agents.

Representative traces were plotted in Origin 6.1 to compare IPSCs evoked under control, CTX, and BIC conditions. Peak amplitudes, used as a quantitative representation of the amount of neurotransmitter release from GABAergic INs, were calculated by subtracting baseline sweep current (pre-IPSC) from the maximum positive-going current of the sweep which occurred just milliseconds after LED stimulation. A time-course plot was created to represent the changes in IPSC peak amplitude (pA) in response to pharmacological conditions over the duration of the recording (min). A two-point segment plot was created to compare average IPSC peak amplitude under control and CTX conditions across the six cellular recordings. Average peak amplitudes were determined after the point at which IPSC peak amplitude remained relatively stable in the time-course plot. A one-tailed paired t-Test was run comparing the average peak amplitude under control and CTX conditions across the six cellular recordings. The mean, standard deviation (SD), and standard error of the mean (SEM) for the average peak amplitude under control and CTX conditions across all recordings were calculated. This mean (gray circles) and SEM (vertical black lines) were added to the two-point segment plot.

Fluorescence Stainings & Confocal Microscopy

Refer to **CHAPTER 1** for more detailed information on fluorescence and confocal imaging in *CCK-Dlx5/6-tdT* mice. Protocols and equipment were conserved in this experiment, except were done to section, stain, and image brain slices containing the mPFC rather than the BLA.

Electrophysiology - Optogenetic Stimulation of IPSCs in CCK+IN/P-cell Synapses

To determine the role of $Ca_v2.2$ in CCK+IN/P-cell synapses in the IL, we determined the sensitivity of IPSCs to $Ca_v2.2$ block via CTX. Whole-cell patch-clamp recordings were performed

on P-cells in the IL of adult *CCK-Dlx5/6-ReaChR* mice ($n = 8$). P-cells were held at 0 mV and IPSCs were evoked using optogenetic stimulation. Recording protocols were programmed in pCLAMP 10 software. 1000 ms sweeps containing a 0.1 ms stimulation began every twenty seconds. ‘Control’ IPSCs were evoked for several minutes to establish a baseline peak amplitude. CTX (300 nM) was then added to bath perfusion. IPSCs were continually evoked until no further CTX-dependent change to peak amplitude were observable. BIC (100 μ M) was then added to the bath perfusion and IPSCs were evoked until eliminated. After recordings were finished, brain slices were discarded and aCSF was replaced. Equipment was washed thoroughly before a subsequent slice was added to the chamber for further recordings. Data analysis was performed in an identical manner as described above for electrically-evoked IPSCs.

Electrophysiology - Modulation of P-Cell Intrinsic Firing Properties by $Ca_v2.2$

To study the role of $Ca_v2.2$ in P-cell intrinsic firing properties in the IL, we determined the sensitivity of action potential spike train firing pattern and spike frequency to CTX and cadmium chloride ($CdCl_2$). $CdCl_2$ is a reversible Ca_v antagonist which allowed us to observe if Ca_v subtypes other than $Ca_v2.2$ modulated P-cell intrinsic firing properties. Whole-cell patches were performed on P-cells in L2/3 of the IL in *wild-type* mice. A current-clamp was applied, and a ramp protocol was run to determine the activation threshold for each P-cell. The amount of current injected to evoke action potential spike trains was then set to +10 pA larger than this threshold and ranged from 50-120 pA across recordings. Initial firing patterns were compared to previous research (Faber et al., 2001; Rainnie et al., 1993; Zaitsev et al., 2012) to confirm we recording from P-cells and not INs. Three second square-pulse currents injections were applied every 45 seconds to produce action potential spike trains at an interval that was both conducive to cell health and

allowed for pharmacologically-induced changes to be observed. Control firing patterns and spike frequencies were determined over a 5-10 min period before pharmacological additions began. Using a valve controller (VC-6; Warner Instruments), three perfusion baths were applied in sequential order. Bath #1, the control condition bath, contained regular aCSF. Bath #2, the CTX condition bath, contained aCSF + 300 nM CTX. Bath #3, the CdCl₂ condition bath, contained aCSF + 100 μM CdCl₂. Given the slow diffusion time of CTX, bath #2 was applied for at least 20 minutes before switching to bath #3. After CdCl₂-dependent effects plateaued, we applied bath #1 for a second time to ‘wash’ the brain slice. Washes removed CdCl₂ from the perfusion and were used to determine if the effects we observed were due to C_{av} block and not damage to the cell. Once recordings were complete, brain slices were discarded, and equipment was washed thoroughly with hydrogen peroxide and MilliQ water to avoid pre-exposing subsequent slices to pharmacological agents.

Representative firing patterns from the control, CTX, and CdCl₂ conditions were plotted in Origin 6.1. Spike frequency was calculated by dividing the number of spikes in an action potential spike train by the duration of the current injection (three seconds). The event detection function in Clampex 10.6 was used to count the number of action potential spikes (or ‘events’) in each sweep. Spike frequencies were charted alongside the time at which the corresponding sweep began (i.e. sweep one = 0 min, sweep two = 0.75 min, sweep three = 1.5 min, etc.). Time-course and two-point segment plots were created in Origin 6.1 to demonstrate represent the effects of pharmacological agents on spike frequency in a single recording and across all cellular recordings, respectively. A one-tailed paired t-Test was run comparing the average spike frequency under control and CTX conditions across six cellular recordings. The mean, SD, and SEM for the average spike frequency amplitude under control and CTX conditions across recordings were calculated.

This mean (gray circles) and SEM (vertical black lines) were added to the two-point segment plot. Additionally, a one-tailed paired t-Test was performed, and the mean, SD, and SEM were calculated for the average spike frequency under control and CdCl₂ conditions in a total of four cellular recordings. This data is not represented in any figure.

Results

Ca_v2.2 Blockade Reduced IPSC Peak Amplitude in GABAergic IN/P-cell Synapses in the IL

Using the recording approach depicted in **Figure 16 - top left/top middle**, we found that IPSC peak amplitude in GABAergic IN/P-cell synapses decreases when Ca_v2.2 is blocked. Electrophysiology recordings were performed in six cells from two male and two female *wild-type* mice. Individual traces comparing IPSC peak amplitude under control, CTX, and BIC conditions were plotted in **Figure 16 - top right**. The control peak amplitude (black) is 743 pA, the CTX peak amplitude (red) is 523 pA, and the BIC peak amplitude (navy) is 28 pA. Ca_v2.2 blockade was slow to take effect; peak amplitude decreased over a thirty-or-so minute window before steadying (**Figure 16 - bottom left**). BIC effects were much quicker, completely eliminating IPSCs in about five minutes. Peak amplitude decreased in response to CTX across all recordings (**Figure 16 - bottom right**). Percentage decrease of peak amplitude from control to CTX conditions ranged from 24% to 70%, averaging to 46% (SD = 20%, SEM = 8%). A one-tailed paired t-Test from the two-point segment plot gives a p-value of 0.00015, meaning the Ca_v2.2-mediated decrease in peak amplitude is statistically significant. The average control peak amplitude was 331.4 pA (SD = 175 pA, SEM = 71 pA) while the average CTX condition peak amplitude was 202 pA (SD = 161 pA, SEM = 66 pA).

Ca_v2.2 Antagonism in GABAergic IN/P-cell Synapses in the IL (Wild-Type)

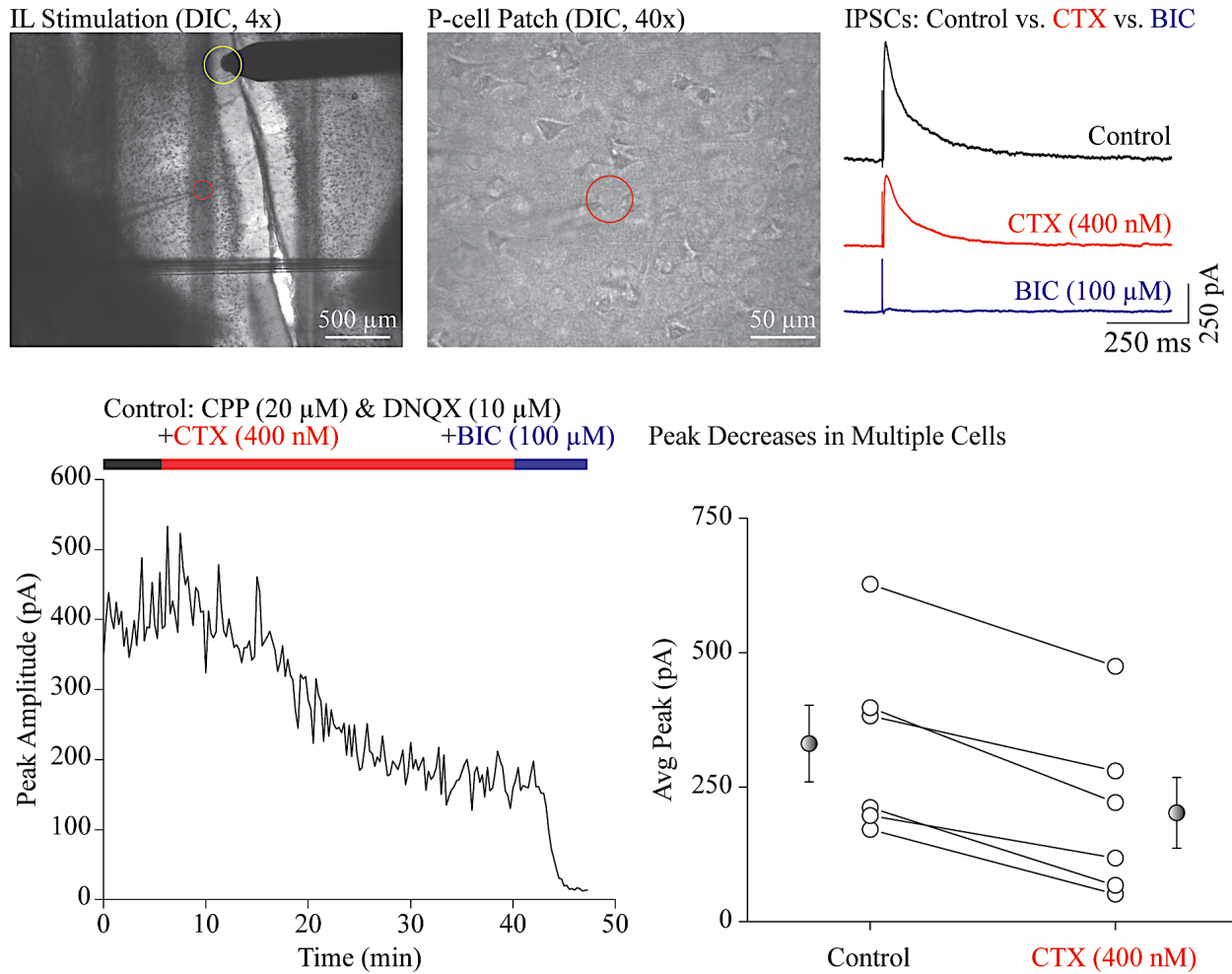


Figure 16| Effects of Cav2.2 antagonism on IPSCs in GABAergic IN/P-cell synapses in the IL. IPSC recordings were performed in the IL of adult wild-type mice. Scale bars represent tissue width in DIC images and time/current values in IPSC traces. Pharmacological conditions are indicated in the color-coded timeline. **Top left:** Electrophysiology setup for IL recordings. A concentric bipolar microelectrode (yellow circle) is placed in the Pia/L1 to stimulate GABA release from INs while P-cells in L2/3 are patched with a micropipette (red circle). **Top middle:** Magnification of the micropipette patch of a L2/3 P-cell (red circle). Axons of surrounding P-cells are directed towards the medial portion of the brain slice, represented by thin projections at the apex of the soma. **Top right:** Representative traces from IPSCs in control, ω-Conotoxin GVIA (CTX), and bicuculline (BIC) conditions. Throughout all recordings, the NMDA and AMPA/Kainate antagonists CPP and DNQX were present in the bath perfusion. The control (black) peak amplitude = 398 pA, the CTX (red) peak amplitude = 222 pA, and the BIC (blue) peak amplitude is < 10 pA. **Bottom left:** Time-course plot of IPSC peak amplitude before and after bath addition of CTX (400 nM) and BIC (100 μM). Peak amplitude begins at 400 pA but drops to under 200 pA following CTX addition. **Bottom right:** Two-point segment plot of average IPSC peak amplitude under control and CTX conditions. Each pair of circles represents one cellular recording (n = 6). CTX addition significantly decreases IPSC peak amplitude (p = 0.00015, one-tailed paired t-Test). The mean decrease was 46% (SD = 20%, SEM = 8%). Grey circles represent the mean IPSC peak amplitude under control (331 pA) and CTX (202 pA) conditions. Vertical black lines represent the SEM of each mean (71 pA and 66 pA, respectively).

Expression of CCK+INs in the IL

We present confocal images of fluorescence staining in the mPFC of an adult *CCK-Dlx5/6-tdT* mouse. The slice contains mostly IL, though the bottom portion contains part of the dorsal peduncle and taenia tecta (Allen Mouse Brain Atlas). CCK+INs and their extensive innervation are observable in what morphologically appear to be L2/3 and L5 of the IL (**Figure 18**). tdTomato (red) fluorescence labels GABAergic CCK+INs and their neuronal processes while SYTO-13 (green) fluorescence labels all cell bodies. CCK+INs are sparse in the medial region of each hemisphere (likely L1) and the anterior forceps of the corpus callosum (**Figure 18 - left**). Neuronal processes of CCK+INs are more apparent in the lateral aspects of the IL, with the highest expression located in what is likely L5. The dorsal peduncle and taenia tecta, considered by some as part of the ventral IL (Swanson, 2004), appear to express a considerable number of CCK+INs and processes. There are many non-labelled cells around which patterns characteristic of perisomatic inhibitory are observable (**Figure 17 - left**). SYTO-13 fluorescence indicates that medial regions of the IL (L1 and the pia) are sparse of cell bodies (**Figure 17 - middle**). There is a clustering of cell bodies in the divide between the two hemispheres, particularly where blood vessels are typically found. Cell bodies appear to be more tightly packed in the most medial portion of L2/3 but more evenly distributed in the outermost aspects of the left-hand hemisphere in **Figure 17 - middle**. An overlay of tdTomato and SYTO-13 signal is located in **Figure 17 - left**. Colocalization (yellow) occurs in all GABAergic CCK+INs, which are not uniformly distributed throughout the slice.

GABAergic CCK Expression in the IL (*CCK-Dlx5/6-tdT*)

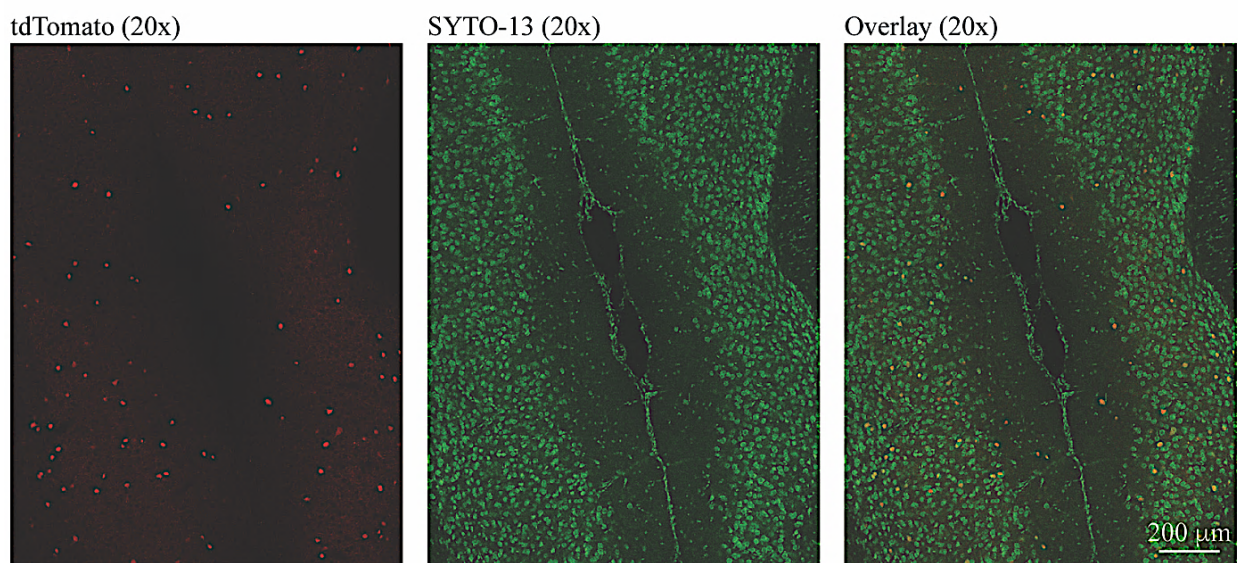


Figure 17| GABAergic CCK Expression in the IL. Fluorescence images of a coronal brain slice containing the IL from an adult *CCK-Dlx5/6-tdT* mice. CCK+INs and their projections are tagged with tdTomato (red) while cell bodies are stained with SYTO-13 (green). Scale bars indicate tissue width and apply to all images within the figure. Left: Expression of GABAergic CCK+INs is prevalent in L2/3 and L5 of the IL. Superficial layers (L1, pia matter) have lower expression. Web-like patterns of GABAergic CCK+IN processes can be seen in L2/3 and L5. Middle: Cell bodies are sparse and disorganized in L1 and the pia matter. However, the deeper layers of the IL show more organized cellular patterns. Right: A two-channel overlay of SYTO-13 and tdTomato signals shows colocalization (yellow) in the cell bodies of GABAergic CCK+INs.

Cav2.2 Blockade did not Significantly Alter IPSC Peak Amplitude in CCK+IN/P-cell Synapses

In **Figure 18** we present data illustrating there is no statistically significant change in IPSC peak amplitude following $\text{Ca}_v2.2$ block in CCK+IN/P-cell synapses of the IL. The effects of CTX and BIC on peak amplitude were studied in eight cells from three male and three female adult *CCK-Dlx5/6-ReaChR* mice. Representative traces of IPSCs from control, CTX, and BIC conditions were plotted in **Figure 18 - top right**. The control peak amplitude (black) was 177 pA, the CTX peak amplitude (red) was 202 pA, and the BIC peak amplitude (navy) was 5 pA. Over a thirty-minute window, no statistically significant change in average peak amplitude was detectable (**Figure 18 - left**). Within ten minutes of addition to the bath perfusion, BIC eliminated IPSCs. Each pair of circles in the two-point segment plot represents the average peak amplitude under

control and CTX conditions for a single cellular recording ($n = 8$) (**Figure 18** - bottom right). Average peak amplitude decreased in four cells and slightly increased in another four. Decreases ranged from 6-49% and increases from 7-23% with a mean change of -9% (SD = 26%, SEM = 9%). The average IPSC peak amplitude was 386 pA (SD = 282 pA, SEM = 100 pA) for control conditions, and 297 pA (SD = 131 pA, SE = 46 pA) for CTX conditions. A one-tailed paired t-Test from this plot gives a p-value of 0.122, meaning there is no statistical significance to the changes in average peak amplitude when $Ca_v2.2$ was blocked.

$Ca_v2.2$ Antagonism in CCK+IN/P-cell Synapses in the IL (*CCK-Dlx5/6-ReaChR*)

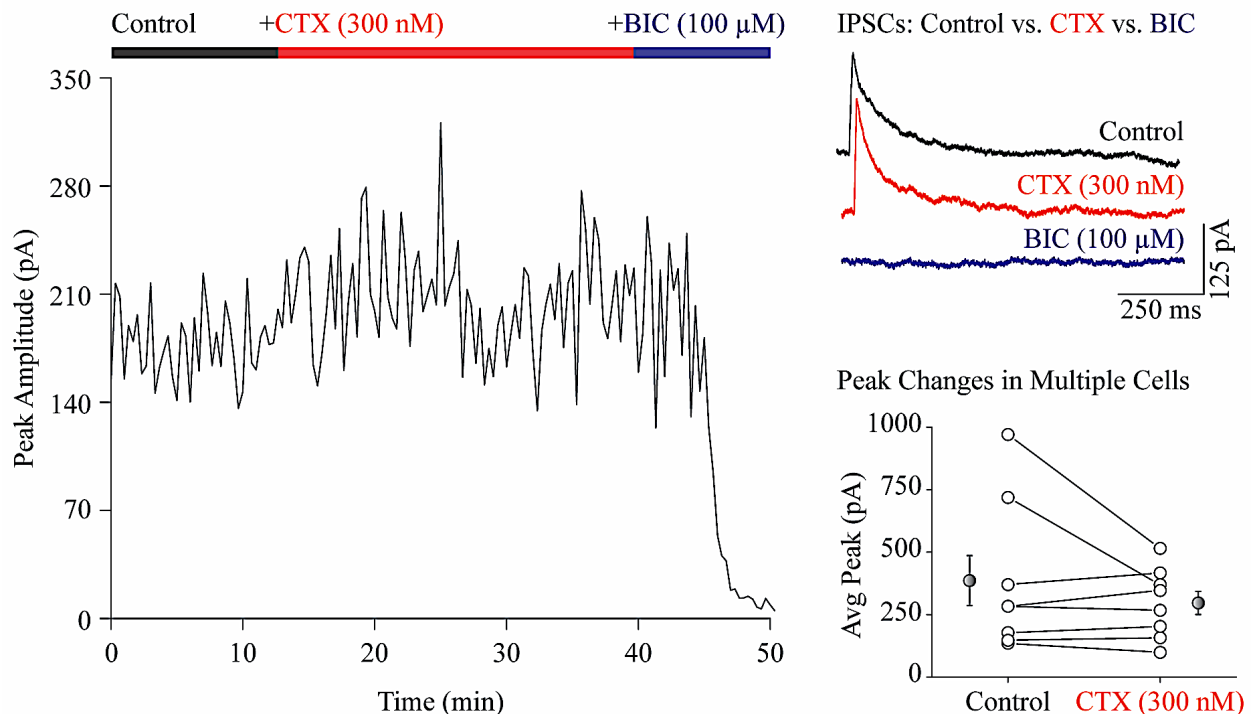


Figure 18 | Effects of $Ca_v2.2$ antagonism on IPSCs in CCK+IN/P-cell synapses in the IL. Optogenetically-evoked IPSCs were recorded from L2/3 P-cells in the IL of adult CCK-Dlx5/6-ReaChR mice. Left: Time-course plot of IPSC peak amplitude under control, ω -Conotoxin GVIA (CTX), and bicuculline (BIC) conditions, indicated in the color-coded timeline. Average peak amplitude was not significantly altered by CTX (300 nM) addition to the bath perfusion. IPSCs were eliminated by BIC (100 μ M). Top right: IPSC traces representing peak amplitude under each pharmacological condition. Peak amplitude under control (black) conditions = 180 pA, CTX (red) conditions = 200 pA, and BIC (blue) conditions = 0 pA. Scale bars represent time and current values for IPSC traces. Bottom right: Two-point segment plot of average IPSC peak amplitude under control and CTX conditions. Each pair of circles represents one cellular recording ($n = 8$). The mean change was -9% (SD = 26%, SEM = 9%). Grey circles

represent the mean IPSC peak amplitude under control (386 pA) and CTX (297 pA) conditions. Vertical black lines represent the SEM (100 pA and 47 pA, respectively). CTX addition to the bath perfusion did not statistically significantly change IPSC peak amplitude ($p = 0.122$, one-tailed paired t-Test).

Cav2.2 Blockade did not Significantly Alter P-cell Intrinsic Firing Properties in the IL

We present data demonstrating that Cav2.2 does not play a statistically significant role in the action potential spike train firing patterns, nor the spike frequency of P-cells L2/3 of the IL. A total of six P-cells were recorded from in this experiment, four cells from two male and two cells from two female *wild-type* mice. Firing patterns of action potential spiking under control, CTX, and CdCl₂ conditions are located in the top-half of **Figure 19**. A non-adapting initial bursting pattern at 3.33 Hz was evoked under control conditions, a non-adapting initial bursting pattern at 4 Hz was evoked under CTX conditions, and an adapting bursting pattern at 9 Hz was evoked under CdCl₂ conditions. Spike frequencies remained between 3.33 Hz and 4.33 Hz under control and CTX conditions but increased to between 7.67 Hz and 9 Hz under CdCl₂ conditions (**Figure 19 - bottom left**). Each pair of circles in the two-point segment plot represents the change in firing frequency after CTX addition for a given cell ($n = 6$) (**Figure 19 - bottom right**). From control to CTX conditions, average spike frequency decreased slightly in three cells and increased slightly in the remaining three. Decreases ranged from 3-6% and increases from 20-39% with a mean change of +13% (SD = 18%, SEM = 7%). A two-tailed paired t-Test from this plot gives a p-value of 0.204, indicating there is no statistically significant change in P-cell spike frequency when Cav2.2 is blocked. CdCl₂ was applied to four recordings (not shown). Increases in spike frequency from control to CdCl₂ conditions ranged from 32-180% with a mean increase of 110% (SD = 62%, SEM = 31%). The average P-cell spike frequency was 4.53 Hz (SD = 1.21 Hz, SEM = .49 Hz) under control conditions, 5.03 Hz (SD = 1.08 Hz, SEM = .44 Hz) under CTX conditions, and 9.77 Hz (SD = 2.82 Hz, SEM = 1.41 Hz) under CdCl₂ conditions.

Ca_v2.2 Antagonism in P-cells in the IL (*Wild-Type*)

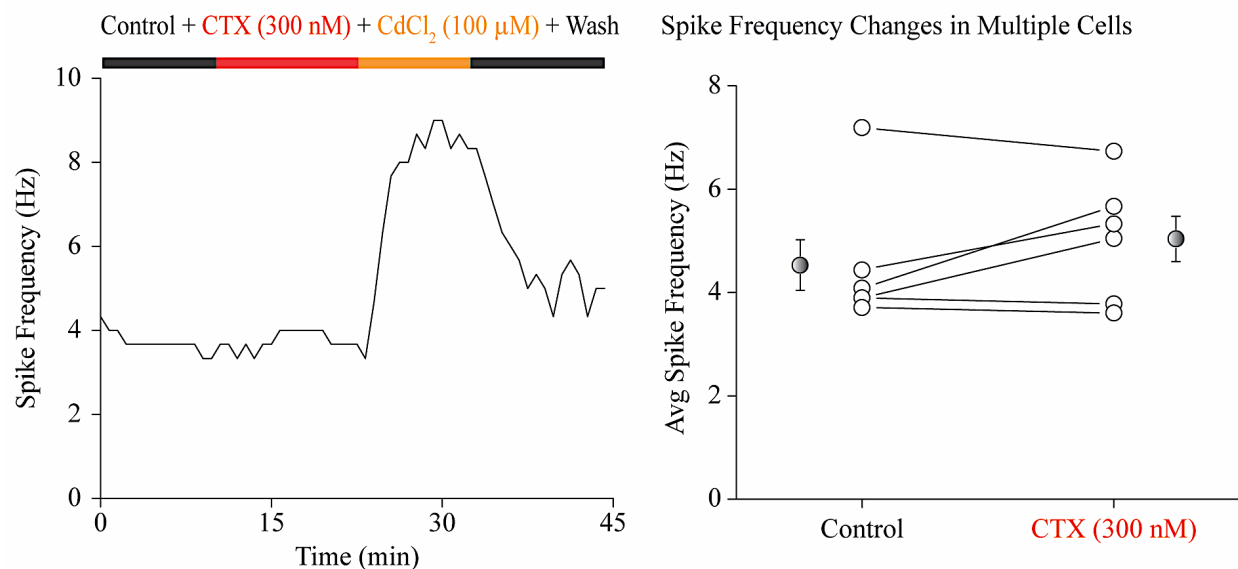
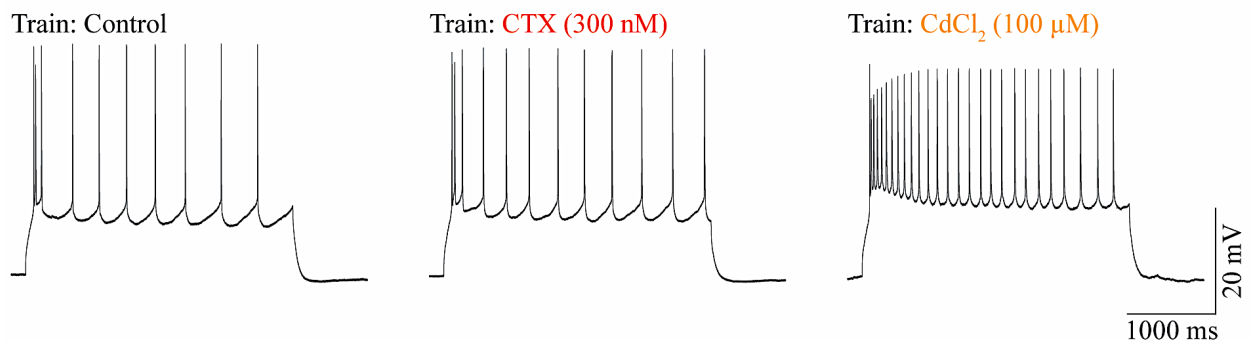


Figure 19| Effects of Cav2.2 antagonism on P-cell intrinsic firing pattern and spike frequency in the IL. Square-pulse currents were injected into P-cells and action potential spike trains were recorded in the IL of adult wild-type mice. Scale bars represents current and time values for the three firing patterns. **Top left:** Spike train evoked under control conditions. P-cell displayed a non-adapting firing pattern with initial bursting (3.33 Hz). **Top middle:** Spike train evoked under CTX conditions. P-cell continued to display a non-adapting firing pattern with initial bursting, but two additional spikes occurred (4 Hz). **Top right:** Spike train evoked under CdCl₂ conditions. P-cell displayed a bursting firing pattern with adaptation. Activation threshold became more positive and the number of spikes increased dramatically (9 Hz). **Bottom left:** Time-course plot of P-cell spike frequency before and after addition of CTX (300nM) and CdCl₂ (100 μM) to the bath perfusion. Pharmacological conditions are indicated in the color-coded timeline. Spike frequency did not significantly change from control to CTX (300nM) conditions, but dramatically increased under CdCl₂ (100 μM) conditions. Wash with clean aCSF partially reduced increases to spike frequency caused by CdCl₂. **Bottom right:** Two-point segment plot of average spike frequency under control and CTX conditions. Each pair of circles represents one cellular recording (n = 6). CTX addition does not statistically significantly affect average spike frequency (p = 0.204, two-tailed paired t-Test). Mean spike frequency increase was +13% (SD = 18%, SEM = 7%) from control to CTX conditions. Grey circles represent the mean spike frequency under control (4.53 Hz) and CTX (5.03 Hz) conditions. Vertical black lines represent the SEM for each mean (.49 Hz and .44 Hz, respectively).

Discussion

GABA Release from GABAergic IN/P-cell Synapses is Partially Cav2.2-dependent in the IL

The reduction of peak amplitude in our IPSC recordings in the presence of CTX indicate that Cav2.2 regulates neurotransmitter release from GABAergic INs onto P-cells in L2/3 of the IL. The validity of this claim is supported by our procedural controls and additional observations. By performing all recordings in the presence of glutamatergic antagonists (CPP and DNQX), we ensured IPSCs contained only GABAergic components, which we additionally validated with BIC. Additionally, we validated that sufficient CTX concentration had been applied during each recording, increasing concentration by 100 nM doses incrementally up to 400 nM, even after the decrease in IPSC amplitude had plateaued. If Cav2.2 were either not present or had no functional role in GABA release, we would observe no significant changes in peak amplitude from control to CTX conditions. While peak amplitude decreases are reproducible, they are not uniform. There is likely variation in Cav2.2 expression in the presynaptic INs located in and around L1, as CTX conditions result in a range of decreases, from 24% to 70%. The larger decreases may represent P-cells that are innervated by more heavily Cav2.2-dependent INs, whereas the lower decreases represent less Cav2.2-dependent innervation. In either case, additional Cav subtypes are likely involved. To determine the identity of these other Caves, further specific Cav antagonists like SNX-482 (Cav2.3) and ω -Agatoxin IVA (Cav2.1) could be applied during future recordings.

Cav2.2-dependent GABA release is likely observable in multiple IL IN subtypes. Transgenic mouse lines labelling various IN populations with optogenetic tools could be used to determine the specific subtypes involved. Previous research may indicate which IN subtypes in the IL are likely to express Cav2.2. A plethora of studies have described laminar organization and cell diversity in the mPFC and neocortex at large. It is possible these properties are conserved in

the IL, despite cytoarchitecture and Cav-dependent neurotransmitter release have not been extensively studied in this region. Cruikshank and colleagues (2012) report that INs in L1 of the PFC are exclusively GABAergic, but heterogeneous otherwise. Several IN subtypes located in L1 have been shown to inhibit P-cells in L2/3. These include neurogliaform cells (Cauli, Zhou, Tricoire, Toussay, & Staiger, 2014) and horizontal cells (Gabbott, 2016), which form inhibitory synapses onto P-cell dendrites. It has been demonstrated that horizontal cells in express N-type calcium channels that are involved in inhibitory feedback circuits (Liu, Hirano, Sun, Brecha, & Barnes, 2013). These findings were from horizontal cells which innervate photoreceptors, thus further studies would need to be done to confirm horizontal cells in the IL also express these properties. More directly associated with Cav2.2 expression in the mPFC, CCK+INs are addressed in their respective section of this discussion.

Previous research may also indicate which IN subtype in the IL are not likely to express Cav2.2. GABA release from neurogliaform cells in L1 (Allene et al., 2015) may be facilitated by L-type Cav_s, as this has been shown for their hippocampal analogues (Li et al., 2014). Martinotti cells, whose soma are distributed in the IL layers which contain P-cells, have long GABAergic projections which synapse onto P-cell dendrites in L1 (Allene et al., 2015; Cauli et al., 2014). Martinotti cells have been shown to express L-type Cav_s (Wang et al., 2004). GABA release from PV+BCs, located in the same layers as Martinotti cells and P-cells, is likely facilitated by P/Q-type Cav_s (Bartos & Elgueta, 2012). As these three IN subtypes have been shown to express non-N-type channels in other brain regions, they may still release GABA onto L2/3 P-cells after Cav2.2 block. Accordingly, it is possible the CTX condition IPSCs we recorded were due to GABA release from PV+BCs, Martinotti cells, and neurogliaform cells.

Localization of CCK+INs in the IL

Fluorescence experiments in our triple transgenic mouse line (*CCK-Dlx5/6-tdT*) reveal CCK+IN expression throughout the mPFC, with variability across layers (**Figure 18 - left**). Perisomatic inhibitory cells, CCK+BCs and PV+BCs, have been described in the superficial and deep layers (L2/3-L6) of the mouse IL, PL, and dorsal peduncular area (DP) (Whissell et al., 2015). CCK+BCs are reported to be the most numerous type of IN in the mPFC, and are significantly more prevalent than PV+BCs in the IL and DP (Whissell et al., 2015). Our fluorescence images appear to display similar patterns of pervasive CCK+IN expression in L2/3 and L5, as most cells appear morphologically to be innervated by the neuronal processes of CCK+INs. Innervations by CCK+INs in the mPFC are vital for regulating excitatory output; dysfunction in this system has been linked to the pathogenesis of anxiety disorders (Bachus, Hyde, Herman, Egan, & Kleinman, 1997). Interestingly, we observe the presence of CCK+INs in what laminarily appears to be L1. This expression pattern has not been specifically reported in the mouse IL before. While CCK+INs have been shown to be present in L1 of the developing mouse neocortex, CCK mRNA was the least abundant compared to other neuropeptide markers like calbindin and neuropeptide-Y (J Ma et al., 2014). Via SYTO-13 labelling, the number of cells located in L1 is relatively low compared to deeper layers. It has been reported that cells in L1 of the PFC are exclusively GABAergic INs (Cruikshank et al., 2012). Only a fraction express GABAergic CCK in our composite image (**Figure 18 - right**), which may be reflective of the low CCK mRNA content described by J Ma and colleagues (2014).

L1 CCK+INs likely possess different intrinsic properties and target different cell populations compared to CCK+INs in L2/3 and L5. As P-cell somas are located in L2/3 and L5 while their dendrites are located in L1 (Riga et al., 2014), L1 CCK+INs may be involved in

dendritic inhibition rather than perisomatic inhibition. Accordingly, the synaptic properties of L1 CCK+INs may be more similar to neurogliaform, horizontal, and/or Martinotti cells than CCK+BCs. It appears the web-like GABAergic CCK+ expression patterns of the deep IL layers are also present in L1, though to a much lesser extent. This could be due to there being a lower number CCK+INs present in L1, but the inhibition patterns of these cells could also be different. Morphological studies like biocytin stainings could be used to determine the neuroanatomical differences between L1 and L2/3 and L5 CCK+INs. The extensive GABAergic CCK+IN expression we observed in confocal images from our *CCK-Dlx5/6-tdT* mouse model are a promising sign for their potential extensive regulatory role on P-cell output in the circuits related to fear extinction.

Cav2.2 Block does not Significantly Affect GABA release in CCK+IN/P-cell Synapses in the IL

Note: While our optogenetic mouse model (*CCK-Dlx5/6-ReaChR*) labels all GABAergic CCK+INs, optogenetic stimulation likely evokes GABA release primarily from CCK+BCs in L2/3. CCK+BCs are involved in perisomatic inhibition networks with local P-cells (Eggan et al., 2010; Freund & Katona, 2007) and are more numerous than non-basket cell CCK+INs (Bachus et al., 1997; J Ma et al., 2014). However, contribution of non-basket cell CCK+INs (possibly in L1) cannot be ruled out, so results must be applied to the entire population of CCK+INs in the IL.

Contrary to our findings regarding CCK+INs in the BLA (**CHAPTER 1**), CCK+INs in the IL did not display Cav2.2-dependent neurotransmitter release properties. Accordingly, CCK+INs may differ in their Cav2.2 expression/function across brain regions. While GABA release from hippocampal CCK+INs is entirely Cav2.2-dependent (Szabo et al., 2014), it may be partially Cav2.2-dependent in the BLA (**CHAPTER 1**), and not statistically significantly Cav2.2-dependent

in the IL. However, the lack of Cav2.2-dependent GABA release may not apply to every CCK+IN in the IL. In two of our recordings, we observed moderate IPSC peak amplitude decreases (47% and 49%) following Cav2.2 blockade. It could be that in these two cells, selected randomly from L2/3 of the IL, GABA release was partially Cav2.2-dependent. However, in the cumulative population of CCK+INs we performed pharmacological recordings in, we did not observe statistically significant Cav2.2-dependent GABA release.

In addition to differential Cav2.2 expression, variations in Cav2.2-dependent GABA release could be the result of differential Cav2.2 modulation across CCK+IN subtypes. In several recordings, we observed an initial decrease in IPSC peak amplitude after CTX addition similar to the time-course plots from **Figures 13 and 16**. However, this initial decrease was temporary; after approximately twenty minutes IPSC peak amplitudes began to return to control condition values. It is possible a compensatory mechanism was responsible for this observation. The presynaptic CCK+IN terminal may have compensated for the Cav2.2 blockade, or the P-cell membrane may have compensated for the decreased GABA binding. Inchauspe and colleagues (2004) report functional compensation between Cav subtypes: N-type channels compensated for the absence of P/Q-type channels and evoked synaptic currents at the Calyx of Held. Given P/Q-type channels contribute to the maintenance of neurotransmission by providing additional facilitatory drive (Inchauspe, 2004), it is theoretically possible they could compensate for N-type calcium channel block if co-expressed in presynaptic terminals. If present in CCK+IN terminals, this compensatory mechanism could lead to much smaller decreases in IPSC peak amplitude following Cav2.2 block when compared to control conditions. In addition to functional compensation by other Cav subtypes, CTX may modulate Cav2.2 differently in the CCK+INs of the IL compared to those in the HPC or BLA. While CTX is generally considered an irreversible blocker, N-type calcium

current recovery was observable under certain conditions, like in the absence of divalent cations (Liang & Elmslie, 2002). It is unlikely we would observe this in the IL and not the BLA however, as our brain slice preparation and internal and external solutions remained consistent.

Comparisons between our two-point segment plots in **Figures 16 and 18** allow for more specific conclusions to be made regarding Cav2.2-dependent neurotransmission. The statistically significant decrease (mean = 46%) in neurotransmitter release from GABAergic INs following Cav2.2 block is not facilitated by CCK+INs. We observed transmitter release from CCK+INs did not significantly change (average 9% decrease) following Cav2.2 block. Speculation as to what presynaptic GABA release is blocked by CTX includes horizontal cells and non-compensatory CCK+INs. Overall, there are many possible reasons as to why we did not see statistically significant changes to IPSC peak amplitude with CTX in CCK+IN/P-cell synapses. Regardless of the underlying mechanism(s), our observations were reproducible. A likely and concise conclusion is that in the IL, Cav2.2 does not play a critical role in GABA release from presynaptic CCK+INs.

Pyramidal Cell Spiking is not Significantly Modulated by Cav2.2 in the IL

Under control, CTX, and CdCl₂ conditions, we observed ‘initial burst’ patterns from L2/3 P-cells in the IL. Initial bursting occurs when a neuron responds with a significantly greater spike frequency upon initial current injection, before slowing to a steady-state pattern. Initial bursting is caused by a series of ‘direct resets’, wherein the cell almost immediately fires from the membrane potential at which its previous spike ended (Gerstner, Kistler, Naud, & Paninski, 2014). We observed two direct resets under control and CTX conditions and four under CdCl₂. Steady-state patterns are the result of ‘detour resets,’ which occur when a neuron makes a ‘detour’ into the region of negative membrane potential (hyperpolarizes) at the beginning of the spike interval

(Schwalger & Lindner, 2013). Detour resets comprise the entirety of the steady-state phase, which can be categorized by the patterns produced by inter-spike intervals (ISIs). Under control and CTX conditions, we observe ‘regular-spiking’ firing patterns (equal ISIs), which are also referred to as normal, tonic, non-adapting, or non-accommodating. Similar patterns have been previously reported from P-cells in the IL (Ferreira et al., 2015), the mPFC (Van Aerde & Feldmeyer, 2015), and the BLA (Rainnie et al., 1993). Under CdCl₂ conditions, we observed what appear to be gradually increasing ISIs, indicative of an adapting or accommodating firing pattern (Gerstner et al., 2014). Though there are multiple ways to classify firing patterns, the intrinsic cellular properties producing these patterns are consistent regardless of naming scheme.

There was a distinct change in firing pattern when CdCl₂ was applied to P-cells in L2/3 of the IL. The ISI decreased dramatically from CTX and control patterns, and the direct reset phase lasted far longer. CdCl₂ acts as a calcium channel antagonist, blocking all Ca_vs (Gadbut, Cash, Noble, Radice, & Weyhenmeyer, 1991). Thus, the changes we observe from CTX to CdCl₂ conditions are due to a combination of P/Q-, L-, T-, and R-type blockade. Ca_vs allow for prolonged calcium conductance during each spike, which produces long-duration action potentials in P-cells when compared to faster spiking interneurons (Rainnie et al., 1993). When Ca_vs are blocked, it is likely that calcium entry is no longer prolonged, and thus action potential duration shortens. Along similar lines, calcium channel modulation has been shown to promote burst firing patterns from regular firing neurons (Friedman & Gutnick, 1989; S. Rudolph, Hull, & Regehr, 2015). These concepts are reflected in our experimental design; as we blocked Ca_vs, we saw greater firing frequency (< 1 Hz with CTX, > 4 Hz with CdCl₂) and an upregulation of bursting. Overall, we can make specific conclusions only for the control and Ca_v2.2 blockade conditions, as CdCl₂ is not a specific antagonist like CTX (Gadbut et al., 1991). The lack of statistically significant changes to

firing properties we observed following CTX addition indicate that Cav2.2 is not an integral somatic modifier of P-cell intrinsic firing properties. Cav2.2 in the presynaptic terminal of INs has a far more important regulatory role over P-cell activity, therefore is likely the more appropriate pharmacological target for regulating anxiety-related neuronal output.

Additional Considerations for Future Research

The infralimbic cortex, as well as the larger medial prefrontal cortex, present many opportunities for novel circuit-level functional studies of Cav_vs. Having observed a robust decrease in IPSC peak amplitude in GABAergic IN/P-cell synapses following Cav2.2 block, further investigations of presynaptic inhibition at the level of P-cell dendrites are warranted. Given the average IPSC peak amplitude decrease was 46%, there are likely other Cav subtypes which facilitate the remaining release of GABA. Emulating our previous recordings, the L-type blocker Nimodipine could be introduced to the bath following Cav2.2 block. Martinotti and neurogliaform cells express L-type channels (Li et al., 2014; Y. Wang et al., 2004), so we predict IPSC peak amplitude would further decrease. If IPSCs are not fully eliminated by N- and L-type blockade, ω -Agatoxin IVA could be added to the bath perfusion to block P/Q-type channels, which are expressed in PV+BCs (Bartos & Elgueta, 2012; Freund & Katona, 2007; Zamponi & Currie, 2013). By altering the layer of the IL in which we recorded and/or stimulated, many additional circuits could be studied. For example, stimulating L1 and recording from L5 would allow for comparisons of dendritic inhibition strength in deep L5 P-cells and superficial L2/3 P-cells. It may be that deeper IL-BLA connections are not as robustly regulated by Cav2.2, in which case other receptors may be better targets for reducing inhibition of fear extinction.

As the PL and IL have been shown to influence distinct fear and anxiety-related processes (Sierra-Mercado et al., 2011), it stands to reason that there could be circuit-level differences between the two mPFC areas. It has been demonstrated that L5 neurons differ morphologically based on projection target; the PL and IL differ greatly in this regard (Ferreira et al., 2015). Irrespective of established cellular differences, functional studies must be run to confirm if morphologically distinctive cells express unique Cav_s and process presynaptic inhibition differently. In a future experiment, we could replicate our IL recordings to test if Cav_v2.2 plays a significant role in neurotransmitter release in the PL, focusing on cell populations with known synaptic and/or intrinsic differences. Our goal would be to describe if and how Cav_v2.2 differentially regulates two distinct mPFC regions involved in fear expression and extinction.

Investigations into the role of eCB-dependent and independent CB₁ modulation of Cav_v2.2 could be performed on dendritic and perisomatic inhibitory networks in L2/3 of the IL. CB₁ receptor signaling within the mPFC has been shown to potentiate emotional associative learning through inputs from the BLA (Laviolette & Grace, 2006). However, Laviolette and Grace (2006) performed extracellular recordings so cell-specific effects were not observable; an entry point from which we could make novel contributions regarding Cav_s. Additionally, CB₁ is known to be expressed in the CCK+INs in the PFC which also express Cav_v2.2 (Marsicano & Lutz, 1999). Combined, there are many opportunities to study the relationship between CB₁/Cav_v2.2 in the infralimbic cortex.

OVERALL CONCLUSIONS

By investigating the regulation of excitatory output from the BLA, we are interested in determining new cell-specific targets to mitigate anxiety. Before this is possible, the basic cellular and molecular mechanisms underlying the relationship between INs and P-cells must be understood. Cav2.2 has been shown to modulate neurotransmitter release from CCK+INs in the hippocampus, but its role in the BLA had not been functionally described. With our novel triple transgenic mouse model, we used optogenetics tools to isolate CCK+IN/P-cell synapses for functional studies. We found that GABA release from CCK+INs was modulated by Cav2.2 in the BLA as hypothesized. But, this modulation was only partial. The average peak amplitude of inhibitory postsynaptic currents was roughly halved following Cav2.2 blockade, whereas studies of CCK+INs in the HPC would suggest total elimination of current. Our data show that while cell circuitry may be conserved, Cav2.2 differentially regulates neurotransmitter release from CCK+INs in the BLA and HPC. We present a challenge to the theory that Cav2.2 is the only Cav involved in regulating neurotransmitter release from CCK+INs. As Cav_vs are vital in regulating neuronal activity, extensive and comprehensive investigations are warranted to uncover more details as to their role in GABA release from INs in the BLA.

CCK+IN terminals in the BLA almost uniformly express type-1 cannabinoid receptor. Upon activation by cannabinoids, these receptors are believed to suppress inhibitory neurotransmitter release and disinhibit P-cells, thus profoundly impacting amygdalar output. The functional studies required to confirm these predictions were not yet published upon the start of our research. Beginning with immunofluorescence experiments, we found comparable colocalization of CB₁ and GABAergic CCK expression in the BLA and HPC. Our initial electrophysiology data suggests that CB₁ is involved in both phasic and tonic inhibition of

neurotransmitter release from CCK+IN in the BLA. CB₁-agonism lead to a decrease in IPSC peak amplitude, as CB₁ inhibits calcium entry through Ca_vs. Contrarily, CB₁-antagonism lead to an increase in IPSC peak amplitude, as tonic levels of CB₁-mediated inhibition of Ca_vs were eliminated. A paper published by Rovira-Esteban and colleagues (2017) comprehensively described the modulation of CCK+IN/P-cell synapses in the BLA by CB₁, thus we discontinued further recordings. Our hypothesis and preliminary data suggest reproducibility of the findings presented by Rovira-Esteban and colleagues (2017). Ultimately, CB₁-containing CCK+INs may control anxiety at the level of the amygdala and are potential targets for regulating anxiety-related neuronal output.

Anxiety disorders are often associated with the inability to extinguish fearful or traumatic memories, a process which in mice is thought to be facilitated by the infralimbic cortex and its connections to the BLA. The IL is a promising target for anxiety research, as Ca_v physiology is relatively understudied despite proposed functional significance. We found that Ca_v2.2 was not an integral modulator of P-cell intrinsic firing properties, as CTX had negligible effects on firing pattern and spike frequency. Ca_v2.2 displayed a far more significant regulatory role over P-cell activity in presynaptic INs, which are likely a more appropriate pharmacological target for regulated neuronal output involved in the extinction of conditioned fear. Our initial electrophysiology experiments suggest that neurotransmitter release from GABAergic inputs in L1 of the IL onto P-cells in L2/3 is partially Ca_v2.2-dependent, similar to our observations in the BLA. However, the approximate halving of IPSC peak amplitude is not facilitated by CCK+INs, as our data show neurotransmitter release from these INs is not significantly modulated by Ca_v2.2.

Overall, our experiments lay groundwork for future functional studies on the role of Ca_vs in anxiety-related circuits. We demonstrate that although CCK+IN/P-cell synapses are found in

the HPC, BLA, and mPFC, they are differentially regulated by Cav2.2. Therefore, novel pharmacological treatments for anxiety that target Cav2.2 should consider region-specific effects. Cav2.2 block likely has therapeutic value in certain neuronal circuits and brain regions, but no value or even detrimental effects on others. For example, anxiety-related brain activity may be suppressed in the HPC while simultaneously upregulated in the BLA. Differential effects may be seen within the mPFC, as upregulation of P-cell activity could facilitate fear-extinction in the IL, but perpetuate fear expression in the PL. Accordingly, more information must be revealed about the role of Cav2.2 in anxiety-related neuronal circuits to ensure the safety and efficacy of developing treatments for anxiety disorders.

As it pertains to the data presented within these chapters, future research should comprehensively describe the role of each Cav subtype involved in CCK+IN/P-cell synapses in the BLA and IL. By blocking Cav subtypes in sequential order, we could fully eliminate IPSCs and determine which are responsible for the remaining IPSC peak amplitude observed in **CHAPTER 1** and **CHAPTER 3**. Pharmacological agents would need to include Nimodipine (L-type blocker), ω -Agatoxin IVA (P/Q-type blocker), and SNX 482 (R-type blocker). Given the discrepancies we observed in CCK+INs across brain regions, it is reasonable to propose investigations into Cav_s in CCK+INs in additional limbic structures like the periaqueductal grey, anterior cingulate, and central amygdala. On a larger scale, our mouse models serve as a tool for potential studies on the anatomical, intrinsic, synaptic, and behavioral properties of CCK+INs throughout the brain.

LIST OF REFERENCES

- Adler, J., & Parmryd, I. (2010). Quantifying colocalization by correlation: The Pearson correlation coefficient is superior to the Mander's overlap coefficient. *Cytometry Part A*, *77A*(8), 733–742. <http://doi.org/10.1002/cyto.a.20896>
- Adolphs, R., Tranel, D., Damasio, H., Damasio, A., Anderson, A. K., Phelps, E. A., ... Vogt, K. E. (2005). The lateral amygdaloid nucleus: sensory interface of the amygdala in fear conditioning. *Neuron*, *62*(6), 655–667.
- Aggleton, J. P., & Passingham, R. E. (1981). Syndrome produced by lesions of the amygdala in monkeys (*Macaca mulatta*). *Journal of Comparative and Physiological Psychology*, *95*(6), 961–977. <http://doi.org/10.1037/h0077848>
- Alger, B. E. (2002). Retrograde signaling in the regulation of synaptic transmission: focus on endocannabinoids. *Progress in Neurobiology*, *68*(4), 247–86. Retrieved from <http://www.ncbi.nlm.nih.gov/pubmed/12498988>
- Ali, A. B. (2011). CB1 modulation of temporally distinct synaptic facilitation among local circuit interneurons mediated by N-type calcium channels in CA1. *Journal of Neurophysiology*, *105*(3), 1051–1062. <http://doi.org/10.1152/jn.00831.2010>
- Allene, C., Lourenço, J., & Bacci, A. (2015). The neuronal identity bias behind neocortical GABAergic plasticity. *Trends in Neurosciences*, *38*(9), 524–534. <http://doi.org/10.1016/j.tins.2015.07.008>
- Altar, C. A., & Boyar, W. C. (1989). Brain CCK-B receptors mediate the suppression of dopamine release by cholecystokinin. *Brain Research*, *483*(2), 321–326. [http://doi.org/10.1016/0006-8993\(89\)90176-5](http://doi.org/10.1016/0006-8993(89)90176-5)
- Alviña, K., & Khodakhah, K. (2008). Selective regulation of spontaneous activity of neurons of the deep cerebellar nuclei by N-type calcium channels in juvenile rats. *The Journal of Physiology*, *586*(10), 2523–2538. <http://doi.org/10.1113/jphysiol.2007.148197>
- Amir, R., Michaelis, M., & Devor, M. (1999). Membrane potential oscillations in dorsal root ganglion neurons: role in normal electrogenesis and neuropathic pain. *The Journal of Neuroscience: The Official Journal of the Society for Neuroscience*, *19*(19), 8589–96. Retrieved from <http://www.ncbi.nlm.nih.gov/pubmed/10493758> <http://www.jneurosci.org/content/19/19/8589.full.pdf>
- Anderson, A. K., & Phelps, E. A. (2001). Lesions of the human amygdala impair enhanced perception of emotionally salient events. *Nature*, *411*(6835), 305–309.
- Andrási, T., Veres, J. M., Rovira-Esteban, L., Kozma, R., Vikór, A., Gregori, E., & Hájos, N. (2017). Differential excitatory control of 2 parallel basket cell networks in amygdala microcircuits. *PLOS Biology*, *15*(5), e2001421. <http://doi.org/10.1371/journal.pbio.2001421>

- Armstrong, C., & Soltesz, I. (2012). Basket cell dichotomy in microcircuit function. *Journal of Physiology*, *590*(4), 683–694. <http://doi.org/10.1113/jphysiol.2011.223669>
- Azad, S. C. (2003). Activation of the Cannabinoid Receptor Type 1 Decreases Glutamatergic and GABAergic Synaptic Transmission in the Lateral Amygdala of the Mouse. *Learning & Memory*, *10*(2), 116–128. <http://doi.org/10.1101/lm.53303>
- Bachus, S. E., Hyde, T. M., Herman, M. M., Egan, M. F., & Kleinman, J. E. (1997). Abnormal cholecystokinin mRNA levels in entorhinal cortex of schizophrenics. *Journal of Psychiatric Research*, *31*(2), 233–256. [http://doi.org/10.1016/S0022-3956\(96\)00041-6](http://doi.org/10.1016/S0022-3956(96)00041-6)
- Baldwin, D., Woods, R., Lawson, R., & Taylor, D. (2011). Efficacy of drug treatments for generalised anxiety disorder: systematic review and meta-analysis. *BMJ*, *342*(mar11 1), d1199–d1199. <http://doi.org/10.1136/bmj.d1199>
- Barsy, B., Szabó, G. G., Andrási, T., Vikór, A., & Hájos, N. (2017). Different output properties of perisomatic region-targeting interneurons in the basal amygdala. *European Journal of Neuroscience*, *45*(4), 548–558. <http://doi.org/10.1111/ejn.13498>
- Bartos, M., & Elgueta, C. (2012). Functional characteristics of parvalbumin- and cholecystokinin-expressing basket cells. *Journal of Physiology*, *590*(4), 669–681. <http://doi.org/10.1113/jphysiol.2011.226175>
- Beinfeld, M. C., Meyer, D. K., Eskay, R. L., Jensen, R. T., & Brownstein, M. J. (1981). The distribution of cholecystokinin immunoreactivity in the central nervous system of the rat as determined by radioimmunoassay. *Brain Research*, *212*(1), 51–57. [http://doi.org/10.1016/0006-8993\(81\)90031-7](http://doi.org/10.1016/0006-8993(81)90031-7)
- Benda, J., & Herz, A. V. M. (2003). A Universal Model for Spike-Frequency Adaptation. *Neural Computation*, *15*(11), 2523–2564. <http://doi.org/10.1162/089976603322385063>
- Bentham Science Publisher, B. S. P. (2013). Pharmacological Inhibition of Voltage-gated Ca²⁺ Channels for Chronic Pain Relief. *Current Neuropharmacology*, *11*(6), 606–620. <http://doi.org/10.2174/1570159X11311060005>
- Biro, A. A., Holderith, N. B., & Nusser, Z. (2006). Release Probability-Dependent Scaling of the Postsynaptic Responses at Single Hippocampal GABAergic Synapses. *Journal of Neuroscience*, *26*(48), 12487–12496. <http://doi.org/10.1523/JNEUROSCI.3106-06.2006>
- Blanchard, D. C., & Blanchard, R. J. (1972). Innate and conditioned reactions to threat in rats with amygdaloid lesions. *Journal of Comparative and Physiological Psychology*, *81*(2), 281–290. <http://doi.org/10.1037/h0033521>
- Bowers, M. E., Choi, D. C., & Ressler, K. J. (2012). Neuropeptide regulation of fear and anxiety: Implications of cholecystokinin, endogenous opioids, and neuropeptide Y. *Physiology & Behavior*, *107*(5), 699–710. <http://doi.org/10.1016/j.physbeh.2012.03.004>
- Bradwejn, J., Koszycki, D., Couetoux du Tertre, A., van Megen, H., & et al. (1994). The

- panicogenic effects of cholecystokinin-tetrapeptide are antagonized by L-365,260, a central cholecystokinin receptor antagonist, in patients with panic disorder. *Archives of General Psychiatry*, 51(6), 486–493. Retrieved from <http://dx.doi.org/10.1001/archpsyc.1994.03950060050005>
- Bremner, J. D., Vermetten, E., Schmahl, C., Vaccarino, V., Vythilingam, M., Afzal, N., ... Charney, D. S. (2005). Positron emission tomographic imaging of neural correlates of a fear acquisition and extinction paradigm in women with childhood sexual-abuse-related post-traumatic stress disorder. *Psychological Medicine*, 35(6), 791–806. Retrieved from <http://www.ncbi.nlm.nih.gov/pubmed/15997600><http://www.pubmedcentral.nih.gov/articlerender.fcgi?artid=PMC3233760>
- Britt, J. P., McDevitt, R. A., & Bonci, A. (2012). Use of channelrhodopsin for activation of CNS neurons. *Current Protocols in Neuroscience*, 1(SUPPL.58). <http://doi.org/10.1002/0471142301.ns0216s58>
- Bystritsky, A., Khalsa, S., Cameron, M., & Schiffman, J. (2013). Current diagnosis and treatment of anxiety disorders. *P&T®*, 38(1), 30–57. Retrieved from <http://www.ncbi.nlm.nih.gov/pubmed/23599668>
- Capogna, M. (2014). GABAergic cell type diversity in the basolateral amygdala. *Current Opinion in Neurobiology*. <http://doi.org/10.1016/j.conb.2014.01.006>
- Cassidy, J. S., Ferron, L., Kadurin, I., Pratt, W. S., & Dolphin, A. C. (2014). Functional exofacially tagged N-type calcium channels elucidate the interaction with auxiliary $\alpha_2\text{-1}$ subunits. *Proceedings of the National Academy of Sciences*, 111(24), 8979–8984. <http://doi.org/10.1073/pnas.1403731111>
- Catterall, W. A. (2011). Voltage-gated calcium channels. *Cold Spring Harbor Perspectives in Biology*, 3(8), 1–23. <http://doi.org/10.1101/cshperspect.a003947>
- Cauli, B., Zhou, X., Tricoire, L., Toussay, X., & Staiger, J. F. (2014). Revisiting enigmatic cortical calretinin-expressing interneurons. *Frontiers in Neuroanatomy* (Vol. 8). <http://doi.org/10.3389/fnana.2014.00052>
- Chhatwal, J. P., Gutman, A. R., Maguschak, K. A., Bowser, M. E., Yang, Y., Davis, M., & Ressler, K. J. (2009). Functional interactions between endocannabinoid and CCK neurotransmitter systems may be critical for extinction learning. *Neuropsychopharmacology*, 34(2), 509–521. <http://doi.org/10.1038/npp.2008.97>
- Cominski, T. P., Jiao, X., Catuzzi, J. E., Stewart, A. L., & Pang, K. C. H. (2014). The Role of the Hippocampus in Avoidance Learning and Anxiety Vulnerability. *Frontiers in Behavioral Neuroscience*, 8, 273. <http://doi.org/10.3389/fnbeh.2014.00273>
- Costes, S. V., Daelemans, D., Cho, E. H., Dobbin, Z., Pavlakakis, G., & Lockett, S. (2004). Automatic and Quantitative Measurement of Protein-Protein Colocalization in Live Cells. *Biophysical Journal*, 86(6), 3993–4003. <http://doi.org/10.1529/biophysj.103.038422>

- Cruikshank, S. J., Ahmed, O. J., Stevens, T. R., Patrick, S. L., Gonzalez, A. N., Elmaleh, M., & Connors, B. W. (2012). Thalamic Control of Layer 1 Circuits in Prefrontal Cortex. *Journal of Neuroscience*, 32(49), 17813–17823. <http://doi.org/10.1523/JNEUROSCI.3231-12.2012>
- Darwin, C., & Francis, D. (2015). *The Expression of the Emotions in Man and Animals*. Oxford University Press, USA. Retrieved from papers3://publication/uuid/5963C8E6-C224-4FBE-9ECC-ACA6D351B6E2
- Davis, M., Rainnie, D., & Cassell, M. (1994). Neurotransmission in the rat amygdala related to fear and anxiety. *Trends in Neurosciences*, 17(5), 208–214. [http://doi.org/10.1016/0166-2236\(94\)90106-6](http://doi.org/10.1016/0166-2236(94)90106-6)
- Dawson, L. A., & Watson, J. M. (2009). Vilazodone: A 5-HT 1A Receptor Agonist/Serotonin Transporter Inhibitor for the Treatment of Affective Disorders. *CNS Neuroscience & Therapeutics*, 15(2), 107–117. <http://doi.org/10.1111/j.1755-5949.2008.00067.x>
- Delaney, A. J., Crane, J. W., & Sah, P. (2007). Noradrenaline Modulates Transmission at a Central Synapse by a Presynaptic Mechanism. *Neuron*, 56(5), 880–892. <http://doi.org/10.1016/j.neuron.2007.10.022>
- Deleuze, C., Pazienti, A., & Bacci, A. (2014). Autaptic self-inhibition of cortical GABAergic neurons: Synaptic narcissism or useful introspection? *Current Opinion in Neurobiology*, 26, 64–71. <http://doi.org/10.1016/j.conb.2013.12.009>
- Do-Monte, F. H., Manzano-Nieves, G., Quinones-Laracuente, K., Ramos-Medina, L., & Quirk, G. J. (2015). Revisiting the Role of Infralimbic Cortex in Fear Extinction with Optogenetics. *Journal of Neuroscience*, 35(8), 3607–3615. <http://doi.org/10.1523/JNEUROSCI.3137-14.2015>
- Douglas, R. J., & Martin, K. A. C. (2004). Neuronal Circuits of the Neocortex. *Annual Review of Neuroscience*, 27(1), 419–451. <http://doi.org/10.1146/annurev.neuro.27.070203.144152>
- Dudok, B., Barna, L., Ledri, M., Szabó, S. I., Szabadits, E., Pintér, B., ... Katona, I. (2015). Cell-specific STORM super-resolution imaging reveals nanoscale organization of cannabinoid signaling. *Nature Neuroscience*, 18(1), 75–86. <http://doi.org/10.1038/nn.3892>
- Dunn, K. W., Kamocka, M. M., & McDonald, J. H. (2011). A practical guide to evaluating colocalization in biological microscopy. *American Journal of Physiology-Cell Physiology*, 300(4), C723–C742. <http://doi.org/10.1152/ajpcell.00462.2010>
- Duvarci, S., & Pare, D. (2014, June 4). Amygdala microcircuits controlling learned fear. *Neuron*. Elsevier. <http://doi.org/10.1016/j.neuron.2014.04.042>
- Eggan, S. M., Melchitzky, D. S., Sesack, S. R., Fish, K. N., & Lewis, D. A. (2010). Relationship of cannabinoid CB1 receptor and cholecystinin immunoreactivity in monkey dorsolateral prefrontal cortex. *Neuroscience*, 169(4), 1651–1661. <http://doi.org/10.1016/j.neuroscience.2010.06.011>

- Ehrlich, I., Humeau, Y., Grenier, F., Ciocchi, S., Herry, C., & Lüthi, A. (2009). Amygdala Inhibitory Circuits and the Control of Fear Memory. *Neuron*.
<http://doi.org/10.1016/j.neuron.2009.05.026>
- Emson, P. C., Lee, C. M., & Rehfeld, J. F. (1980). Cholecystokinin octapeptide: Vesicular localization and calcium dependent release from rat brain in vitro. *Life Sciences*, 26(25), 2157–2163. [http://doi.org/10.1016/0024-3205\(80\)90603-7](http://doi.org/10.1016/0024-3205(80)90603-7)
- Eroglu, Ç., Allen, N. J., Susman, M. W., O'Rourke, N. A., Park, C. Y., Özkan, E., ... Barres, B. A. (2009). Gabapentin Receptor $\alpha 2\delta$ -1 Is a Neuronal Thrombospondin Receptor Responsible for Excitatory CNS Synaptogenesis. *Cell*, 139(2), 380–392.
<http://doi.org/10.1016/j.cell.2009.09.025>
- Etkin, A., Prater, K. E., Schatzberg, A. F., Menon, V., & Greicius, M. D. (2009). Disrupted amygdalar subregion functional connectivity and evidence of a compensatory network in generalized anxiety disorder. *Archives of General Psychiatry*, 66(12), 1361–1372.
<http://doi.org/10.1001/archgenpsychiatry.2009.104>
- Faber, E. S. L., Callister, R. J., & Sah, P. (2001). Morphological and Electrophysiological Properties of Principal Neurons in the Rat Lateral Amygdala In Vitro. *Journal of Neurophysiology*, 85(2), 714–723. <http://doi.org/10.1152/jn.2001.85.2.714>
- Farrant, M., & Nusser, Z. (2005). Variations on an inhibitory theme: Phasic and tonic activation of GABA receptors. *Nature Reviews Neuroscience*. <http://doi.org/10.1038/nrn1625>
- Ferreira, A. N., Yousuf, H., Dalton, S., & Sheets, P. L. (2015). Highly differentiated cellular and circuit properties of infralimbic pyramidal neurons projecting to the periaqueductal gray and amygdala. *Frontiers in Cellular Neuroscience*, 9, 161.
<http://doi.org/10.3389/fncel.2015.00161>
- Foldy, C. (2006). Presynaptic, Activity-Dependent Modulation of Cannabinoid Type 1 Receptor-Mediated Inhibition of GABA Release. *Journal of Neuroscience*, 26(5), 1465–1469.
<http://doi.org/10.1523/JNEUROSCI.4587-05.2006>
- Frankland, P. W., Josselyn, S. A., Bradwejn, J., Vaccarino, F. J., & Yeomans, J. S. (1996). Intracerebroventricular infusion of the CCK(B) receptor agonist pentagastrin potentiates acoustic startle. *Brain Research*, 733(1), 129–132. [http://doi.org/10.1016/S0006-8993\(96\)00756-1](http://doi.org/10.1016/S0006-8993(96)00756-1)
- Freese, J. L., & Amaral, D. G. (2005). The organization of projections from the amygdala to visual cortical areas TE and V1 in the macaque monkey. *Journal of Comparative Neurology*, 486(4), 295–317.
- Freund, T. F. (2003). Interneuron Diversity series: Rhythm and mood in perisomatic inhibition. *Trends in Neurosciences*, 26(9), 489–495. [http://doi.org/10.1016/S0166-2236\(03\)00227-3](http://doi.org/10.1016/S0166-2236(03)00227-3)
- Freund, T. F., & Katona, I. (2007). Perisomatic Inhibition. *Neuron*, 56(1), 33–42.
<http://doi.org/10.1016/j.neuron.2007.09.012>

- Friedman, A., & Gutnick, M. J. (1989). Intracellular Calcium and Control of Burst Generation in Neurons of Guinea-Pig Neocortex in Vitro. *European Journal of Neuroscience*, *1*(4), 374–381. <http://doi.org/10.1111/j.1460-9568.1989.tb00802.x>
- Fukudome, Y., Ohno-Shosaku, T., Matsui, M., Omori, Y., Fukaya, M., Tsubokawa, H., ... Kano, M. (2004). Two distinct classes of muscarinic action on hippocampal inhibitory synapses: M2-mediated direct suppression and M1/M3-mediated indirect suppression through endocannabinoid signalling. *European Journal of Neuroscience*, *19*(10), 2682–2692. <http://doi.org/10.1111/j.0953-816X.2004.03384.x>
- Gabbott, P. L. A. (2016). “Subpial Fan Cell” — A Class of Calretinin Neuron in Layer 1 of Adult Monkey Prefrontal Cortex. *Frontiers in Neuroanatomy*, *10*, 28. <http://doi.org/10.3389/fnana.2016.00028>
- Gadbut, A. P., Cash, S. A., Noble, J. A., Radice, T. R., & Weyhenmeyer, J. A. (1991). The effect of Ca²⁺-channel antagonists (cadmium, ω -conotoxin GIVA, and nitrendipine) on the release of angiotensin II from fetal rat brain in vitro. *Neuroscience Letters*, *123*(1), 91–94. [http://doi.org/10.1016/0304-3940\(91\)90165-P](http://doi.org/10.1016/0304-3940(91)90165-P)
- Gale, G. D. (2004). Role of the Basolateral Amygdala in the Storage of Fear Memories across the Adult Lifetime of Rats. *Journal of Neuroscience*, *24*(15), 3810–3815. <http://doi.org/10.1523/JNEUROSCI.4100-03.2004>
- Gerstner, W., Kistler, W. M., Naud, R., & Paninski, L. (2014). *Neuronal Dynamics: From Single Neurons to Networks and Models of Cognition*. Cambridge: Cambridge University Press. <http://doi.org/10.1007/s13398-014-0173-7.2>
- Gherardi, F., McFarland, D., & Tinbergen, N. (1988). *The Oxford Companion to Animal Behaviour*. Oxford: Oxford University Press. Retrieved from https://books.google.com/books/about/The_Oxford_companion_to_animal_behaviour.html?id=3AEpAQAAAJ
- Goosens, K. A. (2001). Contextual and Auditory Fear Conditioning are Mediated by the Lateral, Basal, and Central Amygdaloid Nuclei in Rats. *Learning & Memory*, *8*(3), 148–155. <http://doi.org/10.1101/lm.37601>
- Greenberg, T., Carlson, J. M., Cha, J., Hajcak, G., & Mujica-Parodi, L. R. (2013). Ventromedial prefrontal cortex reactivity is altered in generalized anxiety disorder during fear generalization. *Depression and Anxiety*, *30*(3), 242–250. <http://doi.org/10.1002/da.22016>
- Guo, J., & Ikeda, S. R. (2004). Endocannabinoids modulate N-type calcium channels and G-protein-coupled inwardly rectifying potassium channels via CB1 cannabinoid receptors heterologously expressed in mammalian neurons. *Molecular Pharmacology*, *65*(3), 665–674. <http://doi.org/10.1124/mol.65.3.665>
- Haller, J., Bakos, N., Szirmay, M., Ledent, C., & Freund, T. F. (2002). The effects of genetic and pharmacological blockade of the CB1 cannabinoid receptor on anxiety. *European Journal of Neuroscience*, *16*(7), 1395–1398. <http://doi.org/10.1046/j.1460-9568.2002.02192.x>

- Hannon, H., & Atchison, W. (2013). Omega-Conotoxins as Experimental Tools and Therapeutics in Pain Management. *Marine Drugs*, *11*(12), 680–699. <http://doi.org/10.3390/md11030680>
- Häring, M., Kaiser, N., Monory, K., & Lutz, B. (2011). Circuit specific functions of cannabinoid CB1 receptor in the balance of onvestigatory drive and exploration. *PLoS ONE*, *6*(11), e26617. Retrieved from isi:000297150900020
- Harris, E. W., & Cotman, C. W. (1986). Long-term potentiation of guinea pig mossy fiber responses is not blocked by N-methyl d-aspartate antagonists. *Neuroscience Letters*, *70*(1), 132–137. [http://doi.org/10.1016/0304-3940\(86\)90451-9](http://doi.org/10.1016/0304-3940(86)90451-9)
- Heidbreder, C. A., & Groenewegen, H. J. (2003, October 1). The medial prefrontal cortex in the rat: Evidence for a dorso-ventral distinction based upon functional and anatomical characteristics. *Neuroscience and Biobehavioral Reviews*. Pergamon. <http://doi.org/10.1016/j.neubiorev.2003.09.003>
- Hill, M. N., McLaughlin, R. J., Morrish, A. C., Viau, V., Floresco, S. B., Hillard, C. J., & Gorzalka, B. B. (2009). Suppression of amygdalar endocannabinoid signaling by stress contributes to activation of the hypothalamic-pituitary-adrenal axis. *Neuropsychopharmacology*, *34*(13), 2733–2745. <http://doi.org/10.1038/npp.2009.114>
- Hill, M. N., Patel, S., Campolongo, P., Tasker, J. G., Wotjak, C. T., & Bains, J. S. (2010). Functional Interactions between Stress and the Endocannabinoid System: From Synaptic Signaling to Behavioral Output. *Journal of Neuroscience*, *30*(45), 14980–14986. <http://doi.org/10.1523/JNEUROSCI.4283-10.2010>
- Hubert, G. W., Li, C., Rainnie, D. G., & Muly, E. C. (2014). Effects of stress on AMPA receptor distribution and function in the basolateral amygdala. *Brain Structure and Function*, *219*(4), 1169–1179. <http://doi.org/10.1007/s00429-013-0557-z>
- Hurley, K. M., Herbert, H., Moga, M. M., & Saper, C. B. (1991). Efferent projections of the infralimbic cortex of the rat. *Journal of Comparative Neurology*, *308*(2), 249–276. <http://doi.org/10.1002/cne.903080210>
- Ikeda, S. R. (1996). Voltage-dependent modulation of N-type calcium channels by G-protein β γ subunits. *Nature*, *380*(6571), 255–258. <http://doi.org/10.1038/380255a0>
- Inchauspe, C. G. (2004). Functional Compensation of P/Q by N-Type Channels Blocks Short-Term Plasticity at the Calyx of Held Presynaptic Terminal. *Journal of Neuroscience*, *24*(46), 10379–10383. <http://doi.org/10.1523/JNEUROSCI.2104-04.2004>
- Ingram, S. M., Krause, R. G., Baldino, F., Skeen, L. C., & Lewis, M. E. (1989). Neuronal localization of cholecystinin mRNA in the rat brain by using in situ hybridization histochemistry. *The Journal of Comparative Neurology*, *287*(2), 260–72. <http://doi.org/10.1002/cne.902870209>
- Janak, P. H., & Tye, K. M. (2015). From circuits to behaviour in the amygdala. *Nature*. <http://doi.org/10.1038/nature14188>

- Jasnow, A. M., Ressler, K. J., Hammack, S. E., Chhatwal, J. P., & Rainnie, D. G. (2009). Distinct Subtypes of Cholecystokinin (CCK)-Containing Interneurons of the Basolateral Amygdala Identified Using a CCK Promoter-Specific Lentivirus. *Journal of Neurophysiology*, *101*(3), 1494–1506. <http://doi.org/10.1152/jn.91149.2008>
- Jinno, S. (2009). Structural organization of long-range GABAergic projection system of the hippocampus. *Frontiers in Neuroanatomy*, *3*, 13. <http://doi.org/10.3389/neuro.05.013.2009>
- Johansen, J. P., Cain, C. K., Ostroff, L. E., & Ledoux, J. E. (2011). Molecular mechanisms of fear learning and memory. *Cell*. <http://doi.org/10.1016/j.cell.2011.10.009>
- Johansen, J. P., Hamanaka, H., Monfils, M. H., Behnia, R., Deisseroth, K., Blair, H. T., & LeDoux, J. E. (2010). Optical activation of lateral amygdala pyramidal cells instructs associative fear learning. *Proceedings of the National Academy of Sciences*, *107*(28), 12692–12697. <http://doi.org/10.1073/pnas.1002418107>
- Josselyn, S. A., Frankland, P. W., Petrisano, S., Bush, D. E. A., Yeomans, J. S., & Vaccarino, F. J. (1995). The CCKB antagonist, L-365,260, attenuates fear-potentiated startle. *Peptides*, *16*(7), 1313–1315. [http://doi.org/10.1016/0196-9781\(95\)02013-M](http://doi.org/10.1016/0196-9781(95)02013-M)
- Katona, I., Rancz, E. A., Acsady, L., Ledent, C., Mackie, K., Hajos, N., & Freund, T. F. (2001). Distribution of CB1 cannabinoid receptors in the amygdala and their role in the control of GABAergic transmission. *The Journal of Neuroscience: The Official Journal of the Society for Neuroscience*, *21*(23), 9506–18. <http://doi.org/10.1523/JNEUROSCI.2123-01.2001> [pii]
- Keifer, O. P., Hurt, R. C., Ressler, K. J., & Marvar, P. J. (2015). The Physiology of Fear: Reconceptualizing the Role of the Central Amygdala in Fear Learning. *Physiology*, *30*(5), 389–401. <http://doi.org/10.1152/physiol.00058.2014>
- Kolosov, A., Aurini, L., Williams, E. D., Cooke, I., & Goodchild, C. S. (2011). Intravenous injection of leconotide, an omega conotoxin: Synergistic antihyperalgesic effects with morphine in a rat model of bone cancer pain. *Pain Medicine*, *12*(6), 923–941. <http://doi.org/10.1111/j.1526-4637.2011.01118.x>
- Krettek, J. E., & Price, J. L. (1977). Projections from the amygdaloid complex and adjacent olfactory structures to the entorhinal cortex and to the subiculum in the rat and cat. *Journal of Comparative Neurology*, *172*(4), 723–752. <http://doi.org/10.1002/cne.901720409>
- Kroenke, K., Spitzer, R. L., Williams, J. B. W., Monahan, P. O., & Löwe, B. (2007). Anxiety disorders in primary care: Prevalence, impairment, comorbidity, and detection. *Annals of Internal Medicine*, *146*(5), 317–325. <http://doi.org/10.7326/0003-4819-146-5-200703060-00004>
- Kullmann, D. M. (2011, October). Interneuron networks in the hippocampus. *Current Opinion in Neurobiology*. <http://doi.org/10.1016/j.conb.2011.05.006>
- Kumar, A. (2011). Long-term potentiation at CA3-CA1 hippocampal synapses with special emphasis on aging, disease, and stress. *Frontiers in Aging Neuroscience*. Frontiers Media

- SA. <http://doi.org/10.3389/fnagi.2011.00007>
- Kurihara, T., & Tanabe, T. (2003). N-type Ca²⁺ channel. *Folia Pharmacologica Japonica*, *121*(4), 211–222. <http://doi.org/10.1254/fpj.121.211>
- Lacaille, J. C., & Williams, S. (1990). Membrane properties of interneurons in stratum oriens-alveus of the CA1 region of rat hippocampus in vivo. *Neuroscience*, *36*(2), 349–359.
- Lafenêtre, P., Chaouloff, F., & Marsicano, G. (2007). The endocannabinoid system in the processing of anxiety and fear and how CB1 receptors may modulate fear extinction. *Pharmacological Research*, *56*(5), 367–381. <http://doi.org/10.1016/j.phrs.2007.09.006>
- Lanza, M., & Makovec, F. (2000). Cholecystokinin (CCK) increases GABA release in the rat anterior nucleus accumbens via CCK B receptors located on glutamatergic interneurons. *Naunyn-Schmiedeberg's Archives of Pharmacology*, *361*(1), 33–38. <http://doi.org/10.1007/s002109900161>
- Laviolette, S. R., & Grace, A. A. (2006). Cannabinoids Potentiate Emotional Learning Plasticity in Neurons of the Medial Prefrontal Cortex through Basolateral Amygdala Inputs. *Journal of Neuroscience*, *26*(24), 6458–6468. <http://doi.org/10.1523/JNEUROSCI.0707-06.2006>
- LeDoux, J. (1996). Emotional networks and motor control: a fearful view. In *Progress in brain research* (Vol. 107, pp. 437–446). [http://doi.org/10.1016/S0079-6123\(08\)61880-4](http://doi.org/10.1016/S0079-6123(08)61880-4)
- LeDoux, J. E. (2009). Emotion Circuits in the Brain. *FOCUS*, *7*(2), 274–274. <http://doi.org/10.1176/foc.7.2.foc274>
- Lee, S.-H., Ledri, M., Toth, B., Marchionni, I., Henstridge, C. M., Dudok, B., ... Katona, I. (2015). Multiple Forms of Endocannabinoid and Endovanilloid Signaling Regulate the Tonic Control of GABA Release. *Journal of Neuroscience*, *35*(27), 10039–10057. <http://doi.org/10.1523/JNEUROSCI.4112-14.2015>
- Lenkey, N., Kirizis, T., Holderith, N., Máté, Z., Szabó, G., Vizi, E. S., ... Nusser, Z. (2015). Tonic endocannabinoid-mediated modulation of GABA release is independent of the CB₁ content of axon terminals. *Nature Communications*, *6*(1), 6557. <http://doi.org/10.1038/ncomms7557>
- Li, G., Stewart, R., Canepari, M., & Capogna, M. (2014). Firing of Hippocampal Neurogliaform Cells Induces Suppression of Synaptic Inhibition. *Journal of Neuroscience*, *34*(4), 1280–1292. <http://doi.org/10.1523/JNEUROSCI.3046-13.2014>
- Liang, H., & Elmslie, K. S. (2002). Rapid and reversible block of N-type calcium channels (Ca_v2.2) by omega-conotoxin GVIA in the absence of divalent cations. *The Journal of Neuroscience: The Official Journal of the Society for Neuroscience*, *22*(20), 8884–90. Retrieved from <http://www.jneurosci.org/content/22/20/8884.abstract>
- Lin, J. Y., Knutsen, P. M., Muller, A., Kleinfeld, D., & Tsien, R. Y. (2013). ReaChR: A red-shifted variant of channelrhodopsin enables deep transcranial optogenetic excitation. *Nature*

Neuroscience, 16(10), 1499–1508. <http://doi.org/10.1038/nm.3502>

- Little, J. P., & Carter, A. G. (2013). Synaptic Mechanisms Underlying Strong Reciprocal Connectivity between the Medial Prefrontal Cortex and Basolateral Amygdala. *Journal of Neuroscience*, 33(39), 15333–15342. <http://doi.org/10.1523/JNEUROSCI.2385-13.2013>
- Liu, X., Hirano, A. A., Sun, X., Brecha, N. C., & Barnes, S. (2013). Calcium channels in rat horizontal cells regulate feedback inhibition of photoreceptors through an unconventional GABA- and pH-sensitive mechanism. *Journal of Physiology*, 591(13), 3309–3324. <http://doi.org/10.1113/jphysiol.2012.248179>
- Loane, D. J., Lima, P. A., & Marrion, N. V. (2007). Co-assembly of N-type Ca²⁺ and BK channels underlies functional coupling in rat brain. *Journal of Cell Science*, 120(6), 985–995. <http://doi.org/10.1242/jcs.03399>
- Lotarski, S. M., Donevan, S., El-Kattan, A., Osgood, S., Poe, J., Taylor, C. P., & Offord, J. (2011). Anxiolytic-Like Activity of Pregabalin in the Vogel Conflict Test in 2 -1 (R217A) and 2 -2 (R279A) Mouse Mutants. *Journal of Pharmacology and Experimental Therapeutics*, 338(2), 615–621. <http://doi.org/10.1124/jpet.111.180976>
- Lozovaya, N., Min, R., Tsintsadze, V., & Burnashev, N. (2009). Dual modulation of CNS voltage-gated calcium channels by cannabinoids: Focus on CB1 receptor-independent effects. *Cell Calcium*, 46(3), 154–162. <http://doi.org/10.1016/j.ceca.2009.07.007>
- Lutz, B., Marsicano, G., Maldonado, R., & Hillard, C. J. (2015). The endocannabinoid system in guarding against fear, anxiety and stress. *Nature Reviews Neuroscience*. <http://doi.org/10.1038/nrn4036>
- Ma, J., Dankulich-Nagrudny, L., & Lowe, G. (2013). Cholecystokinin: An Excitatory Modulator of Mitral/Tufted Cells in the Mouse Olfactory Bulb. *PLoS ONE*, 8(5), e64170. <http://doi.org/10.1371/journal.pone.0064170>
- Ma, J., Yao, X. H., Fu, Y. H., & Yu, Y. C. (2014). Development of Layer 1 Neurons in the Mouse Neocortex. *Cerebral Cortex*, 24(10), 2604–2618. Retrieved from isi:000343408200008
- MACLEAN, P. D. (1955). The Limbic System (“Visceral Brain”) in Relation to Central Gray and Reticulum of the Brain Stem. *Psychosomatic Medicine*, 17(5), 355–366. <http://doi.org/10.1097/00006842-195509000-00003>
- Majak, K., Pikkarainen, M., Kemppainen, S., Jolkkonen, E., & Pitkänen, A. (2002). Projections from the amygdaloid complex to the claustrum and the endopiriform nucleus: A Phaseolus vulgaris leucoagglutinin study in the rat. *Journal of Comparative Neurology*, 451(3), 236–249. <http://doi.org/10.1002/cne.10346>
- Maren, S., & Fanselow, M. (1995). Synaptic plasticity in the basolateral amygdala induced by hippocampal formation stimulation in vivo. *The Journal of Neuroscience*, 15(11), 7548–7564. <http://doi.org/10.1523/JNEUROSCI.15-11-07548.1995>

- Marsicano, G., & Lutz, B. (1999). Expression of the cannabinoid receptor CB1 in distinct neuronal subpopulations in the adult mouse forebrain. *European Journal of Neuroscience*, *11*(12), 4213–4225. <http://doi.org/10.1046/j.1460-9568.1999.00847.x>
- Marsicano, G., Wotjak, C. T., Azad, S. C., Bisogno, T., Rammes, G., Cascioli, M. G., ... Lutz, B. (2002). The endogenous cannabinoid system controls extinction of aversive memories. *Nature*, *418*(6897), 530–534. <http://doi.org/10.1038/nature00839>
- Mascagni, F., & McDonald, A. J. (2003). Immunohistochemical characterization of cholecystinin containing neurons in the rat basolateral amygdala. *Brain Research*, *976*(2), 171–184. [http://doi.org/10.1016/S0006-8993\(03\)02625-8](http://doi.org/10.1016/S0006-8993(03)02625-8)
- Máté, Z., Poles, M. Z., Szabó, G., Bagyánszki, M., Talapka, P., Fekete, É., & Bódi, N. (2013). Spatiotemporal expression pattern of DsRedT3/CCK gene construct during postnatal development of myenteric plexus in transgenic mice. *Cell and Tissue Research*, *352*(2), 199–206. <http://doi.org/10.1007/s00441-013-1552-7>
- McCleskey, E. W., Fox, a P., Feldman, D. H., Cruz, L. J., Olivera, B. M., & Tsien, R. W. (1987). Omega-conotoxin: Direct and persistent blockade of specific types of calcium channels in neurons but not muscle. *Proceedings of the National Academy of Sciences of the United States of America*, *84*(12), 4327–4331. <http://doi.org/10.1073/pnas.84.12.4327>
- McDonald, A. J., & Mascagni, F. (2001). Localization of the CB1 type cannabinoid receptor in the rat basolateral amygdala. *Neuroscience*, *107*(4), 641–652.
- Milad, M. R., Pitman, R. K., Ellis, C. B., Gold, A. L., Shin, L. M., Lasko, N. B., ... Rauch, S. L. (2009). Neurobiological Basis of Failure to Recall Extinction Memory in Posttraumatic Stress Disorder. *Biological Psychiatry*, *66*(12), 1075–1082. <http://doi.org/10.1016/j.biopsych.2009.06.026>
- Milad, M. R., & Quirk, G. J. (2002). Neurons in medial prefrontal cortex signal memory for fear extinction. *Nature*, *420*(6911), 70–74. <http://doi.org/10.1038/nature01138>
- Möhler, H. (2002). Pathophysiological aspects of diversity in neuronal inhibition: A new benzodiazepine pharmacology. *Dialogues in Clinical Neuroscience*, *4*(3), 261–269. <http://doi.org/10.1053/gast.2002.32539>
- Montigny, C. (1989). Cholecystinin Tetrapeptide Induces Panic-like Attacks in Healthy Volunteers: Preliminary Findings. *Archives of General Psychiatry*, *46*(6), 511–517. <http://doi.org/10.1001/archpsyc.1989.01810060031006>
- Moreira, F. A., Grieb, M., & Lutz, B. (2009). Central side-effects of therapies based on CB1 cannabinoid receptor agonists and antagonists: focus on anxiety and depression. *Best Practice & Research Clinical Endocrinology & Metabolism*, *23*(1), 133–144. <http://doi.org/10.1016/j.beem.2008.09.003>
- Morgan, M. A., Romanski, L. M., & LeDoux, J. E. (1993). Extinction of emotional learning: Contribution of medial prefrontal cortex. *Neuroscience Letters*, *163*(1), 109–113.

[http://doi.org/10.1016/0304-3940\(93\)90241-C](http://doi.org/10.1016/0304-3940(93)90241-C)

Neu, A., Földy, C., & Soltesz, I. (2007). Postsynaptic origin of CB1-dependent tonic inhibition of GABA release at cholecystokinin-positive basket cell to pyramidal cell synapses in the CA1 region of the rat hippocampus. *Journal of Physiology*, *578*(1), 233–247.
<http://doi.org/10.1113/jphysiol.2006.115691>

Newton, P. M., & Messing, R. O. (2009). The N-type calcium channel is a novel target for treating alcohol use disorders. *Channels (Austin, Tex.)*, *3*(2), 77–81.
<http://doi.org/10.1523/JNEUROSCI.3621-08.2008>.www.landesbioscience.com

Nyíri, G., Stephenson, F. A., Freund, T. F., & Somogyi, P. (2003). Large variability in synaptic N-methyl-D-aspartate receptor density on interneurons and a comparison with pyramidal-cell spines in the rat hippocampus. *Neuroscience*, *119*(2), 347–363.
[http://doi.org/10.1016/S0306-4522\(03\)00157-X](http://doi.org/10.1016/S0306-4522(03)00157-X)

Onaivi, E. S., Green, M. R., & Martin, B. R. (1990). *Pharmacological characterization of cannabinoids in the elevated plus maze*. *Journal of Pharmacology and Experimental Therapeutics* (Vol. 253).

Pagotto, U., Marsicano, G., Cota, D., Lutz, B., & Pasquali, R. (2006). The Emerging Role of the Endocannabinoid System in Endocrine Regulation and Energy Balance. *Endocrine Reviews*, *27*(1), 73–100. <http://doi.org/10.1210/er.2005-0009>

Palmer, L., Murayama, M., & Larkum, M. (2012). Inhibitory Regulation of Dendritic Activity in vivo. *Frontiers in Neural Circuits*, *6*, 26. <http://doi.org/10.3389/fncir.2012.00026>

Papez, J. (1937). A Proposed Mechanism of Emotion. *Archives of Neurology & Psychiatry*, *258*(March 5), 589–598.

Patel, S., Kingsley, P. J., MacKie, K., Marnett, L. J., & Winder, D. G. (2009). Repeated homotypic stress elevates 2-arachidonoylglycerol levels and enhances short-term endocannabinoid signaling at inhibitory synapses in basolateral amygdala. *Neuropsychopharmacology*, *34*(13), 2699–2709. <http://doi.org/10.1038/npp.2009.101>

Patel, S., Roelke, C. T., Rademacher, D. J., & Hillard, C. J. (2005). Inhibition of restraint stress-induced neural and behavioural activation by endogenous cannabinoid signalling. *European Journal of Neuroscience*, *21*(4), 1057–1069. <http://doi.org/10.1111/j.1460-9568.2005.03916.x>

Paxinos, G., & Watson, C. (2007). *The Rat Brain in Stereotaxic Coordinates* (4th ed.). Academic Press. <http://doi.org/10.1016/j.neulet.2010.11.062>

Phelps, E. A., Delgado, M. R., Nearing, K. I., & Ledoux, J. E. (2004). Extinction learning in humans: Role of the amygdala and vmPFC. *Neuron*, *43*(6), 897–905.
<http://doi.org/10.1016/j.neuron.2004.08.042>

Product, Z., & Support, A. (n.d.). Acquiring and Analyzing Data for Colocalization Experiments

in AIM or ZEN Software. Retrieved March 2, 2018, from https://www.zeiss.com/content/dam/Microscopy/Downloads/Pdf/FAQs/zen-aim_colocalization.pdf

- Qin, Z., Zhou, X., Pandey, N. R., Vecchiarelli, H. A., Stewart, C. A., Zhang, X., ... Chen, H. H. (2015). Chronic Stress Induces Anxiety via an Amygdalar Intracellular Cascade that Impairs Endocannabinoid Signaling. *Neuron*, 85(6), 1319–1331. <http://doi.org/10.1016/j.neuron.2015.02.015>
- Rainnie, D. G., Asproдини, E. K., & Shinnick-Gallagher, P. (1993). Intracellular recordings from morphologically identified neurons of the basolateral amygdala. *Journal of Neurophysiology*, 69(4), 1350–1362. <http://doi.org/10.1152/jn.1993.69.4.1350>
- Ramikie, T. S., & Patel, S. (2012). Endocannabinoid signaling in the amygdala: Anatomy, synaptic signaling, behavior, and adaptations to stress. *Neuroscience*. <http://doi.org/10.1016/j.neuroscience.2011.08.037>
- Rauch, S. L., Shin, L. M., & Wright, C. I. (2006). Neuroimaging Studies of Amygdala Function in Anxiety Disorders. *Annals of the New York Academy of Sciences*, 985(1), 389–410. <http://doi.org/10.1111/j.1749-6632.2003.tb07096.x>
- Rey, A. A., Purrio, M., Viveros, M. P., & Lutz, B. (2012). Biphasic effects of cannabinoids in anxiety responses: CB1 and GABA B receptors in the balance of gabaergic and glutamatergic neurotransmission. *Neuropsychopharmacology*, 37(12), 2624–2634. <http://doi.org/10.1038/npp.2012.123>
- Riga, D., Matos, M. R., Glas, A., Smit, A. B., Spijker, S., & Van den Oever, M. C. (2014). Optogenetic dissection of medial prefrontal cortex circuitry. *Frontiers in Systems Neuroscience*, 8, 230. <http://doi.org/10.3389/fnsys.2014.00230>
- Ritu, Sandeep, Mamta, & Nirja. (2013). Anxiety disorders: A review. *International Journal of Pharma Professional Research*, 4(2), 809–819. Retrieved from <http://www.ijpponline.in/April-2013-Vol-4-issue-2/paper-4.pdf>
- Roberto, M., Cruz, M., Bajo, M., Siggins, G., Parsons, L., & Schweitzer, P. (2010). The Endocannabinoid System Tonicly Regulates Inhibitory. *Neuropsychopharmacology*, 35, 1962–1972.
- Roosendaal, B., McEwen, B. S., & Chattarji, S. (2009). Stress, memory and the amygdala. *Nature Reviews Neuroscience*. <http://doi.org/10.1038/nrn2651>
- Rotzinger, S., & Vaccarino, F. J. (2003). Cholecystokinin receptor subtypes: Role in the modulation of anxiety-related and reward-related behaviours in animal models. *Journal of Psychiatry and Neuroscience*, 28(3), 171–181. Retrieved from <http://www.ncbi.nlm.nih.gov/pubmed/12790157>
- Rovira-Esteban, L., Péterfi, Z., Vikór, A., Máté, Z., Szabó, G., & Hájos, N. (2017). Morphological and physiological properties of CCK/CB1R-expressing interneurons in the

- basal amygdala. *Brain Structure and Function*, 222(8), 3543–3565.
<http://doi.org/10.1007/s00429-017-1417-z>
- Roxo, M. R., Franceschini, P. R., Zubarán, C., Kleber, F. D., & Sander, J. W. (2011). The Limbic System Conception and Its Historical Evolution. *The Scientific World JOURNAL*, 11, 2427–2440. <http://doi.org/10.1100/2011/157150>
- Rudolph, S., Hull, C., & Regehr, W. G. (2015). Active Dendrites and Differential Distribution of Calcium Channels Enable Functional Compartmentalization of Golgi Cells. *The Journal of Neuroscience*, 35(47), 15492–15504. <http://doi.org/10.1523/JNEUROSCI.3132-15.2015>
- Rudolph, U., & Antkowiak, B. (2004). *Molecular and neuronal substrates for general anaesthetics*. *Nature Reviews Neuroscience* (Vol. 5). <http://doi.org/10.1038/nrn1496>
- Saegusa, H. (2001). Suppression of inflammatory and neuropathic pain symptoms in mice lacking the N-type Ca²⁺ channel. *The EMBO Journal*, 20(10), 2349–2356.
<http://doi.org/10.1093/emboj/20.10.2349>
- Schmidtko, A., Lötsch, J., Freynhagen, R., & Geisslinger, G. (2010). Ziconotide for treatment of severe chronic pain. *The Lancet*, 375(9725), 1569–1577. [http://doi.org/10.1016/S0140-6736\(10\)60354-6](http://doi.org/10.1016/S0140-6736(10)60354-6)
- Schwalger, T., & Lindner, B. (2013). Patterns of interval correlations in neural oscillators with adaptation. *Frontiers in Computational Neuroscience*, 7, 164.
<http://doi.org/10.3389/fncom.2013.00164>
- Scott, D. A., Wright, C. E., & Angus, J. A. (2002). Actions of intrathecal ω -conotoxins CVID, GVIA, MVIIA, and morphine in acute and neuropathic pain in the rat. *European Journal of Pharmacology*, 451(3), 279–286. [http://doi.org/10.1016/S0014-2999\(02\)02247-1](http://doi.org/10.1016/S0014-2999(02)02247-1)
- Scotter, E., Graham, S., & Glass, M. (2009). *The Cannabinoid Receptors*. (P. H. Reggio, Ed.). Totowa, NJ: Humana Press. <http://doi.org/10.1007/978-1-59745-503-9>
- Shen, M., Piser, T. M., Seybold, V. S., & Thayer, S. a. (1996). Cannabinoid Receptor Agonists Inhibit Glutamatergic Synaptic Transmission in Rat Hippocampal Cultures. *The Journal of Neuroscience*, 16(14), 4322–4334. <http://doi.org/10.1523/JNEUROSCI.16-14-04322.1996>
- Shin, L. M., Orr, S. P., Carson, M. A., Rauch, S. L., Macklin, M. L., Lasko, N. B., ... Pitman, R. K. (2004). Regional Cerebral Blood Flow in the Amygdala and Medial Prefrontal Cortex during Traumatic Imagery in Male and Female Vietnam Veterans with PTSD. *Archives of General Psychiatry*, 61(2), 168–176. <http://doi.org/10.1001/archpsyc.61.2.168>
- Shin, L. M., Wright, C. I., Cannistraro, P. A., Wedig, M. M., McMullin, K., Martis, B., ... Rauch, S. L. (2005). A functional magnetic resonance imaging study of amygdala and medial prefrontal cortex responses to overtly presented fearful faces in posttraumatic stress disorder. *Archives of General Psychiatry*, 62(3), 273–281.
<http://doi.org/10.1001/archpsyc.62.3.273>

- Sierra-Mercado, D., Corcoran, K. A., Lebrón-Milad, K., & Quirk, G. J. (2006). Inactivation of the ventromedial prefrontal cortex reduces expression of conditioned fear and impairs subsequent recall of extinction. *European Journal of Neuroscience*, *24*(6), 1751–1758. <http://doi.org/10.1111/j.1460-9568.2006.05014.x>
- Sierra-Mercado, D., Padilla-Coreano, N., & Quirk, G. J. (2011). Dissociable roles of prelimbic and infralimbic cortices, ventral hippocampus, and basolateral amygdala in the expression and extinction of conditioned fear. *Neuropsychopharmacology*, *36*(2), 529–538. <http://doi.org/10.1038/npp.2010.184>
- Sills, G. J. (2006). The mechanisms of action of gabapentin and pregabalin. *Current Opinion in Pharmacology*. <http://doi.org/10.1016/j.coph.2005.11.003>
- Soltesz, I., Alger, B. E., Kano, M., Lee, S. H., Lovinger, D. M., Ohno-Shosaku, T., & Watanabe, M. (2015). Weeding out bad waves: Towards selective cannabinoid circuit control in epilepsy. *Nature Reviews Neuroscience*, *16*(5), 264–277. <http://doi.org/10.1038/nrn3937>
- Spampanato, J., Polepalli, J., & Sah, P. (2011). Interneurons in the basolateral amygdala. *Neuropharmacology*, *60*(5), 765–773. <http://doi.org/10.1016/j.neuropharm.2010.11.006>
- Sparta, D. R., Hovelso, N., Mason, A. O., Kantak, P. A., Ung, R. L., Decot, H. K., & Stuber, G. D. (2014). Activation of Prefrontal Cortical Parvalbumin Interneurons Facilitates Extinction of Reward-Seeking Behavior. *Journal of Neuroscience*, *34*(10), 3699–3705. <http://doi.org/10.1523/JNEUROSCI.0235-13.2014>
- Stanton, P. K., Winterer, J., Zhang, X. I., & Müller, W. (2005). Imaging LTP of presynaptic release of FM1-43 from the rapidly recycling vesicle pool of Schaffer collateral-CA1 synapses in rat hippocampal slices. *European Journal of Neuroscience*, *22*(10), 2451–2461. <http://doi.org/10.1111/j.1460-9568.2005.04437.x>
- Steimer, T. (2002, September). The biology of fear- and anxiety-related behaviors. *Dialogues in Clinical Neuroscience*. Les Laboratoires Servier. Retrieved from <http://www.ncbi.nlm.nih.gov/pubmed/22033741>
- Stotz, S. (2001). Structural determinants of fast inactivation of high voltage-activated Ca²⁺ channels. *Trends in Neurosciences*, *24*(3), 176–182. [http://doi.org/10.1016/S0166-2236\(00\)01738-0](http://doi.org/10.1016/S0166-2236(00)01738-0)
- Südhof, T. C. (2012). Calcium control of neurotransmitter release. *Cold Spring Harbor Perspectives in Biology*, *4*(1), a011353. <http://doi.org/10.1101/cshperspect.a011353>
- Sullivan, R., & Gratton, A. (2002). Behavioral effects of excitotoxic lesions of ventral medial prefrontal cortex in the rat are hemisphere-dependent. *Brain Research*, *927*(1), 69–79. Retrieved from www.elsevier.com
- Swanson, C. J., Bures, M., Johnson, M. P., Linden, A.-M., Monn, J. A., & Schoepp, D. D. (2005). Metabotropic glutamate receptors as novel targets for anxiety and stress disorders. *Nature Reviews Drug Discovery*, *4*(2), 131–144. <http://doi.org/10.1038/nrd1630>

- Swanson, L. W. (2004). *Brain Maps: Structure of the Rat Brain. A Laboratory Guide with Printed and Electronic Templates for Data, Models and Schematics*. Academic. Retrieved from <https://books.google.com/books?hl=en&lr=&id=DoL0dzDGxtIC&oi=fnd&pg=PP11&dq=Swanson+LW+Third+Edition,+Elsevier+Academic+Press,+Oxford,+2004&ots=U8ktWY2EwG&sig=RA8vFcljkkFFOSAIrk97xQqIPIA#v=onepage&q&f=false>
- Szabo, G. G., Lenkey, N., Holderith, N., Andrasi, T., Nusser, Z., & Hajos, N. (2014). Presynaptic Calcium Channel Inhibition Underlies CB1 Cannabinoid Receptor-Mediated Suppression of GABA Release. *Journal of Neuroscience*, *34*(23), 7958–7963. <http://doi.org/10.1523/JNEUROSCI.0247-14.2014>
- Talani, G., & Lovinger, D. M. (2015). Interactions between ethanol and the endocannabinoid system at GABAergic synapses on basolateral amygdala principal neurons. *Alcohol*, *49*(8), 781–794. <http://doi.org/10.1016/j.alcohol.2015.08.006>
- Taniguchi, H., He, M., Wu, P., Kim, S., Paik, R., Sugino, K., ... Huang, Z. J. (2011). A Resource of Cre Driver Lines for Genetic Targeting of GABAergic Neurons in Cerebral Cortex. *Neuron*, *71*(6), 995–1013. <http://doi.org/10.1016/j.neuron.2011.07.026>
- Trouche, S., Sasaki, J. M., Tu, T., & Reijmers, L. G. (2013). Fear Extinction Causes Target-Specific Remodeling of Perisomatic Inhibitory Synapses. *Neuron*, *80*(4), 1054–1065. <http://doi.org/10.1016/j.neuron.2013.07.047>
- Truitt, W. A., Johnson, P. L., Dietrich, A. D., Fitz, S. D., & Shekhar, A. (2009). Anxiety-like behavior is modulated by a discrete subpopulation of interneurons in the basolateral amygdala. *Neuroscience*, *160*(2), 284–294. <http://doi.org/10.1016/j.neuroscience.2009.01.083>
- Trzaskowski, B., Latek, D., Yuan, S., Ghoshdastider, U., Debinski, A., & Filipek, S. (2012). Action of Molecular Switches in GPCRs - Theoretical and Experimental Studies. *Current Medicinal Chemistry*, *19*(8), 1090–1109. <http://doi.org/10.2174/092986712799320556>
- Tye, K. M., & Deisseroth, K. (2012). Optogenetic investigation of neural circuits underlying brain disease in animal models. *Nature Reviews Neuroscience*, *13*(4), 251–266. <http://doi.org/10.1038/nrn3171>
- Tye, K. M., Prakash, R., Kim, S.-Y., Fenno, L. E., Grosenick, L., Zarabi, H., ... Deisseroth, K. (2011). Amygdala circuitry mediating reversible and bidirectional control of anxiety. *Nature*, *471*(7338), 358–362. <http://doi.org/10.1038/nature09820>
- Van Aerde, K. I., & Feldmeyer, D. (2015). Morphological and physiological characterization of pyramidal neuron subtypes in rat medial prefrontal cortex. *Cerebral Cortex*, *25*(3), 788–805. <http://doi.org/10.1093/cercor/bht278>
- Vanderhaeghen, J. J., Signeau, J. C., & Gepts, W. (1975). New peptide in the vertebrate CNS reacting with antigastrin antibodies. *Nature*, *257*(5527), 604–605. <http://doi.org/10.1038/257604a0>

- Vereczki, V. K., Veres, J. M., Müller, K., Nagy, G. A., Rácz, B., Barsy, B., & Hájos, N. (2016). Synaptic Organization of Perisomatic GABAergic Inputs onto the Principal Cells of the Mouse Basolateral Amygdala. *Frontiers in Neuroanatomy*. <http://doi.org/10.3389/fnana.2016.00020>
- Veres, J. M., Nagy, G. A., & Hájos, N. (2017). Perisomatic GABAergic synapses of basket cells effectively control principal neuron activity in amygdala networks. *eLife*, 6. <http://doi.org/10.7554/eLife.20721>
- Viveros, M. P., Marco, E. M., & File, S. E. (2005). Endocannabinoid system and stress and anxiety responses. In *Pharmacology Biochemistry and Behavior* (Vol. 81, pp. 331–342). <http://doi.org/10.1016/j.pbb.2005.01.029>
- Wang, G. Q., Cen, C., Li, C., Cao, S., Wang, N., Zhou, Z., ... Wang, Y. (2015). Deactivation of excitatory neurons in the prelimbic cortex via Cdk5 promotes pain sensation and anxiety. *Nature Communications*, 6, 7660. <http://doi.org/10.1038/ncomms8660>
- Wang, Y., Toledo-Rodriguez, M., Gupta, A., Wu, C., Silberberg, G., Luo, J., & Markram, H. (2004). Anatomical, physiological and molecular properties of Martinotti cells in the somatosensory cortex of the juvenile rat. *Journal of Physiology*, 561(1), 65–90. <http://doi.org/10.1113/jphysiol.2004.073353>
- Weiskrantz, L. (1956). Behavioral changes associated with ablation of the amygdaloid complex in monkeys. *Journal of Comparative and Physiological Psychology*, 49(4), 381–391. <http://doi.org/10.1037/h0088009>
- Whissell, P. D., Cajanding, J. D., Fogel, N., & Kim, J. C. (2015). Comparative density of CCK- and PV-GABA cells within the cortex and hippocampus. *Frontiers in Neuroanatomy*, 9(September), 1–16. <http://doi.org/10.3389/fnana.2015.00124>
- Williams, M. E., Brust, P. F., Feldman, D. H., Patthi, S., Simerson, S., Maroufi, A., ... Harpold, M. M. (1992). Structure and functional expression of an ω -conotoxin-sensitive human N-type calcium channel. *Science*, 257(5068), 389–395. Retrieved from <http://science.sciencemag.org/content/257/5068/389.abstract>
- Wilson, R. I., Kunos, G., & Nicoll, R. A. (2001). Presynaptic specificity of endocannabinoid signaling in the hippocampus. *Neuron*, 31(3), 453–462. [http://doi.org/10.1016/S0896-6273\(01\)00372-5](http://doi.org/10.1016/S0896-6273(01)00372-5)
- Womack, M. D. (2004). Calcium-Activated Potassium Channels Are Selectively Coupled to P/Q-Type Calcium Channels in Cerebellar Purkinje Neurons. *Journal of Neuroscience*, 24(40), 8818–8822. <http://doi.org/10.1523/JNEUROSCI.2915-04.2004>
- Wu, L.-G., Borst, J. G. G., & Sakmann, B. (1998). R-type Ca^{2+} currents evoke transmitter release at a rat central synapse. *Proceedings of the National Academy of Sciences*, 95(8), 4720–4725. <http://doi.org/10.1073/pnas.95.8.4720>
- Yoshida, T., Uchigashima, M., Yamasaki, M., Katona, I., Yamazaki, M., Sakimura, K., ...

- Watanabe, M. (2011). Unique inhibitory synapse with particularly rich endocannabinoid signaling machinery on pyramidal neurons in basal amygdaloid nucleus. *Proceedings of the National Academy of Sciences*, *108*(7), 3059–3064. <http://doi.org/10.1073/pnas.1012875108>
- Zaitsev, A. V., Povysheva, N. V., Gonzalez-Burgos, G., & Lewis, D. A. (2012). Electrophysiological classes of layer 2/3 pyramidal cells in monkey prefrontal cortex. *Journal of Neurophysiology*, *108*(2), 595–609. <http://doi.org/10.1152/jn.00859.2011>
- Zamponi, G. W. (2003). Regulation of Presynaptic Calcium Channels by Synaptic Proteins. *Journal of Pharmacological Sciences*, *92*(2), 79–83. <http://doi.org/10.1254/jphs.92.79>
- Zamponi, G. W. (2016). Targeting voltage-gated calcium channels in neurological and psychiatric diseases. *Nature Reviews Drug Discovery*. <http://doi.org/10.1038/nrd.2015.5>
- Zamponi, G. W., & Currie, K. P. M. (2013). Regulation of CaV2 calcium channels by G protein coupled receptors. *Biochimica et Biophysica Acta (BBA) - Biomembranes*, *1828*(7), 1629–1643. <http://doi.org/10.1016/j.bbamem.2012.10.004>
- Zhu, P. J. (2005). Retrograde Endocannabinoid Signaling in a Postsynaptic Neuron/Synaptic Bouton Preparation from Basolateral Amygdala. *Journal of Neuroscience*, *25*(26), 6199–6207. <http://doi.org/10.1523/JNEUROSCI.1148-05.2005>
- Zoppi, S., Pérez Nieves, B. G., Madrigal, J. L. M., Manzanares, J., Leza, J. C., & García-Bueno, B. (2011). Regulatory role of cannabinoid receptor 1 in stress-induced excitotoxicity and neuroinflammation. *Neuropsychopharmacology*, *36*(4), 805–818. <http://doi.org/10.1038/npp.2010.214>

APPENDIX: IACUC APPROVAL LETTER

University of New Hampshire

Research Integrity Services, Service Building
51 College Road, Durham, NH 03824-3585
Fax: 603-862-3564

05-Oct-2015

Andrade, Arturo S
Dept. of Biological Sciences
Rudman Hall
Durham, NH 03824

IACUC #: 150901

Project: Role of Gi/o-protein Inhibition of Cav2.2 Calcium Channels in Anxiety-like Behavior

Category: E

Approval Date: 17-Sep-2015

The Institutional Animal Care and Use Committee (IACUC) reviewed and approved the protocol submitted for this study under Category E on Page 5 of the Application for Review of Vertebrate Animal Use in Research or Instruction - *Animal use activities that involve accompanying pain or distress to the animals for which appropriate anesthetic, analgesic, tranquilizing drugs or other methods for relieving pain or distress are not used.*

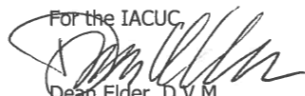
Approval is granted for a period of three years from the approval date above. Continued approval throughout the three year period is contingent upon completion of annual reports on the use of animals. At the end of the three year approval period you may submit a new application and request for extension to continue this project. Requests for extension must be filed prior to the expiration of the original approval.

Please Note:

1. All cage, pen, or other animal identification records must include your IACUC # listed above.
2. Use of animals in research and instruction is approved contingent upon participation in the UNH Occupational Health Program for persons handling animals. Participation is mandatory for all principal investigators and their affiliated personnel, employees of the University and students alike. Information about the program, including forms, is available at <http://unh.edu/research/occupational-health-program-animal-handlers>.

If you have any questions, please contact me at 862-4629 or Julie Simpson at 862-2003.

For the IACUC,



Dean Elder, D.V.M.
Vice Chair

cc: File